11-2012

# Phylogenetic Engineering of the Ribulose-1,5-bisphosphate Carboxylase/Oxygenase Large Subunit in *Chlamydomonas Reinhardtii*

Boon Hoe Lim
*University of Nebraska-Lincoln*, lim@huskers.unl.edu

# PHYLOGENETIC ENGINEERING OF THE RIBULOSE-1,5-BISPHOSPHATE CARBOXYLASE/OXYGENASE LARGE SUBUNIT IN *CHLAMYDOMONAS REINHARDTII*

by

Boon Hoe Lim

A DISSERTATION

Presented to the Faculty of

The Graduate College of the University of Nebraska

In Partial Fulfillment of Requirements

For the Degree of Doctor of Philosophy

Major: Biochemistry

Under the Supervision of Professor Robert J. Spreitzer

Lincoln, Nebraska

November 2012

# PHYLOGENETIC ENGINEERING OF THE RIBULOSE-1,5-BISPHOSPHATE CARBOXYLASE/OXYGENASE LARGE SUBUNIT IN *CHLAMYDOMONAS REINHARDTII*

Boon Hoe Lim, Ph. D.

University of Nebraska, 2012

Advisor: Robert J. Spreitzer

Thirty-four residues in the large subunit of ribulose-1,5-bisphosphate carboxylase/oxygenase (Rubisco) may account for the kinetic differences between Rubisco enzyme from green algae and land plants. By substituting these "phylogenetic residues" as groups and combinations of groups in the large subunit of the green alga *Chlamydomonas reinhardtii* with those of land-plant Rubisco, the functions and relationships of these "phylogenetic groups" were determined.

A phylogenetic-group substitution at the base of catalytic loop 6 of the large subunit decreases the $CO_2/O_2$ specificity of the enzyme, but function is restored by a further phylogenetic-group substitution at the carboxy-terminal tail. Therefore, these two regions of the large subunit, which sandwich loop 6, are complementary. In addition, combining substitutions at the base of loop 6 and the large/small-subunit interface region produces a mutant enzyme that has to be complemented by the land-plant small subunit for function in *Chlamydomonas*. On the other hand, substitutions in α-helix G of the large subunit reduce the holoenzyme level, and, because *Chlamydomonas* mutants with additional substitutions in α-helices 7 and 8 cannot be recovered as photosynthetic-transformants, the three α helices appear to influence holoenzyme assembly.

A previous study showed that substituting five large-subunit residues and a small-

subunit loop with land-plant identities produced an enzyme (termed "penta/ABSO") with land-plant catalytic properties. In the present study, through structural dissection, it is concluded that all the residues substituted in penta/ABSO are required for the shift towards land-plant catalysis. Among the residues substituted in penta/ABSO is methyl-Cys-256, which indicates that posttranslational modifications of the large subunit may also play a role in catalysis. Further study of cysteine methylation and proline hydroxylation showed that mutations of methyl-Cys-256 and hydroxy-Pro-104 influence catalysis.

The current study complements previous knowledge about Rubisco, and provides further structural targets for the beneficial engineering of Rubisco.

## ACKNOWLEDGEMENTS

I am grateful to my Ph. D. advisor, Dr. Robert J. Spreitzer, for providing the opportunity to undertake such an interesting and challenging project. His generosity, patience, and guidance have been essential to the success of this research, and for my development as a scientist. I am also thankful to my committee members, Drs. Donald F. Becker, Heriberto D. Cerutti, Julie M. Stone and Mark A. Wilson for their time and willingness to evaluate the research as it progressed, especially to Drs. Stone and Wilson for critically reading this dissertation. Of course, this research would not be possible without the previous work conducted by past members in our laboratory. Special thanks is due to Dr. Todor N. Genkov not only for "showing me the ropes" and helping me "get my feet wet" when I first started in the lab, but also for creating the *Chlamydomonas rbcL*Δ/SSAT transformation host and other materials. I am also grateful to Dr. Toshihiro Nakano for his contribution to the phenotypic and enzymatic analysis of the posttranslational-modification mutants. To the current members in the Spreitzer group, which include Drs. Asha A. Nesamma, Girish K. Rasineni and Fuqiao Xu, I value their helpful discussions and their willingness to ease my responsibilities in the laboratory as I focused on finishing this dissertation.

# TABLE OF CONTENTS

## LIST OF FIGURES

# LIST OF TABLES

## ABBREVIATIONS USED

| | |
|---|---|
| Bicine | N,N-bis(2-hydroxyethyl)glycine |
| CABP | 2-carboxyarabinitol 1,5-bisphosphate |
| DPM | Disintegrations per minute |
| DTT | dithiothreitol |
| EDTA | ethylenediaminetetraacetate |
| $K_c$ | Michaelis constant ($K_m$) for substrate $CO_2$ |
| $K_o$ | Michaelis constant ($K_m$) for substrate $O_2$ |
| kDa | kilodalton |
| 2-PG | 2-phosphoglycolate |
| 3-PGA | 3-phosphoglycerate |
| Rubisco | ribulose-l,5-bisphosphate carboxylase/oxygenase |
| RUBP | ribulose 1,5-bisphosphate |
| SD | standard deviation |
| SDS-PAGE | sodium dodecyl sulfate-polyacrylamide gel electrophoresis |
| Tris | tris[hydroxymethyl]amino-methane |
| $v_c$ | reaction velocity for Rubisco carboxylation |
| $v_o$ | reaction velocity for Rubisco oxygenation |
| $V_c$ | $V_{max}$ for Rubisco carboxylation |
| $V_o$ | $V_{max}$ for Rubisco oxygenation |
| Ω | $CO_2/O_2$ specificity factor, $V_cK_o/V_oK_c$ |

# INTRODUCTION

## RIBULOSE-1,5-BISPHOSPHATE CARBOXYLASE/OXYGENASE

### Biological importance and function

Ribulose-1,5-bisphosphate carboxylase/oxygenase (Rubisco; EC 4.1.1.39) is the most abundant protein on earth (Ellis, 1979) and is found in all photosynthetic organisms within all three domains of life (Eukarya, Bacteria, Archaea) (Tabita, 1999) from unicellular photosynthetic bacteria and algae to multicellular $C_3$ and $C_4$ plants (Andersson and Backlund, 2008). In earlier experiments, Rubisco was identified as "Fraction 1 protein" because it was the first and only protein to precipitate out of leaf extracts at 35% ammonium sulfate saturation (Wildman and Bonner, 1947; Wildman, 2002). This is not surprising considering that as much as 50% of leaf nitrogen is used by plants to synthesize Rubisco (Ellis, 1979; Spreitzer and Salvucci, 2002). For autotrophic prokaryotes, as much as 40% of total soluble protein can be Rubisco (Ellis, 1979; Tabita *et al.*, 2007). Overall, it is estimated that Rubisco makes up 0.2% of the total protein in our planet's biomass (Ellis, 1979).

The primary function of Rubisco is the reduction of $CO_2$ via the Calvin-Benson-Bassham reductive pentose phosphate pathway (Tabita *et al.*, 2008a). Rubisco captures $CO_2$ by fixing the gaseous molecule onto ribulose 1,5-bisphosphate (RuBP), which is further metabolized into other organic compounds. Although various organisms can reduce $CO_2$ via three other pathways, which are the reductive tricarboxylic acid cycle, the Wood-Ljungdahl acetyl coenzyme A pathway, and the hydroxypropionate pathway, most carbon on earth is fixed through the Calvin cycle (Tabita *et al.*, 2007). Therefore,

Rubisco is also obviously the most important enzyme for all life on Earth (Ellis, 1979). However, the catalytic rate of Rubisco has been unfavorably described as sluggish (Ellis, 1979) because while most enzymes have catalytic rates, $k_{cat}$, of over thousands per second (Wolfenden and Snider, 2001), Rubisco has a carboxylation $k_{cat}$ of only several per second, which is at least two orders of magnitude lower (Tabita *et al.*, 2007). Moreover, the enzyme sometimes fixes $O_2$ instead of $CO_2$, leading to the nonessential, energy-expending and $CO_2$-losing photorespiratory pathway (Bowes *et al.*, 1971). Therefore, there is much interest in understanding and improving the enzyme by overcoming its unusual limitations, especially because the potential benefits of such endeavors include greatly increasing crop and renewable-energy production, and decelerating the rapid rise of atmospheric $CO_2$ levels (reviewed by Spreitzer and Salvucci, 2002).

**$CO_2/O_2$ specificity factor and diversity of kinetic properties**

The $CO_2/O_2$ specificity factor of Rubisco is the ratio of the rate constants for carboxylation ($k_c$) and oxygenation ($k_o$), and is represented by the symbol Ω (Chen and Spreitzer, 1991; Spreitzer, 1993):

$$\Omega = k_c/k_o$$

Ω is also defined by the $V_{max}$ for carboxylation ($V_c$), $V_{max}$ for oxygenation ($V_o$), $K_m$ $CO_2$ ($K_c$) and $K_m$ $O_2$ ($K_o$) (Laing *et al.*, 1974):

$$\Omega = V_c K_o / V_o K_c$$

In addition, Ω is related to the difference in the free energy of activation for oxygenation ($\Delta G_o^{\ddagger}$) and the free energy of activation for carboxylation ($\Delta G_c^{\ddagger}$) (Chen and Spreitzer, 1991):

$$\Omega = e^{(\Delta G_o^{\ddagger} - \Delta G_c^{\ddagger})/RT}$$

where R is the gas constant and T is the absolute temperature. The $\Delta G_o^{\ddagger}$-$\Delta G_c^{\ddagger}$ term is directly related to the difference in the free energy of the transition states of the oxygenation and carboxylation reactions of Rubisco (Chen and Spreitzer, 1991, 1992). Consequently, altering the relative stabilities of the Rubisco transition-state complex of the two reactions through amino-acid modifications or substitutions, environmental pH changes, or metal-cofactor replacements are potential means of altering Ω (Chen and Spreitzer, 1992). Specifically, Ω could be increased by increasing the stability of the Rubisco transition-state complex for carboxylation or decreasing the stability of the complex for oxygenation (Chen and Spreitzer, 1991). Because the highest-resolution x-ray crystal structures of Rubisco from various species and Rubisco mutants can be obtained only when the holoenzyme is in complex with 2-carboxyarabinitol 1,5-bisphosphate (CABP), which is a carboxylation transition-state analog, the structure-function relationships of the holoenzyme are mapped by relating differences in measured Ω values to subtle structural changes that alter the holoenzyme-CABP interactions in these crystal structures (Andersson and Backlund, 2008). Unsurprisingly, there is also a direct relation between Ω and tightness of CABP binding by Rubisco (Satagopan and Spreitzer, 2004). Also, from the Ω-and-free-energy equation, Ω decreases with increased temperature (T) (Chen and Spreitzer, 1992), so increased global temperature would reduce the Ω value of Rubisco in plants.

Even though Ω is a useful measurement in studying the structure-function relationships in Rubisco, the only measurement to model plant growth based on the

kinetic properties of Rubisco is provided by net $CO_2$ fixation, denoted $P_n$ (Laing *et al.*, 1974; Spreitzer, 1993):

$$P_n = V_c K_o ([CO_2]\text{-}t/\Omega\,[O_2]) / (K_c K_o + K_c[O_2] + K_o[CO_2])$$

where t is the fraction of $CO_2$ released in photorespiration. From the $P_n$ equation, net $CO_2$ fixation is not dependent on only Ω, but also on $V_c$, $K_c$, and $K_o$ (Spreitzer, 1993). More importantly, varying the kinetic properties of Rubisco optimizes net $CO_2$ fixation in different photoautotrophic organisms because of the differences in intracellular gaseous $CO_2$ and $O_2$ concentrations around Rubisco (Spreitzer, 1999). Some plants, such as $C_4$ and Crassulacean acid metabolism (CAM) plants, and some photoautotrophic microbes, such as microalgae and cyanobacteria, have biochemical and physiological adaptations that increase the $CO_2$ concentration around Rubisco.

There is an observed trade-off between $V_c$ and Ω in Rubisco from different species, which is like the inverse relationship between activity and specificity that is common among other enzymes (Table 1). Generally, Ω is higher but $V_c$ is lower among eukaryotic Rubiscos compared to the prokaryotic enzymes (Table 1) (Jordan and Ogren, 1981b; Spreitzer and Salvucci, 2002). Therefore, even if a Rubisco with increased Ω was engineered, the resulting decreased $V_c$ might be less than optimal for photosynthetic growth (Spreitzer and Salvucci, 2002). A better understanding of the structure-function relationships of Rubisco is required before attempting to improve the enzyme, bearing in mind that the ultimate measurement for any beneficial improvement is $P_n$ (Spreitzer, 1993).

**Table 1: Diversity of Rubisco kinetic properties.** Values are from Jordan and Ogren (1981b), Andrews and Lorimer (1985), Read and Tabita (1994), Whitney *et al.* (2001), Kubien *et al.* (2008), Genkov *et al.* (2010), and Savir *et al.* (2010).

| Species | Ω | $V_c$ | $K_c$ | $K_o$ |
|---|---|---|---|---|
| | $V_cK_o/V_oK_c$ | *µmol/hr/mg* | *µM* $CO_2$ | *µM* $O_2$ |
| Land plants | | | | |
| *Spinacia oleracea* | 80 | 79 | 23 | 520 |
| *Arabidopsis thaliana* | 77 | 72 | 22 | 474 |
| *Helianthus anuus* | 77 | 69 | 19 | 640 |
| *Nicotiana tabacum* | 82 | 65 | 11 | 295 |
| *Zea mays* | 78 | 84 | 34 | 810 |
| *Amaranthus edulis* | 78 | 79 | 18 | 289 |
| *Flaveria australisica* | 77 | 73 | 22 | 309 |
| Green algae | | | | |
| *Chlamydomonas reinhardtii* | 61 | 112 | 31 | 498 |
| Cyanobacteria | | | | |
| *Synechococcus 7002* | 52 | 255 | 246 | 1300 |
| *Synechococcus 6301* | 43 | 224 | 340 | 972 |

**Holoenzyme structure**

There are three forms of Rubisco, which are usually found in different species (Fig. 1) (Tabita, 1999; Tabita *et. al.*, 2007, 2008a). Form-I Rubisco, which is the focus of this research, has the highest Ω value, and is the common type found in plants, algae, and most autotrophic prokaryotes (Tabita, 1999; Tabita *et al.*, 2007, 2008a; Andersson, 2008, Andersson and Backlund, 2008). The presence of small subunits, and the heterohexadecameric holoenzyme structure composed of eight large subunits and eight small subunits, distinguish form-I Rubisco from the other forms (Fig. 1) (Knight *et al.*, 1990; Schneider *et al.*, 1990; Taylor *et al.*, 2001). The form-I holoenzyme is a ring of four large-subunit dimers, with each open end of the ring capped by four small subunits. A solvent channel runs through the fourfold axis in the middle of the ring (Fig. 1) (Knight *et al.*, 1990).

Unlike form-I Rubisco, forms-II and III Rubisco enzymes lack small subunits. Form II Rubisco, which is found in some photosynthetic prokaryotes and dinoflagellates, is composed of large-subunit dimers (Fig. 1) (Tabita *et al.*, 2008a). The first Rubisco crystal structure solved was for the form-II Rubisco from *Rhodospirillum rubrum* (Schneider *et al.*, 1986). On the other hand, form-III Rubisco, which is found only in archaea, is composed of large-subunit octamers (four dimers in a ring) or decamers (five dimers in a ring), depending on species (Fig. 1) (Andersson, 2008). The unique multi-dimeric structure of form-III Rubisco contributes to the thermostability of the holoenzyme, especially important for the extreme environments where thermophilic archaea would thrive (Maeda *et al.*, 2002). The carboxylase activity of the form-III Rubisco is highly susceptible to $O_2$ inhibition because most archaea with the form-III

**Figure 1: Rubisco holoenzyme structures for form-I, II, and III Rubisco.** Form-I Rubisco is represented by that of *Chlamydomonas* (PDB 1GK8), form-II by that of *R. rubrum* (PDB 9RUB) and form-III by that of *Thermococcus kodakaraensis* (PDB 1GEH). The areas in red denote the active-site regions. For *Chlamydomonas* Rubisco, small subunits are in yellow and orange, with the variable βA-βB loop that surrounds the central solvent channel also shown as ribbons.

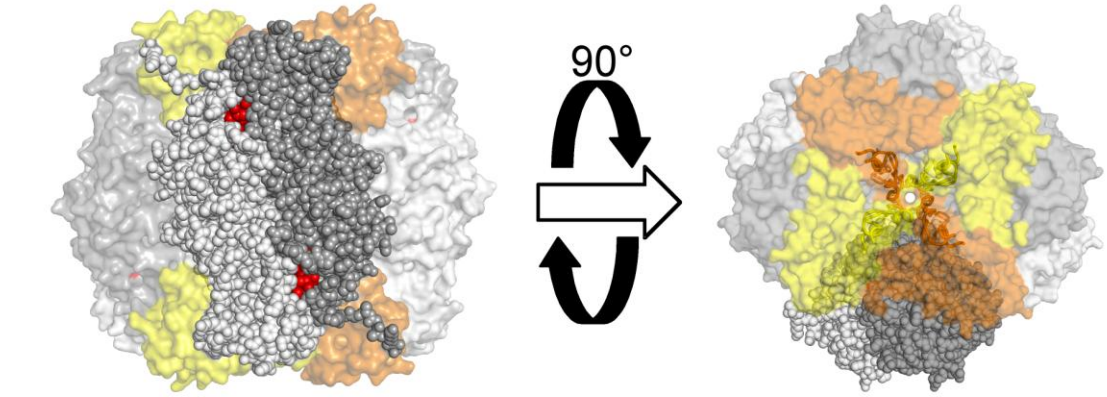


*Chlamydomonas* (Form-I)

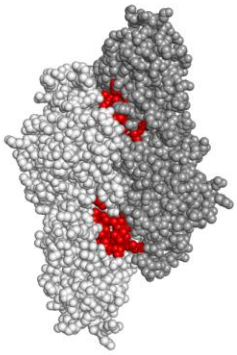

*R. rubrum* (Form-II)

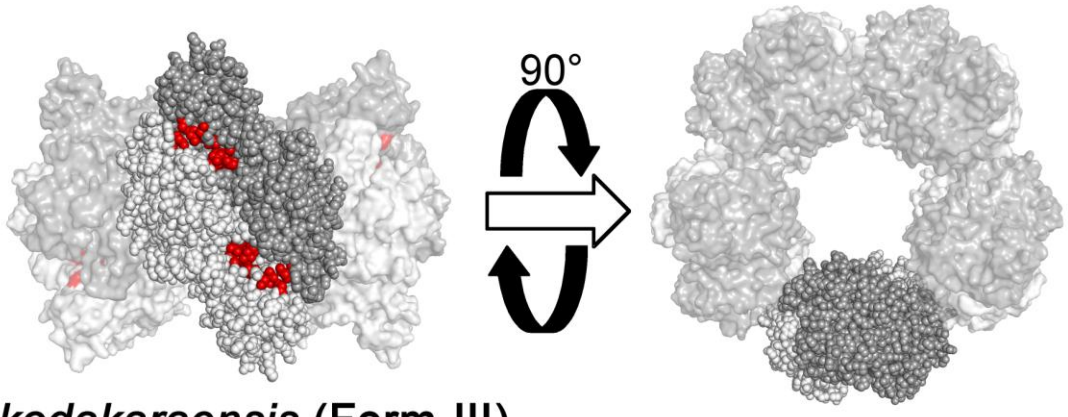


*T. kodakaraensis* (Form-III)

Rubisco are adapted to anaerobic habitats. Based on phylogenetic analysis, form-III Rubisco is the putative ancestor for all Rubisco proteins (Tabita *et al.*, 2008a). Another class of proteins, known as Rubisco-like proteins or form-IV Rubisco, is similarly derived from the form-III ancestral Rubisco, but these proteins lack half of the active-site residues of *bona fide* Rubisco, and do not catalyze carbon fixation (Saito *et al.*, 2009).

In all forms of Rubisco, the active sites are located in the large subunits (Fig. 1) (Knight *et al.*, 1990). Rubisco large subunits are 440-480 amino acids in length (depending on species) and 50-55 kDa in molecular mass (Andersson and Backlund, 2008). The large subunit has an amino-terminal domain composed of a five-stranded mixed β-sheet packed by two α helices on one face of the sheet, and a longer carboxy-terminal domain composed of an eight-stranded parallel α/β-barrel structure (Knight *et al.*, 1990; Andersson and Backlund, 2008).

Despite the structural similarities of the large subunits and active sites, the different forms of Rubisco share as little as 30% protein-sequence identity (Tabita *et al.*, 2008a). However, some photosynthetic prokaryotes such as *Rhodobacter sphaeroides, R. capsulatus*, and *Hydrogenovibrio marinus* harbor both form-I and II Rubisco, but preferentially synthesize the higher-Ω form-I Rubisco under $CO_2$-limiting conditions (Gibson and Tabita, 1977; Tabita, 1999; Tabita *et al.*, 2008a; Andersson, 2008; Andersson and Backlund, 2008).

Among plants and green algae, the Rubisco holoenzyme is localized in the chloroplast stroma, where one large subunit *rbcL* gene is found on each copy of the multicopy chloroplast genome. On the other hand, a family of Rubisco small-subunit *rbcS* genes, ranging from 2 to over 22 genes depending on the species, are found in the

nucleus (Spreitzer, 2003). Nuclear-encoded Rubisco small-subunit proteins have cleavable transit peptides to target and translocate the precursors into the chloroplast for assembly (Schmidt and Mishkind, 1986). The only exception among eukaryotes for separate compartmentalization of the *rbcL* and *rbcS* genes is among non-green algae, which have both small and large subunit genes in a chloroplast *rbcLS* operon (Tabita, 1999; Spreitzer, 2003). Among prokaryotes with form-I Rubisco, the two subunits are cotranscribed in a larger operon containing genes of several other Calvin cycle enzymes (Tabita, 1999).

Most Rubisco small subunits, which are 110-180 amino acids in length and 12-18 kDa in molecular mass, are composed of a four-stranded anti-parallel β-sheet (denoted strands A to D) with two α helices packed on one face of the sheet (Fig. 2). Small subunits from non-green algae and certain prokaryotes also have a longer carboxy-terminal extension with two additional β-strands, which are denoted strands E and F (Fig. 2) (Spreitzer, 2003; Andersson, 2008). A loop between β-strands A and B of the small subunit, known as the βA-βB loop, and a loop between β-strands E and F (when present), known as the βE-βF loop, surround the opening of the the central solvent channel and determine the channel's aperture based on the bulkiness and length of the loops (Fig. 1) (Knight *et al.*, 1990; Spreitzer, 2003). Because the highest measured Ω value is for red-algal Rubisco with the βE-βF loop, and because form-I Rubisco, which has small subunits, has higher Ω than the other Rubisco forms, the architecture of the central solvent channel and the small subunits can influence catalysis (Uemura, 1997; Spreitzer, 2003; Genkov *et al.*, 2010). In addition to playing a role in catalysis, the small subunit is also responsible for aggregating Rubisco molecules into proteinaceous structures known

**Figure 2: Alignment of Rubisco small subunits from *Chlamydomonas* (yellow) (PDB 1GK8), spinach (blue) (PDB 8RUC) and non-green alga *Galdieria partita* (green) (PDB ID 1BWV).** In the structural alignment, the loops between β-strands A and B, and between C and D, and between E and F, which is only in non-green algae, are labeled. In the sequence alignment, the residue positions at the top are based on the *Chlamydomonas* small-subunit sequence, and the secondary structures are shaded and labeled at the bottom.

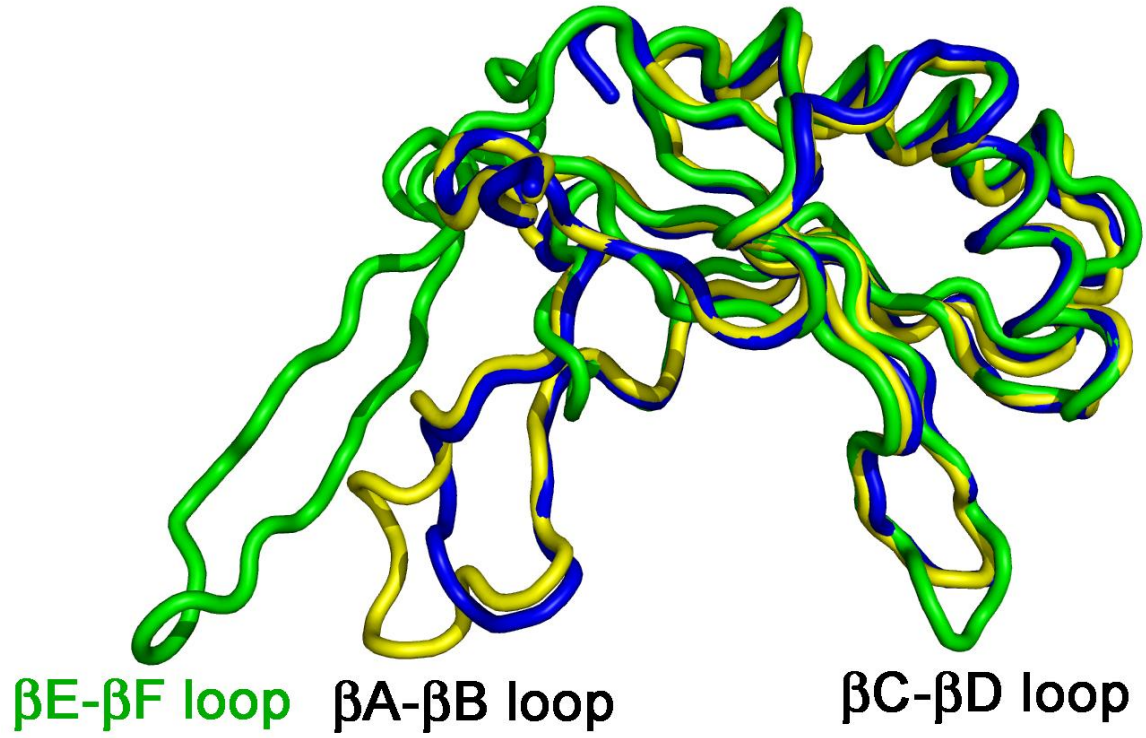


```
                    10         20         30         40
                    |          |          |          |
Chlamydomonas       MMVWTPVNNKMFETFSYLPPLTDEQIAAQVDYIVANGWIP
Spinach             MQVWPILNLKKYETLSYLPPLTTDQLAROVDYLLNNKWVP
Galdieria           -------VRITQGTFSFLPDLTDEQIKKQIDYMISKKLAI
                                                αA

                    50         60         70
                    |          |          |
Chlamydomonas       CLEFAEADKAYVSNESA-IRFGSVSCLYYDNRYWTMWKLP
Spinach             CLEFET-DHGFVYREHHN------SPGYYDGRYWTMWKLP
Galdieria           GIEYTN--DIHPR-----------------NAYWEIWGLP
                    βA                                  βB

                80         90         100        110
                |          |          |          |
Chlamydomonas   MFGCRDPMQVLREIVACTKAFPDAYVRLVAFDNQ--KQVQ
Spinach         MFGCTDPAQVLNELEECKKEYPNAFIRIIGFDSN--REVQ
Galdieria       LFDVTDPAAVLFEINACRKARSNFYIKVVGFSSVRGIEST
                           αB                  βC

                120        130        140        150
                |          |          |          |
Chlamydomonas   IMGFLVQRPKTARDFQPANKRSV----------------
Spinach         CISFIAYKPAGY-----------------------------
Galdieria       IISFIVNRPKHEPGFNLMRQEDKSRSIKYTIHSYESYKPE
                  βD              βE          βF

                160
                |
Chlamydomonas   ----
Spinach         ----
Galdieria       DERY
```

as pyrenoids in algae where $CO_2$ is concentrated to be more efficiently fixed by Rubisco (Genkov *et al.*, 2010).

**Posttranslational modifications**

Posttranslational modifications of the Rubisco holoenzyme have mainly been observed and studied in form-I Rubisco (Houtz *et al.*, 2008). The most important posttranslational modification of the Rubisco large subunit is the carbamylation of catalytic Lys-201 by non-substrate $CO_2$ to activate the enzyme (Lorimer, 1981; Cleland *et al.*, 1998). Besides that, the first two residues of the Rubisco large subunit from plants and green algae are cleaved off by a dipeptidase, and the third residue (Pro-3) is N-acetylated (Houtz *et al.*, 1989). The putative role of this amino-terminal modification is the protection of the protein from proteolysis (Houtz *et al.*, 2008). Amino-terminal modifications of the Rubisco small-subunit also occur, the most obvious being the removal of the transit peptide, which is followed by N-methylation of Met-1 in the mature small subunit (Schmidt and Mishkind, 1986; Houtz *et al.*, 2008).

Other posttranslational modifications occur in the large subunit. Lys-14 of some plant large subunits is Nε-trimethylated by a methyltransferase, but the role of this modification is unknown (Houtz *et al.*, 1989, 2008). In the high-resolution crystal structure of Rubisco from the green alga *Chlamydomonas reinhardtii*, four additional posttranslational modifications of the large subunit were observed (Taylor *et al.*, 2001). These include S-methylation of Cys-256 and Cys-369, and 4-hydroxylation of Pro-104 and Pro-151 (Taylor *et al.*, 2001). Recently, determination of lysine acetylation in *Arabidopsis* proteins using generic anti-LysAc antibody immunodetection followed by

liquid chromatography-tandem mass spectrometry discovered nine acetylated lysine residues in the Rubisco large subunit and one acetylated lysine residue in the small subunit (Finkmeier *et al.*, 2011), which is surprising considering that acetylation of lysines have never been observed in any of the Rubisco crystal structures from diverse species (Schneider *et al.*, 1986; Knight *et al.*, 1990; Taylor *et al.*, 2001; Andersson, 2008).

Despite the vast knowledge on Rubisco posttranslational modification, much is still unknown about the functions or proteins involved. For example, several nuclear mutations in *Chlamydomonas* change the kinetic constants of Rubisco, and decrease Ω, but the genetic loci of these mutations are yet to be identified. These mutations must affect Rubisco posttranslationally (Spreitzer *et al.*, 1988a; Spreitzer *et al.*, 1992; Gotor *et al.*, 1994).

**Holoenzyme assembly**

Assembly of Rubisco is initiated by the folding of large-subunit monomers in an ATP-dependent process, which is mediated by the GroEL/GroES-type chaperonins (Goloubinoff *et al.*, 1989). For form-II Rubisco, the properly-folded large subunits will spontaneously dimerize to form active Rubisco upon release from the chaperonin cage (Goloubinoff *et al.*, 1989). For the hexadecameric form-I Rubisco, an additional chaperone, RbcX, is also involved (Saschenbrecker *et al.*, 2007). The RbcX chaperone binds to the carboxy-terminal tail of the Rubisco large subunit, and facilitates and stabilizes the formation of octameric large subunits after the GroEL/GroES-mediated step (Saschenbrecker *et al.*, 2007; Liu *et al.*, 2010). RbcX is then displaced from the Rubisco

large-subunit octamers by Rubisco small subunits (Liu *et al.*, 2010). In cyanobacteria, the RbcX gene is found in the same operon as the Rubisco large and small-subunit genes (Tabita, 1999) whereas, in plants, the RbcX gene is found in the nucleus (Kolesinski *et al.*, 2011).

**Reaction mechanism and active-site residues**

The carboxylation of RuBP by Rubisco involves five steps, which are enolization, carboxylation, hydration, C2-C3 bond scission, and stereospecific protonation (Fig. 3). The sequence of steps and the nature of the reaction intermediates were mainly deduced by radiolabeling and borohydride trapping experiments, and, more recently, by quantum-chemical modelling, whereas the positions and roles of the active-site residues were identified by chemical affinity labeling, site-directed mutagenesis, and crystal-structure analysis (Miziorko and Lorimer, 1983; Knight *et al*, 1990; Taylor and Andersson, 1997; Kannappan and Gready, 2008). The active sites are located in the interface regions between two large subunits that are assembled head-to-tail. The twenty active-site residues, which are Glu-60, Thr-65, Trp-66, Asn-123, Thr-173, Lys-175, Lys-177, Lys-201, Asp-203, Glu-204, His-294, Arg-295, His-327, Lys-334, Leu-335, Ser-379, Gly-380, Gly-381, Gly-403 and Gly-404, are mainly located in flexible loops in the Rubisco large-subunit. They form electrostatic interactions with the carboxylation transition-state analog CABP, as observed in x-ray crystal structures of CABP-bound Rubisco (Knight *et al.*, 1990; Taylor *et al.*, 2001). Active-site residues Glu-60, Thr-65, Trp-66 and Asn-123, which are from the amino-terminal domain of one large subunit, and the other active-site residues, which are from the carboxy-terminal domain of an adjacent large subunit, form

**Figure 3: Reaction mechanism for Rubisco-catalyzed carboxylation or oxygenation of ribulose 1,5-bisphosphate (Chen and Spreitzer, 1992; Andersson, 2008; Kannappan and Gready, 2008).** Carbon positions are indicated for the substrate ribulose bisphosphate. Reaction steps are in italics and bold.

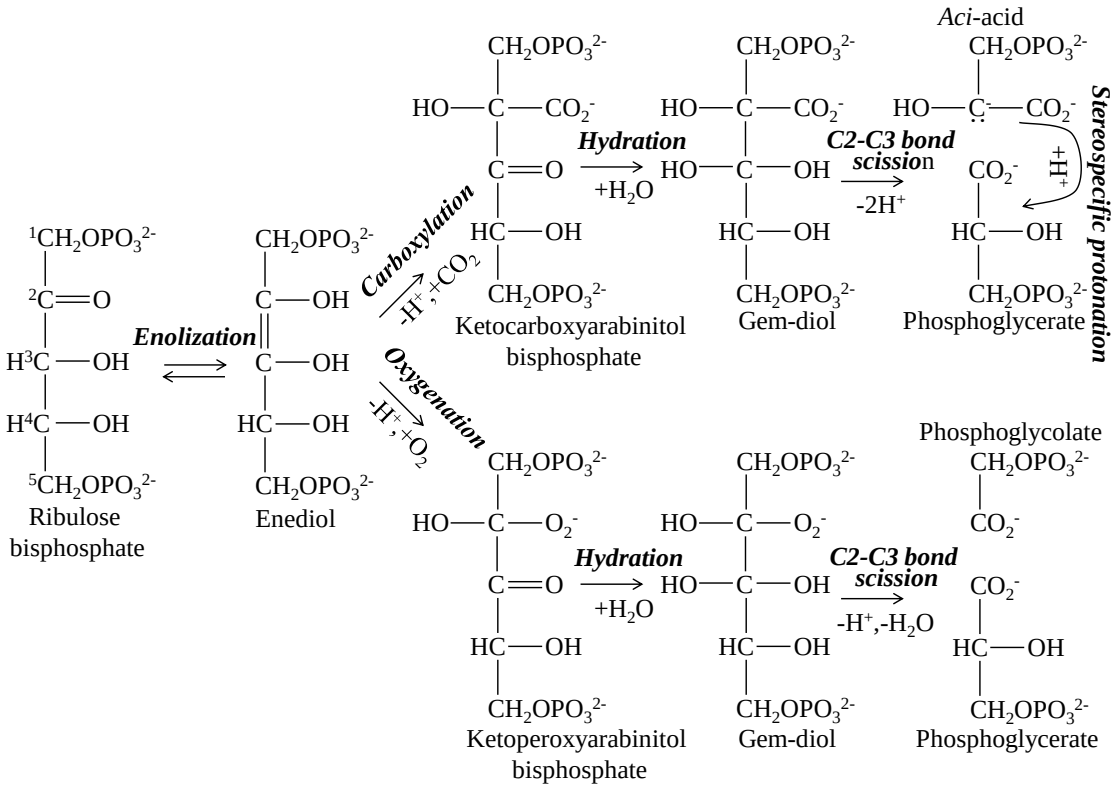
Ribulose bisphosphate
Enediol
Enolization
Carboxylation
Oxygenation
Ketocarboxyarabinitol bisphosphate
Ketoperoxyarabinitol bisphosphate
Hydration
Gem-diol
C2-C3 bond scission
Aci-acid
Stereospecific protonation
Phosphoglycerate
Phosphoglycolate

each active-site pocket. Thus, each dimer of large subunits has two active sites, and each hexadecameric holoenzyme has eight active sites (Knight *et al.*, 1990; Taylor *et al.*, 2001).

Before catalysis, Rubisco has to be activated by $CO_2$ through the carbamylation of Nε of Lys-201 (numbering based on form-I Rubisco). The activator $CO_2$ is distinct from the substrate $CO_2$ used for RuBP carboxylation. After Lys-201 carbamylation, which is reversible, $Mg^{2+}$ binds in the Rubisco active-site, stabilized by the negatively-charged carbamate (Lorimer, 1981). This is followed by RuBP binding to the active-site. If RuBP binds to the unactivated enzyme (i.e. before the carbamylation of Lys-201), a dead-end enzyme-substrate complex is formed that has to be opened by a protein known as Rubisco activase to release the unreacted RuBP (Salvucci *et al.*, 1985).

Lys-201 is essential for the first enolization step in Rubisco catalysis (Fig. 3). To initiate the enolization of RuBP, Lys-201 is carbamylated to enable the abstraction of a proton from the C-3 carbon of RuBP by the negatively-charged carbamate side-group. In addition to that, carbamylation of Lys-201 enables binding of $Mg^{2+}$ at the active site. Two other active-site residues, Asp-203 and Glu-204, also provide negatively-charged side-chains for coordination with the $Mg^{2+}$ cofactor (Gutteridge *et al.*, 1988). Lys-175 is also essential for enolization (Taylor and Andersson, 1997). Based on the atomic coordinates of Lys-175 in the x-ray crystal structures of Rubisco, the position of Lys-175 is close enough to reprotonate the oxygen carbonyl at the C-2 position of RuBP, concurrent with the deprotonation of the C-3 carbon by Lys-201 during enolization (Taylor and Andersson, 1997). Also, Lys-175 forms electrostatic interaction with another active-site residue, Asp-203, which in turn coordinates with the $Mg^{2+}$ cofactor.

The second step in Rubisco catalysis is carboxylation (or oxygenation) of the 2,3-enediol intermediate (Fig. 3). Lys-334 is essential for polarizing the substrate $CO_2$ to facilitate the nucleophilic addition of the gaseous substrate to the C-2 carbon of the enediol intermediate in the carboxylation step, or for polarizing $O_2$ in the corresponding oxygenation step (Gutteridge *et al.*, 1993). Changing Lys-334 to arginine, which would still retain the positive charge on position 334, reduces carboxylation almost completely, but does not affect oxygenation significantly (Gutteridge *et al.*, 1993).

The third and fourth step in Rubisco catalysis are hydration of the ketocarboxyarabinitol bisphosphate (or ketoperoxyarabinitol bisphosphate) intermediate to form a gem-diol, and C2-C3 bond scission of the gem-diol to form one substrate molecule of 3-PGA and one of an *aci*-acid intermediate (or, for oxygenation, 3-PGA and 2-PG) (Fig. 3). There is an additional fifth step in Rubisco catalysis for carboxylation, which is the stereospecific protonation of the three-carbon *aci*-acid intermediate to form another 3-PGA molecule, with Lys-175 as the proton donor (Fig. 3) (Harpel *et al.*, 2002; Kannappan and Gready, 2008). Engineered Rubisco enzymes with mutations at Lys-175 are deficient in the enolization of RuBP, and produce pyruvate instead of 3-PGA in the final stereospecific protonation step (Harpel *et al.*, 2002).

The precise roles of other active-site residues in Rubisco catalysis are less defined. For example, because the imidazole side-chain of His-294 is suitably positioned to either accept or donate a proton to the C-3 hydroxyl group of RuBP, His-294 could play a role in the gas addition, hydration, or C2-C3 bond scission steps (Kannappan and Gready, 2008). However, mutations of His-294 eliminate enolization of RuBP (Harpel *et al.*, 1998). Therefore, through electrostatic interactions, His-294 could also affect the

spatial position and the pKa of carbamate-Lys-201 that is directly responsible for enolization (Kannappan and Gready, 2008). There are other electrostatic interactions between the active-site residues that could affect the pKas of the interacting side chains, such as between Glu-60 and Lys-334, Thr-173 and Lys-201, and Lys-175 and Lys-177. Also, a number of active-site residues, which are Thr-65, Trp-66, Asn-123, Arg-295, His-327, Ser-379, Gly-380, Gly-381, Gly-403 and Gly-404, interact with the negatively-charged terminal phosphates of RuBP (Knight *et al.*, 1990).

**Structural rearrangements during catalysis**

The substrate-free Rubisco holoenzyme is in an initial "open" state whereby the catalytic loop 6 of the large subunit is retracted (Duff *et al.*, 2000). Thus, in the open state, the active site of Rubisco is exposed to solvent (Duff *et al.*, 2000). Substrates RuBP and $CO_2$, and the cofactor $Mg^{2+}$, can access the active site only in the open state (Schreuder *et al.*, 1993; Duff *et al.*, 2000).

Upon binding of substrate RuBP or any organophosphate inhibitor to the Rubisco active site, global conformational changes involving domain movements occur. First, catalytic loop 6 of Rubisco extends over the active site at the top of the large-subunit α/β-barrel. The Rubisco large-subunit carboxy terminus (from residue 462 onwards) folds over loop 6. The amino-terminal domain (residues 1-150) from an adjacent large subunit also rotates toward the carboxy-terminal domain to cover the top of the α/β-barrel, with a corresponding shift of the small subunit (Duff *et al.*, 2000). As a result, the active site of Rubisco is shielded from solvent, and the active-site residues from two adjacent large

subunits are also near enough to substrate RuBP to catalyze the reaction (Schreuder *et al.*, 1993; Duff *et al.*, 2000).

The solvent-occluded state of Rubisco is known as the "closed" state. Catalysis takes place during the closed state where there is less chance of the reaction intermediates being released prematurely or being misprotonated by external solvent (Schreuder *et al.*, 1993). Crystal structures of the closed state of Rubisco most often contain the carboxylation transition-state analog CABP, which is analogous to the ketocarboxyarabinitol-bisphosphate intermediate (Andersson and Backlund, 2008). Loop 6 and the carboxy-terminal tail are ordered in the closed state, but these structural elements are disordered in the open state. The conformational stabilization of loop 6 and the carboxy terminus in the closed state occurs because of interactions between loop 6, RuBP, reaction intermediates, the carboxy terminus, and residues from an adjacent large subunit. Specifically, Lys-334 in loop 6 forms electrostatic interactions with a terminal phosphate of RuBP, the carboxylate group in the ketocarboxyarabinitol bisphosphate intermediate, and also Glu-60 and Thr-65 from an adjacent large subunit. Glu-338 in loop 6 also interacts with Asp-473 in the carboxy-terminal tail of Rubisco (Schreuder *et al.*, 1993; Duff *et al.*, 2000). Mutations of Asp-473 produce functional Rubisco, but caused the carboxy terminus to be disordered in the crystal structures (Satagopan and Spreitzer, 2004; Karkehabadi *et al.*, 2007).

The closed state of Rubisco becomes open only when the six-carbon ketocarboxyarabinitol-bisphosphate intermediate of RuBP is converted into two three-carbon 3-PGA carboxylation products or into the single three-carbon 3-PGA and two-carbon 2-PG oxygenation products within the active site. Duff *et al.* (2000) proposed that

the shift from a closed-state Rubisco to an open state is caused by the increased distance between the terminal phosphates after scission of the six-carbon ketocarboxyarabinitol bisphosphate, but this was disproved by subsequent mutagenesis experiments involving the carboxy terminus (Satagopan and Spreitzer, 2004).

## DISSECTION OF RUBISCO

### Random mutant screening and genetic selection

Early genetic studies of Rubisco were focused on attempts to select a better enzyme (Somerville and Ogren, 1982; Spreitzer *et al.*, 1982). However, no Rubisco mutants were recovered by screening or selection in *Arabidopsis* (Somerville and Ogren, 1982). In contrast, screening of *Chlamydomonas* for mutants that were photosynthesis-deficient yielded the first Rubisco large-subunit mutant, which has a Gly-171-to-Asp (G171D) substitution (Spreitzer and Mets, 1980; Dron *et al.*, 1983). The G171D substitution eliminates the activity of the holoenzyme without affecting structural stability (Spreitzer and Mets, 1980). A multitude of other mutations in *Chlamydomonas* Rubisco that negatively affect holoenzyme activity and/or stability were isolated using this prolific screen (Spreitzer, 1993). Mutants T173I and G237S lacked Rubisco activity, whereas G54D and R217S lacked the holoenzyme (Spreitzer *et al.*, 1988b; Spreitzer, 1993; Thow *et al.*, 1994). Several mutants with nonsense mutations at amino-acid positions 45, 66, and 451 were also isolated through this screen (Spreitzer and Chastain, 1987). However, unlike the other *Chlamydomonas* Rubisco mutants discovered by random mutant screening, mutants V331A and L290F, had measurable but decreased carboxylase activity and Ω (Chen *et al.*, 1988; Chen and Spreitzer, 1989). Rubisco-

mutant V331A was isolated by screening for photosynthesis-deficient mutants, but L290F was isolated by screening for mutants that were photosynthesis-deficient only at elevated temperature (Chen *et al.*, 1988; Chen and Spreitzer, 1989).

The *Chlamydomonas* missense mutations are distributed in four regions of the Rubisco large subunit. The first region, highlighted by the G54D mutation, is in the amino-terminal domain near the loop containing active-site residues Glu-60, Thr-65, and Trp-66 (Spreitzer *et al.*, 1995). The second region, highlighted by the R217S and G237S mutations, is near the active-site residue Lys-201 that has to be activated for catalysis (Thow *et al.*, 1994). The third region, highlighted by the V331A mutation, is near catalytic loop 6 (Chen and Spreitzer, 1989). Finally, the fourth region, highlighted by the L290F mutation, is at the bottom of the large-subunit α/β-barrel (Chen *et al.*, 1988). Unlike the other three regions, which are in close proximity to the Rubisco active-site, the region at the bottom of the barrel is 20 Å from the active-site, thus providing the first indication that residues far from the active site could affect catalysis (Du and Spreitzer, 2000).

Reversion experiments were carried out on the photosynthesis-deficient Rubisco mutants by subjecting the mutant cells to photosynthetic selection (Spreitzer *et al.*, 1982). The basis for the reversion experiments was that suppressor mutations in the Rubisco primary-structure would be isolated if these suppressor residues complement and interact with the original mutated residue to restore Rubisco function *in vivo* (Spreitzer *et al.*, 1985). From the reversion experiments, it was discovered that the V331A substitution, which is at the amino-terminal end of loop 6 is complemented by suppressor mutations T342I and G344S, which are on the carboxy-terminal end of the loop (Chen and

Spreitzer, 1989; Chen *et al*., 1991). On the other hand, mutation R217S, which affects Rubisco assembly, is complemented by A242V, and, because both the mutation and suppressor residues are within the hydrophobic wall of the α/β-barrel, the residues could influence the structure of the barrel (Thow *et al.*, 1994). Another significant result from the reversion experiments is that Rubisco large-subunit mutation L290F, which causes a decrease in Ω, can be complemented by A222T and V262L suppressor substitutions in the large subunit as well as by N54S, A57V, and C65S substitutions in the small subunit, indicating that the small subunit can affect Ω through interactions with the large subunit (Hong and Spreitzer, 1997; Du and Spreitzer, 2000; Du *et al.*, 2000; Genkov *et al.*, 2006). Unlike the other Rubisco mutations, G54D within the hydrophobic core of the amino-terminal domain cannot be complemented by other suppressor-residue substitutions. Instead, the mutated residue can pseudorevert to alanine or valine, which are non-polar residues, signifying the role of residue 54 in retaining the hydrophobicity of the structural core (Spreitzer *et al*., 1995).

Screening for photosynthesis-deficient *Chlamydomonas* mutants also found other non-Rubisco nuclear-gene mutations that could reduce the mRNA level and posttranslationally affect the kinetic properties of Rubisco (Spreitzer *et al.*, 1988a; Gotor *et al.*, 1994; Hong and Spreitzer, 1994). The mutated proteins likely play a role in Rubisco transcription and posttranslational modification, but, as of yet, only one of the mutations has been identified, and found to have occurred in an mRNA-stabilizing protein that has orthologs in plants (Johnson *et al.*, 2010).

**Directed mutagenesis**

Site-directed mutagenesis studies of Rubisco active-site residues have been extensively carried out on prokaryotic Rubisco from *R. rubrum* and *Synechococcus*, but the prokaryotic enzymes were expressed only in *Escherichia coli* for study (Hartman and Harpel, 1994; Gutteridge *et al.*, 1993; Harpel *et al.*, 2002). Eukaryotic Rubisco cannot be expressed in *E. coli*, and the reason for that is still unclear (Cloney *et al.*, 1993). Mutations of the prokaryotic Rubisco active-site residues eliminate activity, which indicates that the active-site residues are immutable for proper function, consistent with the fact that these residues are almost 100% conserved among species (Hartman and Harpel, 1994). Similarly, mutating the active-site residues of eukaryotic Rubisco in *Chlamydomonas* decreases the carboxylase activity to less than 5% and Ω to less than 30% of the wild type value, and eliminates photosynthetic growth of the organism (Zhu and Spreitzer, 1994).

Directed mutagenesis of non-active-site residues, guided by phylogenetic data, has also been pursued to understand the structure-function relationships of Rubisco. Certain stretches of Rubisco amino-acid sequences were changed from one species to that of another, with the expectation of a corresponding shift in kinetic properties. The non-active-site residues in and around loop 6 were one of the earlier targets for these directed-mutagenesis experiments because earlier mutant screening in *Chlamydomonas* found that changes in the region, specifically V331A, could modify Ω (Chen and Spreitzer, 1989). A stretch of four amino acids, from residue 338 to 341, at the carboxy-terminal end of loop 6, was changed in Rubisco of the cyanobacterium *Synechococcus* to the sequence found in plants, but did not cause any alterations in kinetic properties, even though the

plant Rubisco should have higher Ω and lower $V_c$ (Gutteridge *et al.*, 1993). On the other hand, mutating residues that flank loop 6 in *Chlamydomonas* Rubisco to that of plants decreased Ω and $V_c$ (Zhu and Spreitzer, 1996). Creating the suppressor substitutions of V331A in *Chlamydomonas* Rubisco, which are T342I and G344S, alone decreased Ω and $V_c$, even though these substitutions improve the catalytic properties of the previous V331A mutant enzyme (Karkehabadi *et al.*, 2007). Therefore, residue engineering in the region around loop 6 does not improve the net $CO_2$ fixation of the enzyme, but, instead, is deleterious to catalysis.

Because substitutions in the amino-terminal domain of the Rubisco large subunit affect both Ω and enzyme stability, evidenced by the G54D Rubisco-deficient *Clamydomonas* mutant and the pseudorevertant G54V, which has a 17% decrease in Ω, a couple of variable non-active-site residues in the region were targeted for directed-mutagenesis studies (Spreitzer *et al.*, 1995; Du *et al.*, 2003). Met-42 and Cys-53 were changed singly or as a pair to the Val-42 and Ala-53 residues of plants, but the mutant enzymes had no significant changes in catalysis (Du *et al.*, 2003). Thus, residue differences in the amino-terminal domain alone cannot account for the differences in Rubisco kinetic properties among species.

Because of the phylogenetic diversity in the Rubisco large-subunit carboxy-terminus, which folds over loop 6 during catalysis, site-directed mutagenesis experiments of this region have been pursued extensively (Gutteridge *et al.*, 1993; Zhu *et al.*, 1998; Satagopan and Spreitzer, 2008). When the carboxy terminus, residues 470-475, of the *Chlamydomonas* large subunit was substituted with the residues from spinach, there was an increase in Ω by 10%, but a decrease in carboxylation catalytic efficiency (Satagopan

and Spreitzer, 2008). On the other hand, no significant increase in Ω was measured when the carboxy terminus of *Synechococcus* Rubisco was changed to that of plants (Gutteridge *et al.*, 1993). Also, because red-algal Rubisco has 10 additional residues at the carboxy terminus and higher Ω when compared to *Synechococcus* Rubisco, the extra residues were engineered into the *Synechococcus* enzyme, but did not cause a marked increase in Ω (Zhu *et al.*, 1998). Truncations of the carboxy-terminal region of the *Synechococcus* and *R. rubrum* enzymes eliminate enzymatic activity, and for the *R. rubrum* Rubisco, also alter the quarternary structure of the holoenzyme (Ranty *et al.*, 1990; Gutteridge *et al.*, 1993). Thus, the carboxy terminus most likely plays a role in Rubisco catalysis, possibly through interactions with loop 6, which is also evidenced by the fact that mutations of Asp-473, a latch residue that holds the carboxy terminus over loop 6, decrease Ω (Duff *et al.*, 2000; Satagopan and Spreitzer, 2004; Karkehabadi *et al.*, 2007).

Directed mutagenesis experiments of Rubisco should also consider the interactions between Rubisco and Rubisco activase (Spreitzer and Salvucci, 2002). Activase from Solanaceae species (e.g. tobacco) will not activate Rubisco from non-Solanaceae species (e.g. *Chlamydomonas* and spinach), and *vice versa* (Wang *et al.*, 1992). In fact, substitutions P89R and D94K in the *Chlamydomonas* Rubisco large subunit produced enzymes that could be activated by activase from tobacco but not spinach, effectively switching the activase-recognition site from that of non-Solanaceae to Solanaceae (Larson *et al.*, 1997; Ott *et al.*, 2000). Because changes in other residues around this region may also affect activase interaction with Rubisco, future experiments should keep that possibility in mind.

***The penta/ABSO mutant and the large/small-subunit interface***

Another region of the Rubisco holoenzyme analyzed by site-directed mutagenesis experiments is the interface between the large and small subunit, at the bottom of the α/β barrel, which is on the opposite end from the active site (Du and Spreitzer, 2000; Spreitzer *et al.*, 2005; Genkov *et al.*, 2006). The large/small-subunit interface region became of interest when it was discovered that an L290F mutation in the region is the cause for photosynthesis deficiency at elevated temperatures in a *Chlamydomonas* mutant (Chen *et al.*, 1988; Spreitzer *et al.*, 1988a). Further reversion experiments and site-directed mutagenesis studies indicated that the region affects both catalysis and stability of Rubisco (Chen *et al.*, 1988; Hong and Spreitzer, 1997; Du *et al.*, 2000; Du and Spreitzer, 2000; Genkov *et al.*, 2006). More importantly, a phylogenetic *Chlamydomonas*-to-plant substitution involving five residues of the Rubisco large-subunit, V221C/V235I/C256F/K258R/I265V, together with changing the small-subunit loop between β-strands A and B to that of spinach (*Spinacia oleracea*) (ABSO), all at the interface region, produces a Rubisco mutant in *Chlamydomonas*, named "penta/ABSO", with kinetic properties shifted towards the plant Rubisco properties, marked by an increase in Ω and decrease in $V_c$ (Table 1) (Spreitzer *et al.*, 2005).

***Hybrid enzymes***

A more elaborate directed-engineering approach for studying Rubisco structure-function relationships is swapping the whole large or small subunit of Rubisco from different species, which have different catalytic properties (Table 1) (Jordan and Ogren, 1981b; Read and Tabita, 1992; Kanevski *et al.*, 1999; Whitney *et al.*, 2001, 2011;

Genkov *et al.*, 2010). However, a limitation to swapping the whole subunit is that prokaryotic Rubisco large subunits cannot be expressed in eukaryotes and *vice versa*, with the exception of the prokaryotic *R. rubrum* Rubisco, which can be expressed in tobacco plants, but the transgenic plants require elevated $CO_2$ (5% v/v in air) for growth (Cloney *et al.*, 1993; Whitney and Andrews, 2001). Even transgenic tobacco plants that express the sunflower or *Flaveria* Rubisco large subunits produce less than 50% of wild-type holoenzyme level, and mainly require elevated $CO_2$ or sucrose supplementation for growth (Kanevski *et al.*, 1999; Whitney *et al.*, 2011). Moreover, even though the Rubisco small subunit is not hindered by the eukaryotic/prokaryotic-expression barrier, plant Rubisco small subunits are encoded by a family of nuclear genes (Spreitzer *et al.*, 2003). Thus, the native small subunits are still present in experiments where transgenic plants were transformed with foreign small subunits, which complicates the analysis of the experiments (Read and Tabita, 1992; Getzoff *et al.*, 1998; Ishikawa *et al.*, 2011). On the other hand, all the native Rubisco small-subunit genes in *Chlamydomonas* have been successfully knocked out and replaced by the foreign small-subunit genes from *Arabidopsis*, spinach, and sunflower, and the mutant Rubisco enzymes have increases in Ω by 3-11% (Genkov *et al.*, 2010). When the cyanobacterial *Synechococcus* Rubisco small subunit was replaced with that from marine algae, an increase in Ω was also observed (Read and Tabita, 1992). Thus, even though the active-site region is located in the Rubisco large subunit, the small subunit also influences catalysis (Read and Tabita, 1992; Karkehabadi *et al.*, 2005; Spreitzer *et al.*, 2005; Genkov *et al.*, 2010).

**Directed evolution**

The first directed-evolution experiment that specifically targeted the Rubisco genes was performed in the photosynthetic bacteria *Rhodobacter capsulatus* using a library of cyanobacterial *Synechococcus* Rubisco large and small-subunit genes that were mutagenized in the *E. coli* mutator-strain XL-1 Red (Smith and Tabita, 2003). Because the *R. capsulatus* mutant depends on *Synechococcus* Rubisco for photosynthetic growth at elevated $CO_2$ (5%), any *Synechococcus* Rubisco mutant enzyme that enabled the *R. capsulatus* strain to grow at lower $CO_2$ (1.5%) should harbor positive mutations that increased $CO_2$ fixation of the enzyme *in vivo* (Smith and Tabita, 2003). Instead of changes in kinetic properties with regard to $CO_2$ fixation, the positive Rubisco mutants had increased affinity for the substrate RuBP (Smith and Tabita, 2003). In other Rubisco selection experiments, Rubisco-dependent *E. coli* strains were engineered by expressing the enzyme phosphoribulose kinase, which diverted carbon to RuBP (Parikh *et al.*, 2006; Mueller-Cajar *et al.*, 2007; Mueller-Cajar and Whitney, 2008). Rubisco libraries created by PCR-based mutagenesis were transformed into the Rubisco-dependent *E. coli*, and the fastest-growing colonies were picked for analysis (Parikh *et al.*, 2006; Mueller-Cajar *et al.*, 2007; Mueller-Cajar and Whitney, 2008). Similar to the *R. capsulatus* selection system, the *E. coli* Rubisco selection system selected for enzymes with improved expression and RuBP affinity, but not catalysis (Parikh *et al.*, 2006; Mueller-Cajar *et al.*, 2007; Mueller-Cajar and Whitney, 2008). On the other hand, improvements in $\Omega$ and $V_c$ of Rubisco by 20% and 50%, respectively, were reported after screening 60,000 *Chlamydomonas* transformants that were transformed with a library of gene-shuffled Rubisco variants, but the residue-substitutions were not included in the report (Zhu *et al.*,

2005). Therefore, selection strategies with Rubisco have yet to produce a better plant enzyme.

### *Chlamydomonas reinhardtii* as a model organism

The most well-developed and expedient genetic system for study of eukaryotic Rubisco is the green alga *Chlamydomonas*, with the goal of eventually transferring any identified improvements into crops (Spreitzer, 1998). Unlike plants, which are obligate photoautotrophs, *Chlamydomonas* can grow heterotrophically when supplemented with acetate as an alternate carbon source, thus allowing expression and analysis of defective Rubisco mutants (Spreitzer and Mets, 1980, 1981). More importantly, the Rubisco large and small-subunit genes have been knocked out in *Chlamydomonas* to create hosts for transformation with genetically-engineered Rubisco genes (Spreitzer and Mets, 1980; Newman *et al.*, 1991; Khrebtukova and Spreitzer, 1996; Dent *et al.*, 2005; Zhu *et al.*, 2005). Chloroplast and nuclear transformation of the Rubisco large and small-subunit genes, respectively, have been routinely carried out for *Chlamydomonas* (Zhu and Spreitzer, 1994, 1996; Satagopan and Spreitzer, 2004; Genkov *et al.*, 2006). Even though genetic studies of eukaryotic Rubisco have also been carried out in tobacco, there are several drawbacks to the tobacco system. There is a need to use a co-transformation system with a selectable antibiotic-resistance marker instead of direct selection for photoautotrophy, an inability to fully replace the family of native Rubisco small-subunit genes, and a longer transformation time of three weeks (Svab and Maliga, 1993; Whitney and Andrews, 2001). Also, more Rubisco mutants can be screened or selected for in

*Chlamydomonas* compared to plants (Spreitzer and Mets, 1980; Somerville and Ogren, 1982).

Mating of *Chlamydomonas* mutants is also an available tool to combine several non-allelic mutations into a single strain. Tetrad analysis can be done to determine genetic linkage, and, through the inheritance pattern, the organelle-localization of the mutations (Spreitzer and Mets, 1980; Hong and Spreitzer, 1994).

The wealth of bioinformatics resources also benefits *Chlamydomonas* Rubisco research. The availability of both the chloroplast and nuclear-genome sequences facilitates genetic analysis and engineering of mutants (Maul *et al.*, 2002; Merchant *et al.*, 2007). In addition, the availability of over ten x-ray crystal-structures of separate *Chlamydomonas* mutant Rubisco enzymes provides extensive data for structural studies (Andersson and Backlund, 2008).

**Bioinformatics analysis**

With the increased abundance of *rbcL* sequences, more elaborate and intricate computational phylogenetic analysis can be undertaken to define catalysis-influencing residue changes within the Rubisco large subunit. One of the studies, which coupled phylogenetic and crystal structure data, forms the basis for the present study and for the engineering of the penta/ABSO mutant (Du *et al.*, 2003; Spreitzer *et al.*, 2005).

In a recent phylogenetic analysis, Kapralov *et al.* (2011) sought to determine the residues that could be responsible for the differences in kinetic properties between Rubisco enzymes from the C3 and C4 species within the *Flaveria* genus. Changes in large-subunit residues 149 and 309 correlate with changes in Rubisco kinetic properties,

though large-subunit residue 265 and small-subunit residues 20, 24 and 57 are also changed in different *Flaveria* species (Kapralov *et al.*, 2011). To test the importance of residues 149 and 309, Whitney *et al.* (2011) expressed the *Flaveria rbcL* gene in tobacco, and changed residues 149 and 309 separately to that of either the C3 or C4 species, and found that only residue 309 is responsible for the switch in the kinetic properties.

However, most of the other phylogenetic studies of Rubisco did not necessarily focus on evolutionary forces acting on the kinetic properties of Rubisco (Nozaki *et al.*, 2002; Yu *et al.*, 2005; Kapralov and Filatov, 2006, 2007). Instead, the positively-selected residues from these studies could play a role in Rubisco stability, or interaction with activase or other molecules. For example, Nozaki *et al.* (2002) sought to determine the large-subunit residues that could explain the presence or absence of the pyrenoid within the green algal *Chloromonas* lineage. Kapralov and Filatov (2006) sought to determine the residues that could facilitate the environmental adaptation of the Hawaiian-plant genus *Schiedea* between rainforest and dry coastal cliffs. Yu *et al.* (2005) sought to determine the clusters of surface residues that differentiate green plants, cyanobacteria and non-green algae Rubiscos. Additional bioinformatics-based, site-directed mutagenesis and biochemical analysis of Rubisco is required.

## RATIONALE AND OBJECTIVES

The structural basis for the differences in kinetic properties between Rubisco from diverse species has yet to be elucidated (Spreitzer, 1993, 1999; Spreitzer and Salvucci, 2002). Understanding the structure-function relationship of Rubisco would allow future engineering of the holoenzyme for improved photosynthesis in crops (Spreitzer and

Salvucci, 2002). In other words, defining the structural regions or residues in Rubisco to be targeted for engineering is crucial.

The active-site residues are almost 100% conserved among the ~2500 Rubisco large-subunit sequences in the NCBI Entrez Proteins database. Moreover, crystal-structure data indicate that all Rubisco holoenzymes adopt similar tertiary folds (Andersson and Backlund, 2008). Therefore, differences in the non-active-site residues of Rubisco, which cause subtle structural changes, must account for the differences in kinetic properties, and, because the small subunit is too divergent, it is reasonable to focus on differences within only the large subunit. Moreover, the catalytic subunit of Rubisco is the large subunit (Knight *et al.*, 1990).

Because site-directed mutagenesis and transformation of Rubisco in *Chlamydomonas* is well-established, and the crystal structures of various mutant forms of *Chlamydomonas* Rubisco have been solved, including the highest-resolution structure, *Chlamydomonas* has been extensively used for structure-function and genetic-engineering studies (Zhu and Spreitzer, 1994, 1996; Taylor *et al.*, 2001; Andersson and Backlund, 2008). The kinetic properties of *Chlamydomonas* Rubisco are different from plants, but most strikingly, for *Chlamydomonas* Rubisco, $\Omega \approx 60$, whereas for plants, $\Omega \approx$ 80-100 (Jordan and Ogren, 1981b; Genkov *et al.*, 2010). Therefore, knowing the phylogenetic-residue changes responsible for the differences in kinetic properties between *Chlamydomonas* and plant Rubiscos could be important for defining genetic-engineering targets.

Even though the phylogenetic residues changed in the penta/ABSO enzyme are suitable targets for genetic engineering, there are other diverse residues within the large

subunit that may also influence catalysis. Therefore, a global subunit-wide inquiry, that would encompass all the other phylogenetically-diverse residues of the Rubisco large subunit, might identify other residues that contribute to phylogenetic differences in catalysis. This is the first global structure-function study of the Rubisco large subunit by directed mutagenesis. The only other Rubisco study to attempt such a broad scope focused on substituting only conserved glycine residues with alanines and prolines (Cheng and McFadden, 1998).

# MATERIALS AND METHODS

## MATERIALS

### Molecular biology

DNA-miniprep kits for plasmid purification and gel-extraction kits for agarose-gel-embedded DNA-fragment purification were purchased from Qiagen. Restriction endonucleases and T4 DNA ligase for plasmid recombination were from New England Biolabs. *Taq* DNA polymerase was from Invitrogen. *Pfu* Turbo DNA Polymerase and the Quikchange Mutagenesis Kit for site-directed mutagenesis were from Stratagene. Oligonucleotides for site-directed mutagenesis and for sequencing were from Sigma-Aldrich. Tungsten (M-10, 0.7 μm) for chloroplast transformation was from Biorad Laboratories.

### Biochemistry

Most reagents, including 2-phosphoglycolate (tri(monocyclohexylammonium) salt) (2-PG), 3-phosphoglycerate (sodium salt) (3-PGA), and ribulose 1,5-bisphosphate (sodium salt hydrate) (RuBP), and enzymes for synthesis of D-[1-$^{3}$H]ribulose 1,5-bisphosphate ([1-$^{3}$H]RuBP), which are hexokinase, glucose 6-phosphate dehydrogenase, 6-phosphogluconate dehydrogenase, phosphoribulokinase and pyruvate kinase, were purchased from Sigma-Aldrich. $NaH^{14}CO_3$ was from ViTrax. D-[2-$^{3}$H]glucose was from Amersham Bioscience.

**STRAINS AND CULTURE CONDITIONS**

*Chlamydomonas reinhardtii* 2137 *mt+* was used as the wild-type strain (Spreitzer and Mets, 1981) and, in most cases, MX3312 *mt+* was used as the host for chloroplast transformation with mutant *rbcL* genes (Satagopan and Spreitzer, 2004; Zhu *et al.*, 2005). *Chlamydomonas* MX3312 has the chloroplast 1428-bp *rbcL* gene replaced by the 786-bp bacterial *aadA* gene, which confers spectinomycin resistance (Hollingshead and Vapnek, 1985). Except for the photosynthesis-deficient, acetate-requiring phenotype, the MX3312 strain is indistinguishable from wild type because the *rbcL* gene knock-out was created in *Chlamydomonas* 2137 *mt+* through homologous recombination, preserving the *rbcL* 5' and 3' flanking sequences (Satagopan and Spreitzer, 2004; Zhu *et al.*, 2005). For co-expression of engineered large subunits with the small-subunit βA-βB loop from spinach (*Spinacia oleracea*), the *rbcL*Δ/ABSO transformation host was used, which was created by replacing the *rbcL* gene of *Chlamydomonas* penta/ABSO with the *aadA* gene (Spreitzer *et al.*, 2005; Genkov and Spreitzer, unpublished). For co-expression of mutant large subunits with the entire small subunit from *Arabidopsis,* the *rbcL*Δ/SSAT transformation host was used, which was created by replacing the *rbcL* gene with the *aadA* gene in a cell-walled SSAT strain (Genkov *et al.*, 2010; Genkov and Spreitzer, unpublished). All strains were maintained in the dark at 25°C on medium containing 10 mM acetate solidified with 1.5% Difco Bacto-Agar (Spreitzer and Mets, 1981).

Electrocompetent *Escherichia coli* XL-1 Blue was used for propagating plasmid DNA (Stratagene). XL-1 Blue was prepared for electrocompetence in Biorad's Gene Pulser Xcell system (Miller and Nickoloff, 1995). Briefly, a starter culture of cells was grown overnight at 37ºC in 5 mL of LB medium with 10 µg/mL tetracycline, shaking at

280 RPM. The starter culture was then poured into 500 mL of LB medium, and the new culture was grown until the OD was between 0.4-0.7, which took about 4 hr. The cells were pelleted and washed twice with 10% ice-cold glycerol, and finally resuspended in 2 mL of 10% ice-cold glycerol. Aliquots of cells (50 µL) were stored at -80ºC for at least 6 months.

## MOLECULAR-BIOLOGY METHODS

### Site-directed mutagenesis and mutant-plasmid construction

Site-directed mutagenesis was performed using the Quikchange Mutagenesis Kit (Papworth *et al.*, 1996). A 25-µL PCR reaction mix was made consisting of 1.25 U *Pfu* Turbo DNA Polymerase, 1X *Pfu* Turbo buffer (20 mM, Tris-HCl, pH 8.8, 10 mM KCl, 10 mM $(NH_4)_2SO_4$, 2 mM $MgSO_4$, 1.0% Triton X-100 and 1 mg/mL BSA), 25 ng of template DNA, 62.5 ng each of a pair of complementary 30-40 bp primers, which contain the desired base changes, and 0.4 mM of each dNTP. The mix was heated to 95ºC for 30 sec, followed by 18 cycles of 95ºC for 30 sec, 55ºC for 1 min, and 68ºC for 6 min. Then, 5 U of restriction-endonuclease *Dpn*I was added to the PCR mix and incubated at 37ºC for 1 hr to fully digest the template DNA. Finally, 1 µL of the reaction mix was electroporated into *E. coli* XL-1 Blue, and transformants were selected on LB medium containing 100 µg/mL ampicillin at 37ºC overnight. *E. coli* colonies were inoculated into 7 mL of liquid LB medium for DNA miniprep using the Qiagen kit, which is based on the alkaline lysis procedure (Birnboim and Doly, 1979), and mutant plasmids were screened by restriction-enzyme digestion.

The template DNA used for site-directed mutagenesis is the pLS-H plasmid,

which consists of a 2670-bp *Hpa*I fragment of *Chlamydomonas* chloroplast DNA, including the Rubisco *rbcL* gene, cloned into the *Sma*I site of the pUC19 plasmid (Yanisch-Perron *et al.*, 1985; Du and Spreitzer, 2000). Codon changes were strictly limited to only those codons commonly used in *rbcL*, and, when possible, introduced or removed a restriction site for ease of mutant-plasmid screening. In certain cases, a silent mutation was introduced at a second site, to alter the restriction pattern for mutant screening. Mutations were combined by restriction-enzyme digestion and ligation.

**Chloroplast transformation**

Chloroplast transformation was performed using a particle-inflow gun (Finer *et al.*, 1992; Zhu and Spreitzer, 1994, 1996). Strains MX3312, *rbcL*Δ/ABSO, or *rbcL*Δ/SSAT were grown in 50 mL of liquid acetate medium in the dark at 25ºC on a rotary shaker at 220 RPM until they reached the late-log phase of growth (~2.5 X $10^6$ cells/mL). The cells were pelleted, resuspended at a concentration of 2.5 X $10^8$ cells/mL in liquid minimal medium (without acetate), and 0.5 X $10^7$ cells were plated on solid acetate medium. When the plates were dry, the cells were bombarded with DNA-coated tungsten. The tungsten particles were coated with DNA by mixing 2.5 µg of plasmid, 25 µL of tungsten (60 mg/mL in $H_2O$), 25 µL of 2.5 M $CaCl_2$ and 10 µL of 0.1 M spermidine (free base). The tungsten-DNA suspension was allowed to sediment at room temperature for 30 min. Forty microliters of the supernatant was removed, and the tungsten-DNA sediment was resuspended in the remaining liquid and loaded for bombardment, which was performed at a vacuum of 28 inches Hg and helium pressure of 70 PSI (Boynton *et al.*, 1988; Boynton and Gillham, 1993; Finer *et al.*, 1992).

To select for photosynthetic *Chlamydomonas* transformants, cells were scraped off the plate and replated on six minimal-medium plates, which were incubated at 25°C under 80 microeinsteins/$m^2$/s fluorescent lamps. The *Chlamydomonas* SSAT strain required 5% $CO_2$ for growth. For the other *Chlamydomonas* strains, incubation at 5% $CO_2$ reduced transformation time to 6 days, from 2-4 weeks, before colonies were visible. Transformant colonies were picked and maintained on acetate medium in darkness. Because there are multiple copies of the chloroplast genome, all transformants were cloned to homoplasmicity by plating on acetate medium to obtain single colonies and then by replica-plating on minimal medium to screen for photosynthetic growth. Cells were usually homoplasmic after three cloning cycles, which was confirmed by PCR.

**DNA extraction from *Chlamydomonas***

Extraction of DNA from *Chlamydomnas* was carried out according to a previously-established protocol with slight modifications (Newman *et al.*, 1990). Briefly, a whole 100-mm acetate-medium plate of fresh *Chlamydomonas* cells, which had been growing for less than a week, was scraped and resuspended in 0.5 mL of 150 mM NaCl, 10 mM EDTA and 10 mM Tris-HCl, pH 8.0. Cells were pelleted by spinning at 14,000 RPM for 10 sec, and the supernatant was discarded. The pelleted cells were then completely lysed by vortexing in 0.45 mL of 1.3% SDS, 250 mM NaCl, 25 mM EDTA, and 66 mM Tris-HCl, pH 8.0. The cell lysate was phenol/chloroform extracted with 350 µL of 1:1 phenol:chloroform three times, keeping the aqueous layer each time. DNA from the final clear, aqueous solution was precipitated with 800 µL of 100% ethanol at -20ºC overnight, washed with 200 µL of 70% ethanol, and dissolved in 40 µL of $H_2O$.

**PCR and sequencing of the *Chlamydomonas rbcL* gene**

PCR was carried out in a 100-µL reaction mix consisting of 5 µL of genomic DNA, 2.5 U *Taq* DNA polymerase, 20 mM Tris-HCl, pH 8.4, 50 mM KCl, 0.2 mM of each dNTP, 3 mM of $MgCl_2$, and 0.5 µM each of a pair of primers flanking the *rbcL* gene (5'-GTAAGACGACCGACATATACCTAAAGGCC-3' and 5'-CGCACTCTACCGATT GAGTTACATCCGC-3'). The PCR steps were 94°C initial denaturation for 3 min, followed by 30 cycles of 94°C for 1 min, 56ºC for 2 min, and 72ºC for 2 min. A final 72°C extension was performed for 10 min. The 1907-bp PCR product was run on a 1% agarose TAE gel, purified with a Qiagen Gel Extraction kit, and sequenced by Eurofins MWG Operon or the University of Nebraska DNA sequencing facility.

**BIOCHEMICAL-ANALYSIS METHODS**

**Protein extraction and Rubisco purification from *Chlamydomonas* (Spreitzer and Chastain, 1987)**

*Chlamydomonas* for protein extraction was grown in 250-500 mL of acetate medium in the dark at 25°C on a rotary shaker at 220 RPM until late-log phase of growth (~2.5 X $10^6$ cells/ml). Cells were pelleted by centrifuging at 1,500 g at 4ºC, washed once with 4ºC $H_2O$, pelleted again, resuspended in 1.5 mL of ice-cold extraction buffer (2 mM DTT, 50 mM Bicine-NaOH, pH 8.0, 10 mM $MgCl_2$, 10 mM $NaHCO_3$), and sonicated for 3 min in an ice bath with 30-sec pulses. Sonicated cells were centrifuged at 30,000 g for 15 min at 4ºC to sediment the cell debris, and the supernatant containing total soluble protein was transferred to a new 4ºC pre-chilled microfuge tube and kept on ice. Protein

concentration was determined with the Coomassie Brilliant Blue binding assay with BSA as the standard (Bradford, 1976). Proteins were kept at -80ºC.

To further purify Rubisco from the soluble cell protein, 1 mL of the protein solution was separated in a linear 10% to 30% 12-mL sucrose gradient (2 mM DTT, 50 mM Bicine-NaOH, pH 8.0, 10 mM $MgCl_2$, 10 mM $NaHCO_3$) at 37,000 RPM for 20 hr at 4°C using a SW40 Ti swinging-bucket rotor (Beckman Coulter). The protein gradient was fractionated with a Model 185 density-gradient fractionator (ISCO, Inc.) while scanning at 280 nm with a UA-5 absorbance/fluorescence monitor (ISCO, Inc.). The hexadecameric-Rubisco fraction, which forms a distinct peak, was collected. Rubisco was dialyzed overnight at 4°C in 2 mM DTT, 50 mM Bicine-NaOH, pH 8.0, 10 mM $MgCl_2$, and 10 mM $NaHCO_3$ (or 2 mM $NaHCO_3$ for enzyme assays), to remove the sucrose, and re-concentrated to ~100 µL using a Centricon YM-100 column (Amicon). Purified Rubisco was used directly in enzyme assays or stored at -20ºC.

**Determination of Rubisco $N_2/O_2$ ratio**

The Rubisco $N_2/O_2$ ratio, is the ratio of the carboxylase activity in the absence of $O_2$ divided by the activity in the presence of $O_2$. The $N_2/O_2$ ratio is a measurement of the susceptibility of Rubisco carboxylation to inhibition by $O_2$ (Spreitzer and Chastain, 1987; Chen *et al.*, 1988). Briefly, 20 µg of purified Rubisco in 10 µL of 1 mM DTT, 50 mM Bicine-NaOH, pH 8.0, 10 mM $MgCl_2$, and 2 mM $NaHCO_3$ was injected with a Hamilton syringe into a rubber-stopper-sealed 7-mL scintillation vial containing reaction buffer for a total of 0.5 mL of reaction mix (20 µg of purified Rubisco, 0.4 mM RuBP, 50 mM Bicine-NaOH, pH 8.0, 10 mM $MgCl_2$, 0.98 mM $NaHCO_3$). The reaction buffers were

gassed at 7 PSI for 15 min with either 100% $N_2$ (to create an environment without $O_2$) or 100% $O_2$, before adding $NaHCO_3$, which included trace amounts of radiolabeled $NaH^{14}CO_3$ (7.2 Ci/mol). The reaction was allowed to proceed for 1 min in a 25ºC water-bath, and then stopped with 400 µL of 3 M formic acid in methanol. The rubber stopper was removed from the scintillation vial, and the reaction mix was dried in a force-draft oven at 65ºC overnight. Then, 250 µL of 0.25 M HCl was added to the dried product, and the acid-stable $^{14}CO_2$ was measured in a liquid scintillation counter (after addition of 5 mL of scintillation cocktail). A third reaction was also carried out to measure the specific activity of Rubisco, with a similar procedure, except that a saturating 12.4 mM $NaHCO_3$ concentration was used, and the reaction was pre-gassed with 100% $N_2$.

**Determination of Rubisco specificity factor (Ω)**

The Rubisco Ω assay is based on the simultaneous measurement of $^{14}C$ DPM for carboxylation and $^{3}H$ DPM for oxygenation of [1-$^{3}H$]RuBP (Jordan and Ogren, 1981a; Spreitzer *et al.*, 1982). A reaction mix containing Rubisco, [1-$^{3}H$]RuBP, $^{14}CO_2$ from $NaH^{14}CO_3$, and $O_2$ is incubated, and then the carboxylation product, [1-$^{14}C$]phosphoglycerate, and oxygenation product, [1-$^{3}H$]phosphoglycolate, are measured by liquid scintillation spectroscopy (Jordan and Ogren, 1981a).

Briefly, 10 µL (22 nmol, 0.34 µCi) of [1-$^{3}H$]RuBP was injected with a Hamilton syringe into a rubber-stopper-sealed 7-mL scintillation vial at 25ºC containing reaction buffer for a total of 0.5 mL of reaction-mix (20 µg of purified Rubisco, 50 mM Bicine-NaOH pH 8.3, 10 mM $MgCl_2$, 2 mM of 5 Ci/mol $NaH^{14}CO_3$). The reaction buffer was gassed with 100% $O_2$ at 7 PSI for 15 min before the addition of the $NaH^{14}CO_3$ and

Rubisco. The reaction was allowed to proceed for 30 min in a 25ºC water bath, and then stopped with 0.1 ml of 50 mM $ZnSO_4$ in 0.5 M HCl. The reaction mix was adjusted to pH 6.3 with 0.1 mL of 1.5 M sodium cacodylate, added with 0.1 mL of 0.2 M 3-PGA/0.5 mM 2-PG, 0.1 mL (0.25 units) of phosphoglycolate phosphatase, and incubated at 30°C for 30 min in a water bath to convert the [1-$^3$H]phosphoglycolate into [1-$^3$H]glycolate. The phosphatase reaction was stopped with the addition of 0.9 mL of 1 M formic acid, which brings the total reaction volume to 1.8 mL. Of the 1.8 mL reaction-mix, 0.75 mL was mixed with 0.1 mL of 1 M HCl, dried in a force-draft oven at 65ºC overnight, redissolved in 350 µL $H_2O$, and the acid-stable $^{14}CO_2$ was measured by liquid scintillation spectroscopy. Another 0.75 mL of the 1.8-mL reaction mix was loaded onto a Dowex AG 1-X8 formate column (Biorad) that was pre-equilibrated with $H_2O$, and the flow-through was collected. The column was further eluted with 3 mL of 1 M formic acid, collecting a total of 3.75 mL of flow-through, which contained the uncharged non-phosphorylated [1-$^3$H]glycolate. Two separate 1.5-mL aliquots of flow-through was lyophilized at -40ºC overnight, re-dissolved in 250 µL of $H_2O$, and the $^3$H measured by liquid scintillation spectroscopy. Ω is simply calculated as the rate of carboxylation ($v_c$) per the rate of oxygenation ($v_o$) times the concentration of $O_2$ per $CO_2$ (Laing *et al.*, 1974):

$$\Omega = v_c/v_o \times [O_2]/[CO_2]$$

where $v_c/v_o$ is equivalent to the moles of $CO_2$ fixed per moles of phosphoglycolate formed, $[O_2]$ is 1.15 mM, and $[CO_2]$ is 30 µM (Jordan and Ogren, 1981a). However, even before the specificity-factor assay can be carried out, the [1-$^3$H]RuBP had to be

synthesized and the phosphoglycolate phosphatase enzyme had to be partially purified (Christeller and Tolbert, 1978; Kuehn and Hsu, 1978; Jordan and Ogren, 1981a).

[1-$^3$H]RuBP was previously synthesized by Dr. Todor N. Genkov from D-[2-$^3$H]glucose according to an established method (Kuehn and Hsu, 1978; Jordan and Ogren, 1981a). An 8-mL reaction mixture comprised of 40 mM Hepes-NaOH, pH 7.6, 5 mM $MgCl_2$, 1 mM KCl, 2 mM ATP, 15 mM phosphoenol pyruvate, 15 mM NADP, 2 mM DTT, 0.2 mM EDTA, and 6 mM D-glucose was prepared at 0°C and adjusted to pH 7.6 with 1 M NaOH. Then, 1 mg of BSA, 100 U of pyruvate kinase, 150 U of glucose-6-phosphate dehydrogenase, 25 U of 6-phosphogluconate dehydrogenase, 25 U of phosphoribulokinase, and 1 mCi of D-[2-$^3$H]glucose were added. When the reaction mix returned to room temperature, the pH was adjusted to 7.6 with 1 M NaOH, and RuBP-synthesis was initiated by the addition of 325 U of hexokinase. During RuBP synthesis, which took about 45 min, the mixture was continuously stirred, and the pH was monitored and maintained at 7.6 with drop-wise additions of 1 M NaOH until there was no further change in pH, indicating the completion of the reaction. The reaction mix was adjusted to pH 3.5 using 3 M HCl, loaded onto a Dowex AG 1-X8 $Cl^-$ column (200-400 mesh) that was pre-equilibrated with $H_2O$, and sequentially washed with 300 mL of $H_2O$, 300 mL of 10 mM LiCl/1 mM HCl, and 200 mL of 10 mM to 100 mM LiCl/1 mM HCl as a linear gradient. [1-$^3$H]RuBP fractions, which were eluted with 300 mL of 100 mM to 350 mM LiCl/1 mM HCl as a linear gradient, were identified by liquid scintillation spectroscopy, concentrated to 20 mL by lyophilization at -40ºC, and then adjusted to pH 6.5 with $Ba(OH)_2$. To precipitate out the [1-$^3$H]RuBP, 1 mL of 1 M barium acetate and 20 mL of 100% ethanol were added. The [1-$^3$H]RuBP was pelleted, resuspended in 1 mL

$H_2O$ and mixed with 0.75 g AG 50W-X4 $H^+$- resin, which had been prewashed with $H_2O$. The flow-through from the resin mix was collected, and the resin mix was further eluted with 5 mL $H_2O$, collecting the flow-through as well. The total flow-through, which contained [1-$^3$H]RuBP, was adjusted to pH 6.5 with 1 M NaOH. The mole-amount of [1-$^3$H]RuBP was determined by measuring the [$^{14}$C]carboxylation product in a Rubisco reaction with unknown but limited amount of substrate [1-$^3$H]RuBP, but excess amounts of Rubisco and NaH$^{14}$CO3. [1-$^3$H]RuBP was stored at -20ºC.

The phosphoglycolate phosphatase enzyme was partially purified from tobacco leaves (Christeller and Tolbert, 1978; Jordan and Ogren, 1981a). Homogenate from 300 g of leaves ground in 1 L of Buffer A (20 mM sodium cacodylate pH 6.3, 2 mM $ZnSO_4$, 2 mM citrate), with 2% w/v polyvinylpolypyrrolidone added, was filtered through cheesecloth and centrifuged at 12,000 g for 20 min at 4°C to pellet leaf debris. The supernatant containing the leaf extract was acetone-precipitated, and the precipitate between 25% to 40% v/v acetone was pelleted, air-dried, dissolved in 50 mL of Buffer A and loaded on a Buffer A-equilibrated DEAE-cellulose column (2.5 X 30 cm). The column was then washed with 150 mL of Buffer A and the phosphoglycolate phosphatase was eluted with a linear gradient of 0 M to 0.4 M KCl in Buffer A. Eluate-fractions were assayed for phosphoglycolate phosphatase activity by adding 50 µL of eluate to 0.5 mL of Buffer A containing 2 µmol of $MgCl_2$ and 1 µmol of 2-phosphoglycolate, incubated at 30ºC for 5 min, and stopped with 0.2 mL of 10% w/v trichloroacetic acid. To determine the phosphatase activity, absorbance at 820 nm by free inorganic-phosphate released from 2-phosphoglycolate was measured and compared to a phosphate standard curve. Eluate fractions containing peak phosphatase activities were pooled and subjected to

ammonium-sulfate fractionation. The precipitate between 50% and 80% ammonium sulfate, which contained phosphoglycolate phosphatase, was pelleted, resuspended in 10 mL of Buffer A, and stored at -80ºC. When needed for the Rubisco Ω assay, the required amount of phosphoglycolate phosphatase was adjusted to 2.5 U/mL with Buffer A.

**Determination of Rubisco kinetic-properties**

The kinetic properties of Rubisco were determined from measurements of Rubisco carboxylase activity at six different $CO_2$ concentrations with or without $O_2$ (Chen *et al.*, 1988). $V_o$ was calculated from the Ω value ($V_cK_o/V_oK_c$) and the $V_c$, $K_c$, and $K_o$ values (Laing *et al.*, 1974; Chen *et al.*, 1988). Purified Rubisco (10 µg) in 20 µL of buffer (1 mM DTT, 50 mM Bicine-NaOH, pH 8.0, 10 mM $MgCl_2$, 10 mM $NaHCO_3$) was injected with a Hamilton syringe into a rubber-stopper-sealed 7-mL scintillation vial containing reaction buffer for a total of 1 mL of reaction mix (10 µg Rubisco, 0.4 mM RuBP, 50 mM Bicine-NaOH, pH 8.0, 10 mM $MgCl_2$, and $NaHCO_3$ concentrations of 0.6 mM, 1.6 mM, 2.6 mM, 4.6 mM, 8.6 mM, or 16.6 mM). The reaction buffers had been gassed at 7 PSI for 15 min with either 100% $N_2$ (to create an environment without $O_2$) or 100% $O_2$ before the addition of the $NaHCO_3$, which included 25 µL of radiolabeled $NaH^{14}CO_3$ (0.4 mCi/mL, 60 Ci/mol). The reaction was allowed to proceed for 1 min in a 25ºC water bath, and then stopped with 1 mL of 3 M formic acid in methanol. The rubber stopper was removed from the scintillation vial, the reaction mix was dried in a force-draft oven at 65ºC overnight, 350 µL of 0.25 M HCl was added to the dried product, and the remaining fixed, acid-stable $^{14}CO_2$ was measured by liquid scintillation spectroscopy. The $V_c$ and $K_c$ values were determined from the double-reciprocal plot of

1/[$CO_2$] (x-axis) to 1/$v_c$ (y-axis) for the 100% $N_2$-gassed $O_2$-free carboxylase reactions. $V_c$ is the 1/x-intercept and $K_c$ is the $V_c$ times the slope. $K_o$ is determined from the relation between [$CO_2$] and the ratio (R) of the carboxylase activity in the absence and presence of $O_2$ where $R = 1 + K_c[O_2]/(K_cK_o+K_o[CO_2])$, which can be rearranged as $1/(R-1) = K_o[CO_2]/K_c[O_2] + K_o/[O_2]$. (Chen *et al.*, 1988). By plotting [$CO_2$] (x-axis) to 1/(R-1) (y-axis), $K_o$ is simply the x-intercept times 1.15 mM, which is [$O_2$] for the 100% $O_2$-gassed reactions (Jordan and Ogren, 1981a; Chen *et al.*, 1988).

**Determination of Rubisco thermostability**

Rubisco stability was determined with a thermostability assay (Chen *et al.*, 1993). Purified Rubisco (5 µg) in 50 µL of buffer (1 mM DTT, 50 mM Bicine-NaOH, pH 8.0, 10 mM $MgCl_2$, 10 mM $NaHCO_3$) was incubated at 35ºC, 45ºC, 50ºC, 55ºC, 60ºC, 65ºC, or 70ºC for 10 min, cooled on ice for 5 min, and then injected with a Hamilton syringe into a rubber-stopper-sealed 7-mL scintillation vial containing reaction buffer for a total of 0.5 mL of reaction-mix (5 µg of purified Rubisco, 0.4 mM RuBP, 50 mM Bicine-NaOH, pH 8.0, 10 mM $MgCl_2$, 10 mM of 2 Ci/mol $NaH^{14}CO_3$). The reaction was allowed to proceed for 1 min in a 25ºC water bath, and then stopped with 0.5 mL of 3 M formic acid in methanol. The rubber stopper was removed from the scintillation vial, the reaction mix was dried in a force-draft oven at 65ºC overnight, 350 µL of 0.25 M HCl was added to the dried product, and the remaining fixed, acid-stable $^{14}CO_2$ measured by liquid scintillation spectroscopy.

**SDS-PAGE of *Chlamydomonas* total soluble proteins**

Total soluble proteins from sonicated *Chlamydomonas* cells were separated with a linear-gradient SDS-PAGE method that gives high resolution of chloroplast stromal proteins (Chua, 1980). A 14 x 16 x 0.15-cm gel was poured consisting of 28 mL of resolving linear-gradient gel of 7.5% to 15% w/v polyacrylamide/N,N'-methylene-bis-acrylamide (37.5:1), 5% to 17% w/v sucrose, 85 mM Tris-HCl, pH 9.18, and 0.1% w/v SDS. The resolving gel was then overlaid with 6 mL of stacking gel of 6% w/v acrylamide/N,N'-methylene-bis-acrylamide (37.5:1), 13.5 mM Tris-$H_2SO_4$, pH 6.1, and 0.1% w/v SDS. The lower reservoir buffer was 85 mM Tris-HCl, pH 9.18, and 0.1% w/v SDS whereas the upper reservoir buffer was 2 mM Tris-borate, pH 8.64. Each well of the gel was loaded with 60 µg of *Chlamydomonas* protein, which had been mixed with sample loading buffer (5% w/v SDS, 30% w/v sucrose, 0.05% w/v bromophenol blue, 100 mM DTT) at a 3:2 ratio and boiled for 3 min. Electrophoresis was carried out at 25ºC, and initially set to 15 mA per gel, but turned up to 30 mA per gel after the dye front had passed the stacking/resolving gel interface. Electrophoresis was stopped as soon as the dye front moved off the end of the gel. The gel was stained overnight with 0.25% w/v Coomassie Brilliant Blue R, 50% v/v methanol, and 7% v/v acetic acid (Chua, 1980). Destaining was then carried out with a solution of 40% v/v methanol and 7% v/v acetic acid until bands were visible. The gel was then further destained and stored in 10% acetic acid.

**Western blotting of Rubisco**

SDS-PAGE gels were run in duplicate, and one was used for western blotting

(Towbin *et al.*, 1979). Proteins from the gel were transferred to a nitrocellulose membrane at 15 V for 12 hr at 4ºC in blotting buffer (25 mM Tris, 192 mM glycine, 20% v/v methanol). Then, the membrane was blocked with 3% w/v gelatin in TBS buffer (500 mM NaCl, 20 mM Tris-HCl, pH 7.4) for 1 hr at room temperature. The membrane was probed with rabbit anti-*Chlamydomonas* Rubisco large (0.76 µg) and small-subunit IgGs (0.68 µg) (Karkehabadi *et al.*, 2005) in 50 mL of 1% w/v gelatin in TBS buffer for 7 hr. It was then washed with TTBS buffer (0.05% v/v Tween 20 in TBS buffer), incubated with 12.5 µL of goat anti-rabbit IgG/horseradish peroxidase conjugate (Biorad) in 1% w/v gelatin in 50 mL TBS buffer for 2 hr, washed with TTBS buffer, washed with TBS buffer, and visualized on an x-ray film using horseradish peroxidase chemiluminescence (National Diagnostics).

# RESULTS AND DISCUSSION

## PHYLOGENETIC GROUPS

### Defining phylogenetic groups

Protein-sequence alignment of the Rubisco large subunit of *Chlamydomonas* with 500 flowering-plant large subunits showed that there are 34 "phylogenetic residues" that differ between *Chlamydomonas* and plants (Du *et al.*, 2003). Phylogenetic residues are those that differ between *Chlamydomonas* Rubisco and over 95% of the 500 flowering-plant sequences (Du *et al.*, 2003). These phylogenetic residues may account for the differences in kinetic properties between algae and plants, and are potential targets for engineering. A direct approach to determine the phylogenetic-residue combinations that can influence Rubisco catalysis would be to change the *Chlamydomonas* residues to plant residues, and then assay the mutant enzymes for changes in kinetic properties. However, site-directed mutagenesis of all possible combinations of the 34 phylogenetic residues would involve creating $2^{34}$ mutant enzymes, which is over 17 billion mutant strains (Du *et al.*, 2003).

Instead, to simplify the problem, phylogenetic residues can be first clustered into "phylogenetic groups" based on the closeness of the residues in the highest-resolution, 1.4-Å x-ray crystal structure of *Chlamydomonas* Rubisco (Table 2 and Fig. 4) (Taylor *et al.*, 2001; Du *et al.*, 2003). Specifically, a phylogenetic group consists of phylogenetic residues within 5 Å of each other (Du *et al.*, 2003). Each phylogenetic group defines a structural region, and directed mutagenesis of each group as a whole would determine whether a structural region influences catalysis. Single-residue changes are often not

**Table 2: Phylogenetic groups in the catalytic large subunit of *Chlamydomonas* Rubisco (Du *et al.*, 2003).**

| Group number [a] | Group notation [b] | Residue substitutions |
|---|---|---|
| 1 | 11 | A11V |
| 2 | 30-32 | V30E, V31T, R32K |
| -- | 42-53 | M42V, C53A |
| 3 | 86 | D86H |
| 4 | 105-369 [c] | I105L, C369V [c] |
| 5 | 149-282 | V149Q, I282H |
| 6 | 168-399 | G168P, L326I, M349L, M375L, A398S, C399V |
| 7 | 221 | V221C |
| -- | 235 | V235I |
| -- | 256-258 | C256F, K258R |
| -- | 265 | I265V |
| 8 | 305-474 | R305K, D470E, T471A, I472M, K474T |
| -- | 341 | V341I |
| 9 | 391-428 | V391T, T428V |
| 10 | 442-447 | G442N, D443E, V444I, S447E |

[a] Group number, which is based on the order of the phylogenetic groups, will be used for labeling of western-blot and phenotype-data figures where space is limited. Mutant phylogenetic groups that were previously created and analyzed are designated "--" (Zhu and Spreitzer, 1996; Du *et al.*, 2003; Spreitzer *et al.*, 2005).

[b] Group notation, which is based on the first and last residue substituted in a phylogenetic group, is the favored method for referring to specific phylogenetic groups throughout the text.

[c] The phylogenetic-residues Ile-105 and Cys-369 are from neighboring large-subunits.

**Figure 4: Distribution of the 34 phylogenetic residues, which cluster into 15 groups, in the large subunit of *Chlamydomonas* Rubisco (PDB 1GK8) (Taylor *et al.*, 2001).** Each color represents a phylogenetic group. Only one large subunit is shown with the backbone represented as white ribbon. At the left is the N-terminal domain. At the right is the C-terminal α/β-barrel active-site domain with the bound transition-state analog CABP shown as black sticks. Residues Ile-105 and Cys-369 are in contact between two large subunits. The βA-βB loops from two different small subunits are shown as yellow and orange ribbons at the bottom right of the figure. These loops vary in size among species, and interact with phylogenetic groups 256-258 and 235 at the bottom of the α/β barrel (Spreitzer *et al.*, 2005).

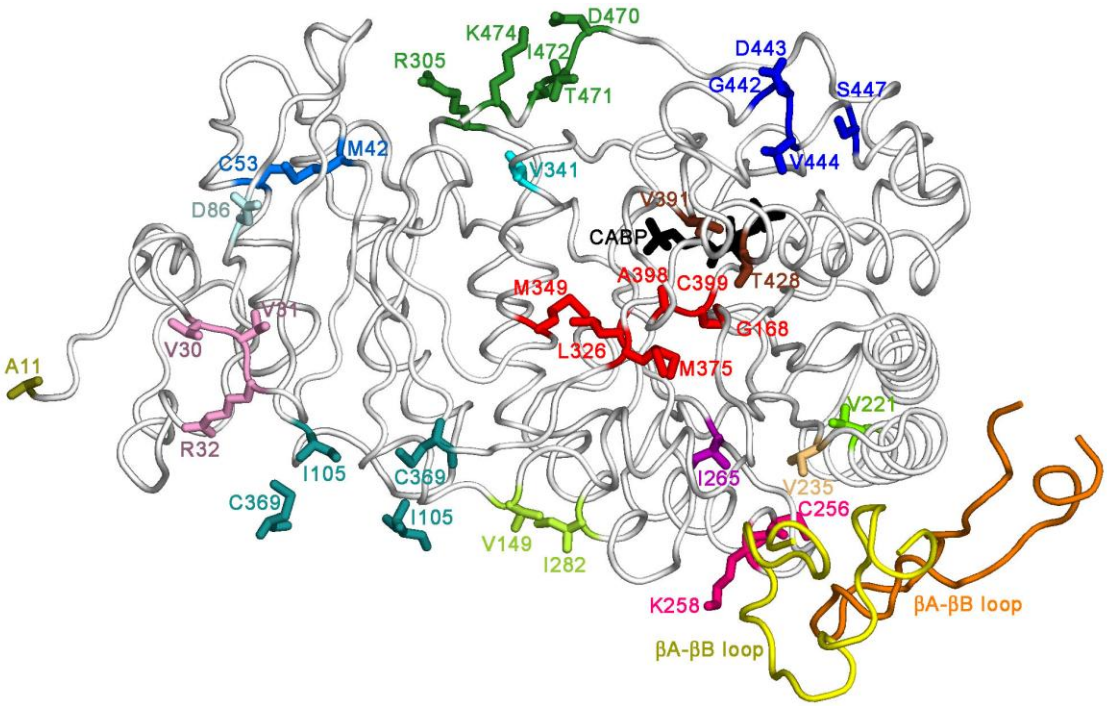
D470
K474
I472
R305
T471
D443
G442
S447
V444
M42
C53
V341
D86
V391
CABP
A398
C399
T428
M349
G168
L326
M375
V81
V30
A11
V221
R32
I105
C369
I265
V235
C256
C369
I105
V149
I282
K258
βA-βB loop
βA-βB loop

sufficient to cause a noticeable change in catalysis, but residue-group changes have greater effects on structure (Zhu and Spreitzer, 1996; Du *et al.*, 2003; Spreitzer *et al.*, 2005; Satagopan and Spreitzer, 2008).

The objective of the first phase of this study was to determine which phylogenetic groups contribute to the differences in kinetic properties between *Chlamydomonas* and plant Rubisco enzymes, and possibly determine their other roles in Rubisco structure and function. Some of the groups have only one residue (i.e., groups 11, 86, 221, 235, 265 and 341) (Table 2 and Fig. 4). Five of the phylogenetic groups (i.e., groups 42-53, 235, 256-258, 265 and 341) were studied previously, but did not result in any significant changes in catalysis (Zhu and Spreitzer, 1996; Du *et al.*, 2003; Spreitzer *et al.*, 2005). Thus, only ten remaining phylogenetic-group mutants needed to be created and analyzed in this study.

**Recovery of phylogenetic-group mutants and their phenotypes**

*Chlamydomonas* phylogenetic-group mutants were recovered by chloroplast transformation of the MX3312 *rbcL*-knockout strain (Satagopan and Spreitzer, 2004, 2008; Zhu *et al.*, 2005) followed by photosynthetic selection. All ten phylogenetic-group mutant strains could grow photoautotrophically, and the transformation frequencies with the mutant genes were not significantly different from that of wild type *rbcL* ($1 \times 10^{-6}$ per cells shot). Thus, none of the mutations affected essential functions of Rubisco (Fig. 5). Moreover, similar to wild-type *rbcL* transformation, all the phylogenetic-group mutant transformants started appearing as photosynthetic colonies on minimal medium within 2 to 4 weeks.

**Figure 5: Growth phenotypes of *Chlamydomonas* wild type (WT) and phylogenetic-group mutants.** About 2 X $10^5$ cells were spotted at each position, and grown for one week with the conditions indicated (Spreitzer and Mets, 1981). Spot numbering is based on Table 2.

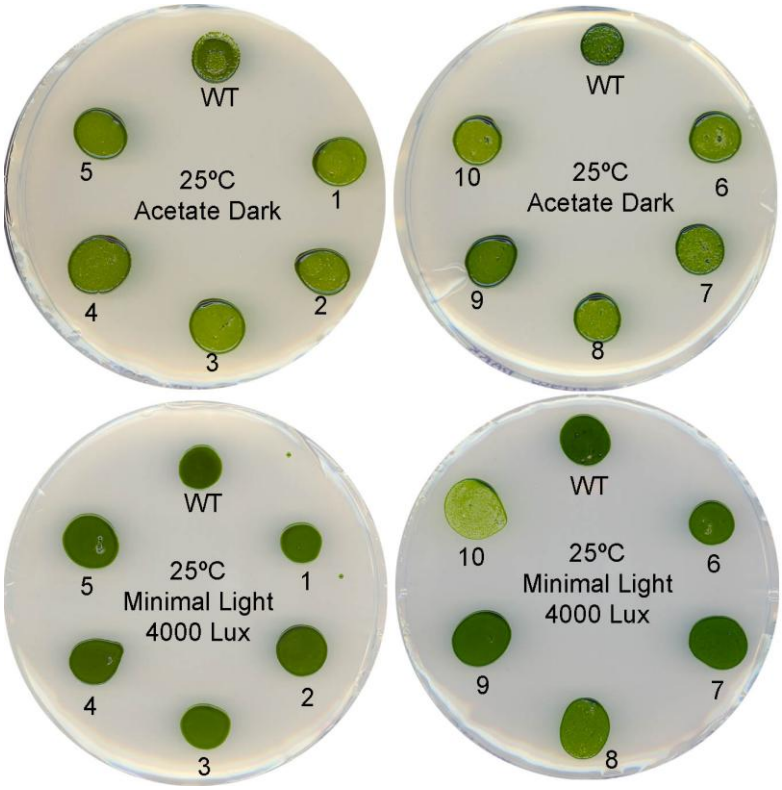
WT
5
1
25ºC
Acetate Dark
4
2
3
WT
10
6
25ºC
Acetate Dark
9
7
8
WT
5
1
25ºC
Minimal Light
4000 Lux
4
2
3
WT
10
6
25ºC
Minimal Light
4000 Lux
9
7
8

Comparison of the growth phenotypes of the phylogenetic-group mutants (Spreitzer and Mets, 1981) indicated that only the 442-447 phylogenetic-group mutant (G442N/D443E/V444I/S447E) had reduced photosynthetic growth on minimal medium in the light (spot 10, Fig. 5). When grown heterotrophically on acetate medium in the dark, the 442-447 mutant-Rubisco strain was indistinguishable from wild type indicating that the reduction in growth on minimal medium must result from a decrease in photosynthesis.

**Rubisco holoenzyme level**

To determine the effects of the mutations on the amount of Rubisco *in vivo*, which would depend on holoenzyme expression, stability, or assembly, cell extracts were subjected to SDS-PAGE and western blotting (Fig. 6). The amount of assembled Rubisco *in vivo* is directly related to the observed subunit levels *in vitro* because free small subunits are rapidly degraded *in vivo*, and expression of large subunits is blocked at translation in the absence of small subunits (Spreitzer *et al.*, 1985; Khrebtukova and Spreitzer, 1996). Almost all the phylogenetic-group mutant strains expressed equal amounts of Rubisco when compared with wild type except for the 442-447 mutant strain, which had reduced *in vivo* holoenzyme level as evidenced by the western blot (lane 10, Fig. 6). Thus, the decreased holoenzyme level of the 442-447 mutant strain could account for its decreased photosynthetic growth (spot 10, Fig. 5).

A thermal-inactivation experiment (Chen *et al.*, 1993) was performed with the 442-447 mutant Rubisco to determine whether the enzyme was unstable. As shown in Fig. 7, the wild-type and 442-447 mutant enzymes have similar thermal inactivation.

**Figure 6: SDS-PAGE (left) and western-blot (right) analysis of total soluble protein from *Chlamydomonas* wild type (WT) and phylogenetic-group mutants (lanes 1 through 10).** Sixty micrograms of total soluble protein from sonicated dark-grown cells were run in each lane. Mutant numbering is based on Table 2. LS denotes the Rubisco large subunit, and SS denotes the small subunit.

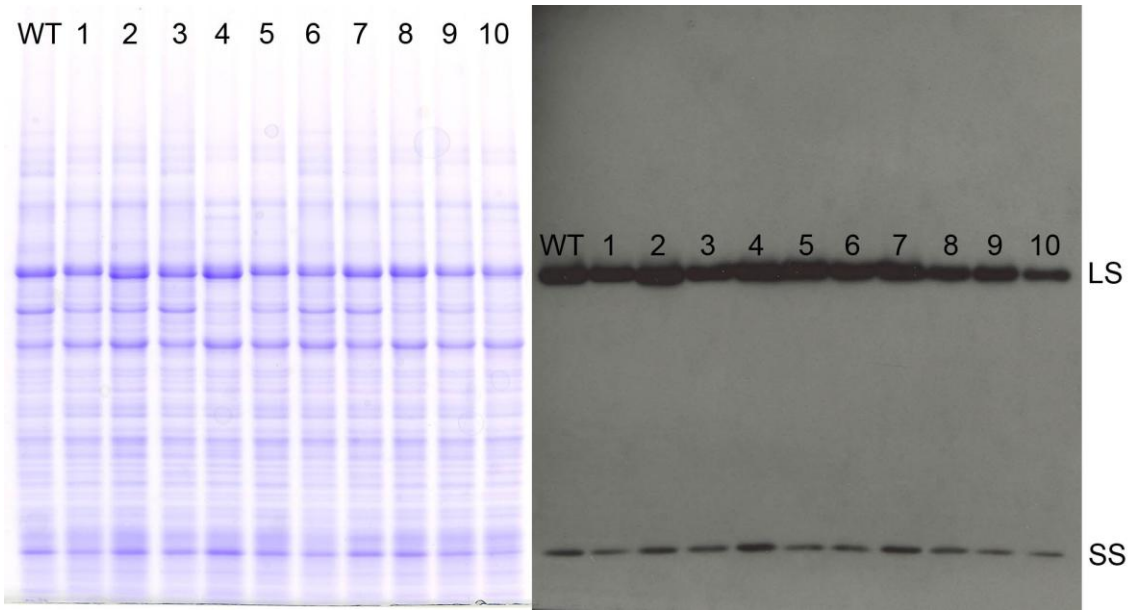
WT 1 2 3 4 5 6 7 8 9 10
WT 1 2 3 4 5 6 7 8 9 10
LS
SS

**Figure 7: Thermal inactivation of Rubisco purified from *Chlamydomonas* wild type (WT) and the 442-447 phylogenetic-group mutant.** Five micrograms of Rubisco were pre-incubated at the indicated temperatures for 10 min, and then cooled on ice for 5 min, before assaying carboxylase activity at 25ºC for 1 min. The measured activity was normalized to that of the 35ºC pre-incubation. The specific activity after the 35ºC pre-incubation was 1.1 µmol $CO_2$ fixed/min/mg protein for wild-type Rubisco, and 0.9 µmol/min/mg for the mutant enzyme.

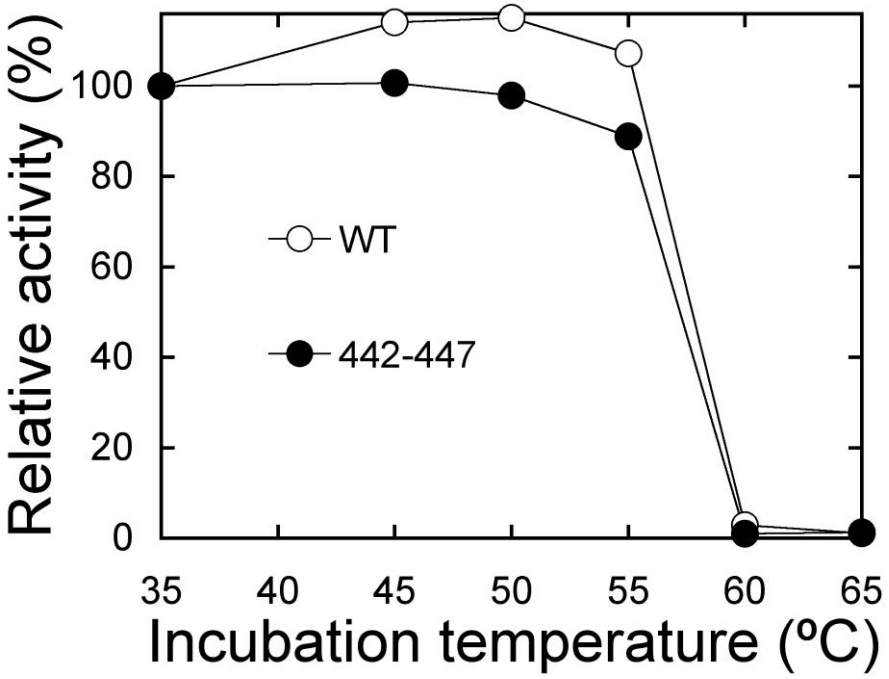
Relative activity (%)
100
80
60
40
20
0
WT
442-447
35
40
45
50
55
60
65
Incubation temperature (ºC)

Therefore, the phylogenetic substitutions G442N/D443E/V444I/S447E in the 442-447 mutant do not affect stability *in vitro*, but may affect structure leading to degradation *in vivo*.

**Kinetic properties**

Despite the reduced holoenzyme level of the 442-447 phylogenetic-group mutant, sufficient amounts of Rubisco could be purified from all the mutants for kinetic analysis. An initial $N_2/O_2$-ratio assay (Spreitzer and Chastain, 1987) was performed with all the phylogenetic-group mutant enzymes to determine whether the phylogenetic substitutions affected the $O_2$ sensitivity of Rubisco (Ratio A/B, Table 3). Carboxylase specific activities were measured at saturating $CO_2$ (12.4 mM $NaHCO_3$, Table 3), and the Ω values were also measured (Table 3).

Only the 168-399, 305-474 and 442-447 phylogenetic-group mutant enzymes have altered $O_2$-sensitivity in comparison with wild type Rubisco, which has an $N_2/O_2$ ratio of 2.4 (Table 3). The rest of the phylogenetic mutants have ratios within ±10% of the wild-type value. The 168-399 and 442-447 mutants have increases in the $N_2/O_2$ ratio to 3.2 and 2.9, respectively, which indicates that the phylogenetic substitution G168P/L326I/M349L/M375L/A398S/C399V in phylogenetic-group 168-399, close to catalytic loop-6, increased the sensitivity of Rubisco to $O_2$, causing the carboxylase reaction to be more prone to $O_2$ inhibition (Table 3). The phylogenetic substitution G442N/D443E/V444I/S447E in phylogenetic-group 442-447 also caused a similar but less pronounced increase in $O_2$ inhibition. On the other hand, phylogenetic-group 305-474, consisting of R305K/D470E/T471A/I472M/K474T substitutions at the carboxy

**Table 3: Ω values, specific activities, and oxygen inhibition of Rubisco purified from *Chlamydomonas* wild type and phylogenetic-group mutants.** Values are the means ±S.D. (*n* - 1) of three separate enzyme preparations.

| Enzyme | Ω<br>$V_cK_o/V_oK_c$ | RuBP carboxylase activity<br>100% $N_2$<br>12.4 mM<br>$NaHCO_3$ | 100% $N_2$<br>0.98 mM<br>$NaHCO_3$<br>(A) | 100% $O_2$<br>0.98 mM<br>$NaHCO_3$<br>(B) | Ratio<br>(A/B) |
|---|---|---|---|---|---|
| | | *µmol $CO_2$/hr/mg of protein* | | | |
| Wild type | 59 ± 1 | 101 ± 2 | 28.6 ± 0.4 | 11.8 ± 1.0 | 2.4 |
| 11 | 62 ± 3 | 115 ± 5 | 33.6 ± 0.4 | 13.7 ± 0.8 | 2.5 |
| 30-32 | 61 ± 3 | 107 ± 9 | 31.1 ± 0.4 | 13.0 ± 0.3 | 2.4 |
| 86 | 58 ± 2 | 92 ± 5 | 22.8 ± 1.3 | 8.7 ± 1.2 | 2.6 |
| 105-369 | 63 ± 2 | 115 ± 16 | 35.5 ± 1.0 | 13.8 ± 0.3 | 2.6 |
| 149-282 | 61 ± 1 | 122 ± 7 | 33.7 ± 2.9 | 13.3 ± 1.6 | 2.5 |
| 168-399 | 56 ± 2 | 46 ± 4 | 10.7 ± 1.1 | 3.3 ± 0.3 | 3.2 |
| 221 | 59 ± 1 | 116 ± 10 | 32.3 ± 2.0 | 14.6 ± 0.8 | 2.2 |
| 305-474 | 61 ± 2 | 99 ± 16 | 21.7 ± 0.8 | 11.5 ± 0.4 | 1.9 |
| 391-428 | 62 ± 3 | 57 ± 9 | 18.1 ± 1.1 | 8.3 ± 0.2 | 2.2 |
| 442-447 | 61 ± 4 | 98 ± 11 | 28.5 ± 2.9 | 9.9 ± 1.2 | 2.9 |

terminus of the Rubisco large subunit, decreased the sensitivity of Rubisco to $O_2$, evidenced by the reduction of the $N_2/O_2$ ratio to 1.9 (Table 3). Of the three phylogenetic mutants 168-399, 305-474 and 442-447, only the 168-399 mutant has a decrease in specific carboxylase activity, which is over 50% (Table 3).

Because of the decrease in specific activity and increase in oxygen sensitivity, the 168-399 mutant enzyme has the lowest Ω value among the phylogenetic-group mutants, with Ω = 59 for the wild-type enzyme, and Ω = 56 for the 168-399 mutant enzyme (Table 3). On the other hand, it was surprising that none of the phylogenetic substitutions increases Ω by at least 10% considering that plant Rubisco enzymes have Ω values at least 15% higher than that of *Chlamydomonas* Rubisco (Jordan and Ogren, 1981b; Genkov *et al.*, 2010). Perhaps further combinations of phylogenetic-group substitutions are required to achieve the shift in catalytic properties observed between *Chlamydomonas* and plant Rubisco enzymes.

Detailed kinetic analysis was performed on the 168-399, 305-474 and 442-447 phylogenetic-group mutant Rubisco enzymes to determine the specific changes in kinetic constants (Table 4). For the 168-399 and 442-447 mutants, which have increases in $O_2$ inhibition, the $K_o$ values are decreased to 386 and 352 μM $O_2$, respectively, compared with 458 μM $O_2$ for the wild-type enzyme (Table 4).

For the 305-474 mutant, which has a decrease in $O_2$-inhibition, $K_o$ is increased to 637 μM $O_2$ (Table 4). However, the beneficial decrease in $O_2$ sensitivity of the 305-474 mutant is offset by an increase in $K_c$ to 58 μM $CO_2$, compared to 35 μM $CO_2$ for the wild-type enzyme (Table 4). In addition, for the 168-399 mutant, $V_c$ is reduced to 65 μmol $CO_2$ fixed/hr/mg protein, from 105 μmol/hr/mg for the wild-type enzyme, which,

**Table 4: Kinetic properties of Rubisco purified from *Chlamydomonas* wild type and three phylogenetic-group mutants with altered oxygen inhibition.**

| Enzyme | $\Omega$ [a,b] $V_cK_o/V_oK_c$ | $V_c$ [b] | $K_c$ [b] | $K_o$ [b] | $V_c/K_c$ [c] | $K_o/K_c$ [c] | $V_c/V_o$ [c] |
|---|---|---|---|---|---|---|---|
| | | *µmol/hr/mg* | *µM* $CO_2$ | *µM* $O_2$ | | | |
| Wild type | 59 ± 1 | 105 ± 2 | 35 ± 1 | 458 ± 3 | 3.0 | 13 | 4.5 |
| 168-399 | 56 ± 2 | 65 ± 11 | 36 ± 3 | 386 ± 29 | 1.8 | 11 | 5.1 |
| 305-474 | 61 ± 2 | 96 ± 10 | 58 ± 7 | 637 ± 7 | 1.7 | 11 | 5.5 |
| 442-447 | 61 ± 4 | 82 ± 8 | 34 ± 4 | 352 ± 32 | 2.4 | 10 | 6.1 |

[a] Values are from Table 3.

[b] Values are the means ± S.D. ($n$ - 1) of three separate enzyme preparations.

[c] Calculated values.

together with the reduced $K_o$, contributes to a lower Ω (Table 4).

**Structural analysis of the phylogenetic-group mutant enzymes**

The decrease in Ω caused by the 168-399 phylogenetic-group substitutions (G168P/L326I/M349L/M375L/A398S/C399V) (Table 4), at the base and flank of catalytic loop 6 (Fig. 8), is reminiscent of the decreased Ω previously observed for an L326I/M349L mutant enzyme (Zhu and Spreitzer, 1996). The side chains of Leu-326 and Met-349 are in van der Waals contact, and, because the two residues are located in β-strand 6 and α-helix 6, respectively (Fig. 8), substituting the two residues could directly affect the flexibility of the loop, and affect the stability of the interactions between Lys-334 and the gaseous substrates (Gutteridge *et al.*, 1993; Zhu and Spreitzer, 1996). Besides that, changes of Leu-326 could also affect the adjacent active-site residue His-327 (Fig. 8). Mutations of His-327 have been previously found to weaken the binding of the CABP carboxylation transition-state analog to Rubisco, which would decrease Ω (Harpel *et al.*, 1991).

Because the base-of-loop-6 phylogenetic-group 168-399 mutant enzyme, which has four substitutions G168P/M375L/A398S/C399V additional to the previous L326I/M349L, does not have Ω restored to the wild-type value or increased to plant values (Table 4), it must be concluded that these additional phylogenetic-residue changes are not sufficient to complement the L326I/M349L substitutions in terms of Ω (Zhu and Spreitzer, 1996). The four additional phylogenetic-residue substitutions are at the amino-terminal ends of the β strands forming the β-sheet wall of the active-site barrel (Fig. 8). In fact, as part of the network of hydrogen bonds keeping the β-sheet intact, there is a

**Figure 8: Structural comparison of residues in the 168-399 phylogenetic group (red) at the base of catalytic loop 6 between *Chlamydomonas* (left, PDB 1GK8) and spinach Rubisco (right, PDB 8RUC).** Except for Leu-326 and Met-349, which flank loop 6, the other phylogenetic residues are at the N-terminal ends of β-strands β1, β8, and β7, which are also part of the α/β-barrel active-site domain. The CABP carboxylation transition-state analog denotes the active site with the side chain of Lys-334 stabilizing the partial negative charge on the $CO_2$ (or $O_2$) moiety that is represented by a carboxylate side group of CABP. His-327 at the C-terminal end of β6, adjacent to Leu-326, is another active-site residue that can influence Ω (Harpel *et al.*, 1991).

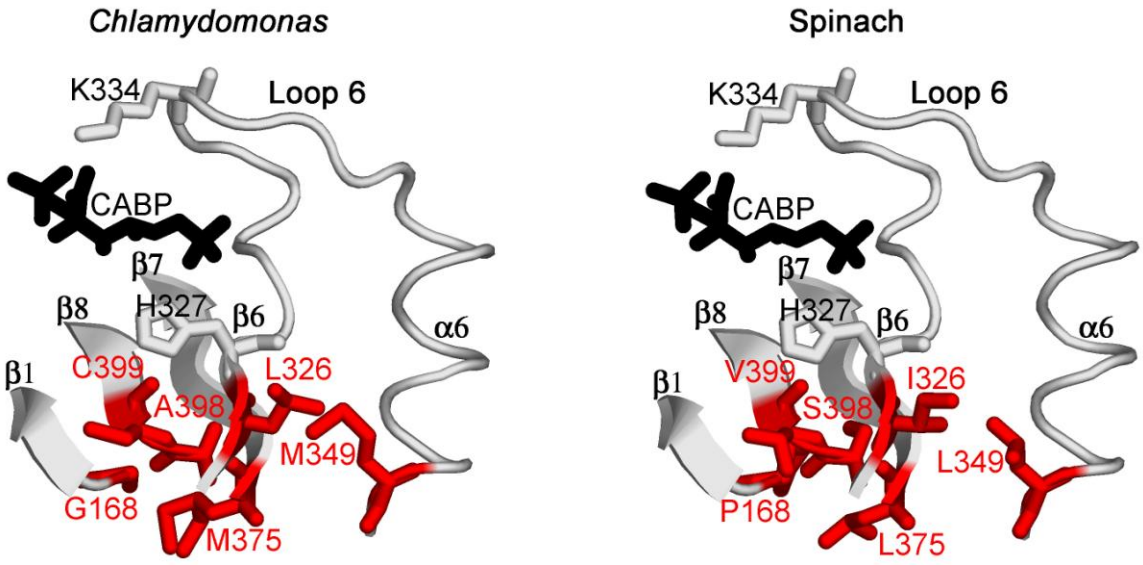
Chlamydomonas
K334
Loop 6
CABP
β7
β8
H327
β6
α6
β1
C399
L326
A398
M349
G168
M375
Spinach
K334
Loop 6
CABP
β7
β8
H327
β6
α6
β1
V399
I326
S398
L349
P168
L375

hydrogen bond between the backbone carbonyl oxygen of Met-375 and the amide nitrogen of Leu-326, suggesting that there could be some other complementary effects between the phylogenetic residues unrelated to Ω.

As for the phylogenetic-group 305-474 substitutions (R305K/D470E/T471A/I472M/K474T) at the carboxy terminus, the increase in $K_o$ (Table 4) is reminiscent of the increased $K_o$ observed in a previous mutant *Chlamydomonas* Rubisco that had the carboxy terminus changed to that of spinach (D470P/T471A/I472M/K474T) (Satagopan and Spreitzer, 2008). Whereas the previous D470P/T471A/I472M/K474T mutant enzyme had a 10% increase in Ω (Satagopan and Spreitzer, 2008), the 305-474 phylogenetic-group mutant enzyme has no change in Ω despite an increase in $K_o$ because of a concomitant increase in $K_c$ (Table 4).

The 305-474 mutant enzyme (R305K/D470E/T471A/I472M/K474T) is different from the previous D470P/T471A/I472M/K474T enzyme in that Asp-470 was replaced with Glu-470, found in 41% of plant-Rubisco sequences, as opposed to being replaced with Pro-470, found in only 18% of the plant sequences including spinach (Du *et al.*, 2003). Also, an additional Arg-305-to-Lys substitution was included in the 305-474 mutant because Arg-305 in *Chlamydomonas* Rubisco is in van der Waals contact with Lys-474 (Fig. 9). It was previously suggested that the increase in Ω for D470P/T471A/I472M/K474T might be attributed to an increase in carboxy-terminal flexibility caused by the elimination of the salt bridge between Asp-470 and Lys-474 (Satagopan and Spreitzer, 2008). For the 305-474 mutant enzyme, even though the salt bridge between residue 470 and 474 is disrupted, the increased flexibility of the carboxy terminus could be offset by the formation of an ionic interaction between Thr-474 and

**Figure 9: Structural comparison of residues in phylogenetic group 305-474 (green) at the carboxy-terminal tail between *Chlamydomonas* (top) and spinach Rubisco (bottom).** The Asp-470-Lys-474 salt bridge present in *Chlamydomonas* is absent among plants. Instead, Lys-305 and Thr-474 form an ionic interaction in plants. Phe-467 packs against catalytic Lys-334, which interacts with the carboxylation transition-state analog CABP. Residues Glu-336 and Glu-338 in loop 6 interact with the 305-474 phylogenetic residues, and could be responsible for transmitting changes in 305-474 directly to the loop, especially to Glu-338, which has a different conformation between *Chlamydomonas* and spinach Rubisco.

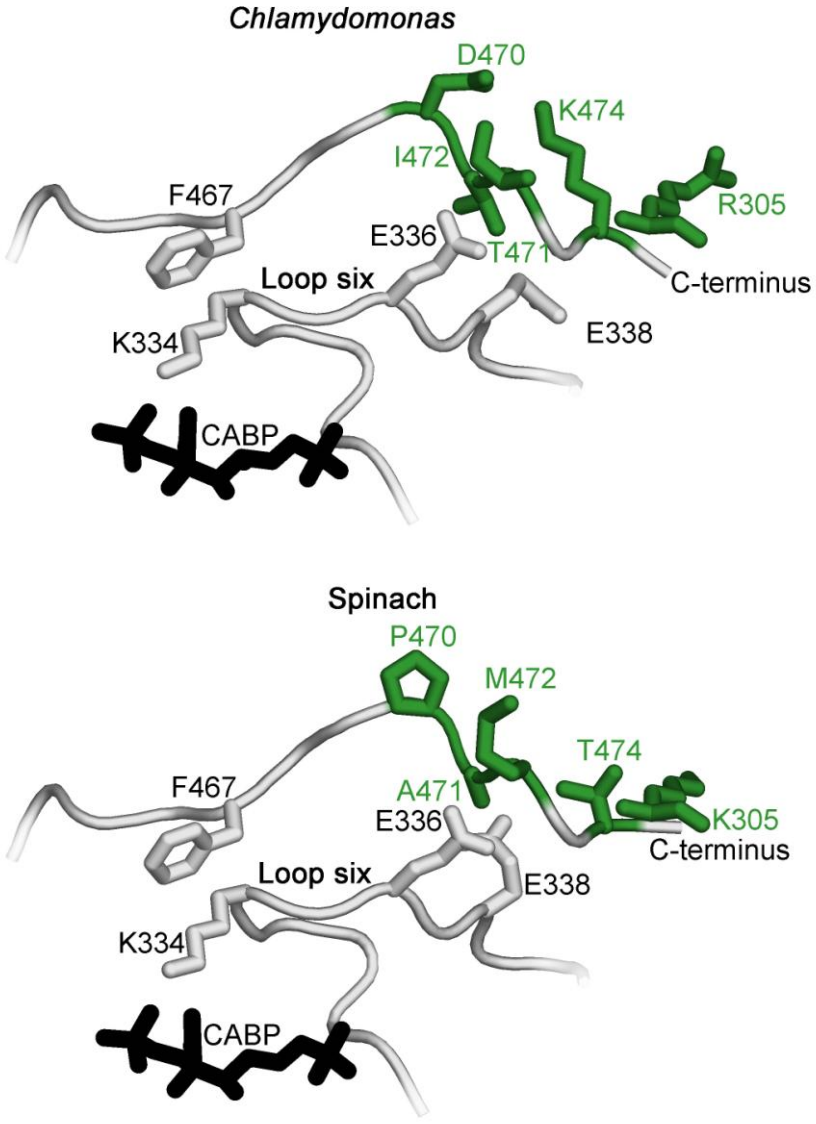
Chlamydomonas
D470
K474
I472
F467
R305
E336
T471
Loop six
C-terminus
K334
E338
CABP
Spinach
P470
M472
T474
F467
A471
K305
E336
C-terminus
Loop six
E338
K334
CABP

Lys-305, which was an additional phylogenetic substitution in the 305-474 mutant (Fig. 9). Nonetheless, the conformational rigidity of the carboxy terminus could affect Phe-467, which packs against active-site Lys-334, thus transmitting changes in the carboxy terminus to the active-site (Fig. 9). Also, interactions between the 305-474 residues and Glu-336 and 338 directly affects catalytic loop 6 (Fig. 9).

As for 442-447 mutant Rubisco, the phylogenetic substitutions are mainly in α-helix G, on the surface of the large-subunit, over 20Å away from the active-site. Thus, it is difficult to map the network of interactions between the 442-447 phylogenetic group and the active site to account for the decreased $K_o$ of the mutant enzyme (Table 4). Nevertheless, the 442-447 phylogenetic group could play a greater role in holoenzyme assembly, which would account for the decreased growth and *in vivo* Rubisco level of the mutant strain (Figs. 5 and 6).

Even though phylogenetic groups 168-399, 305-474 and 442-447 do play a role in Rubisco catalysis, more extensive combinations of phylogenetic groups could be responsible for the shift in kinetic properties between *Chlamydomonas* and plant Rubisco.

## ASSOCIATED GROUPS

### Defining associated groups

Because individual phylogenetic-group substitutions in *Chlamydomonas* Rubisco do not produce plant Rubisco kinetics, combinations of the phylogenetic groups might be required (Tables 3 and 4). However, to create all possible combinations of the 15 phylogenetic groups, which is $2^{15}$ or over 32,000 combinations, would still be overwhelming. Instead, phylogenetic groups can be combined into "associated groups," which are each defined as a combination of a phylogenetic group and all other surrounding phylogenetic groups (Table 5). To be included in an associated-group, the surrounding phylogenetic groups have to be within interacting distance (5 Å) of a non-phylogenetic residue that also interacts with the center phylogenetic group (Table 5). It is not possible for two separate phylogenetic groups to interact with a common phylogenetic residue directly, because the two groups, including the bridging phylogenetic residue, would have been clustered as one phylogenetic group.

Because the previous penta/ABSO mutant had plant-like kinetic properties, the small-subunit βA-βB loop also influences catalysis (Spreitzer *et al.*, 2005). Therefore, this loop was also considered in the associated-group analysis. The βA-βB loop is variable between *Chlamydomonas* and plant Rubisco enzymes (Spreitzer, 2003). The penta/ABSO mutant was created by combining five phylogenetic-residue substitutions and a chimeric Rubisco small subunit that has the βA-βB loop from spinach (Spreitzer *et al.*, 2005). To test the possible role of the βA-βB loop in the associated groups, any associated-group mutants that have the center phylogenetic group in direct contact with the βA-βB loop was combined with the chimeric Rubisco small subunit that has the

**Table 5: Associated groups in *Chlamydomonas* Rubisco.** Phylogenetic groups are based on Table 2. Residue substitutions are listed in Table 6.

| Center phylogenetic group | Surrounding phylogenetic groups | Shared non-phylogenetic residues between groups [a] | Associated groups | |
|---|---|---|---|---|
| | | | Name | Letter |
| 11 | None | None | | |
| 30-32 | 86<br>105-369 | Y85<br>T34 | 30-32Assoc | A |
| 42-53 | 86<br>305-474 | A99<br>R41 | 42-53Assoc | B |
| 86 | 30-32<br>42-53 | Y85<br>A99 | 86Assoc | C |
| 105-369 | 30-32<br>149-282 | T34<br>M371 | 105-369Assoc | D |
| 149-282 | 105-369<br>256-258<br>265 | M371<br>Y283<br>L280, C284 | 149-282Assoc | E |
| 168-399 | 265<br>341<br>391-428 | Y239<br>F345<br>F394, L424 | 168-399Assoc | F |
| 221 | 256-258<br>265 | F218<br>L240 | 221Assoc | G |
| 235 | βA-βB loop [b] | Direct contact | 235Assoc | H |
| 256-258 | 149-282<br>221<br>265<br>βA-βB loop [b] | Y283<br>F218<br>A257<br>Direct contact | 256-258Assoc | I |
| 265 | 149-282<br>168-399<br>221<br>256-258 | L280, C284<br>Y239<br>L240<br>A257 | 265Assoc | J [c] |
| 305-474 | 42-53<br>341 | R41<br>L475 | 305-474Assoc | K |
| 341 | 168-399<br>305-474 | F345<br>L475 | 341Assoc | L |
| 391-428 | 168-399<br>442-447 | F394, L424<br>A426, A430 | 391-428Assoc | -- [d] |
| 442-447 | 391-428 | A426, A430 | 442-447Assoc | -- [d] |

[a] Shared non-phylogenetic residues are within 5 Å from both the center and surrounding phylogenetic groups.

[b] Because the βA-βB loop from the Rubisco small subunit also influences catalysis, phylogenetic-groups that interact with residues in the βA-βB loop are combined with the spinach βA-βB loop when substituted as associated groups.

[c] The 265Assoc associated group alone cannot be recovered by photosynthetic selection, but, when combined with the Rubisco small subunit from *Arabidopsis*, can support photosynthesis. Thus, this strain is noted as "J" in further studies.

[d] The 391-428Assoc and 442-447Assoc associated groups cannot be recovered by photosynthetic selection, and thus, cannot be analyzed.

spinach βA-βB loop. Therefore, the βA-βB loop was also considered a phylogenetic group with regard to associated groups, but it is included in an associated group only if residues of the βA-βB loop are in contact with a phylogenetic group (Table 5).

Different regions of Rubisco can interact. Thus, directed mutagenesis of the associated groups as a whole, coupled with data from separately substituting each phylogenetic group, may provide information about complementation between regions of the holoenzyme. Perhaps combinations of structurally-related phylogenetic groups complement to produce catalytic changes, which might not be obvious from separate phylogenetic-group substitution.

Because each phylogenetic group and the other surrounding phylogenetic groups form each associated group, like the number of phylogenetic groups, there are 15 associated group, for which mutant enzymes can be created and analyzed. However, for phylogenetic group 11, Ala-11 is too distant from any other phylogenetic groups to form an associated group (Table 5). Thus, only 14 associated-group mutants need to be created.

**Recovery of associated-group mutants and their phenotypes**

*Chlamydomonas* associated-group mutants were recovered by chloroplast transformation of the MX3312 (Satagopan and Spreitzer, 2004, 2008; Zhu *et al.*, 2005) and *rbcL*Δ/ABSO *rbcL*-knockout strains followed by photosynthetic selection. The *rbcL*Δ/ABSO strain, which has the spinach-substituted Rubisco small-subunit βA-βB loop (Spreitzer *et al.*, 2005), was used to create associated-group mutants that involve the βA-βB loop (235Assoc and 256-258Assoc) (Table 5). Eleven of the fourteen associated-

group mutant strains could grow photoautotrophically. The 265Assoc, 442-447Assoc, and 391-428Assoc mutants could not be recovered (Table 5). For the mutants that could be recovered, the transformation frequencies were 1-3 X $10^{-6}$ per cells transformed, and the transformants started appearing as photosynthetic colonies on minimal medium within 2 to 4 weeks, which was similarly observed for the wild-type *rbcL* transformants.

Comparison of the growth phenotypes between the associated-group mutants and wild-type *Chlamydomonas* by spot tests (Spreitzer and Mets, 1981) indicated that the 30-32Assoc, 86Assoc, 149-282Assoc, and 221Assoc mutants have reduced photosynthetic growth on minimal medium in the light at the restrictive temperature of 35ºC (spots A, C, E, and G, respectively, Fig. 10). Because these "temperature-conditional phenotypes" are limited to photosynthetic growth, but not heterotrophic growth at 35ºC (Fig. 10), the temperature sensitivity must be specific to a defect in Rubisco. Considering that the 30-32Assoc mutant (V30E/V31T/R32K/D86H/I105L/C369V) and the 86Assoc mutant (D86H/V30E/V31T/R32K/M42V/C53A) have substitutions V30E/V31T/R32K/D86H in common, which is also a combination of phylogenetic groups 30-32 and 86 (Tables 2 and 5), the temperature-conditional phenotypes might be caused by combining the 30-32 and 86 phylogenetic-group substitutions. Similarly, considering that the 149-282Assoc mutant (V149Q/I282H/I105L/C369V/C256F/K258R/I265V) and the 221Assoc mutant (V221C/C256F/K258R/I265V) have substitutions C256F/K258R/I265V in common, which is a combination of phylogenetic groups 256-258 and 265 (Tables 2 and 5), the temperature-conditional phenotypes might be caused by combining the 256-258 and 265 phylogenetic-group substitutions. Moreover, a previous study has shown that combining

**Figure 10: Growth phenotypes of *Chlamydomonas* wild type (WT) and associated-group mutants (spots A through L).** About 2 X $10^5$ cells were spotted at each position at the conditions indicated (Spreitzer and Mets, 1981). Panel A (top) cells were grown for a week. Panel B (bottom) cells were supplemented with 5% $CO_2$ in air and scanned after one week (bottom-left) and after two weeks (bottom-right). Spot letter is based on Table 5.

A

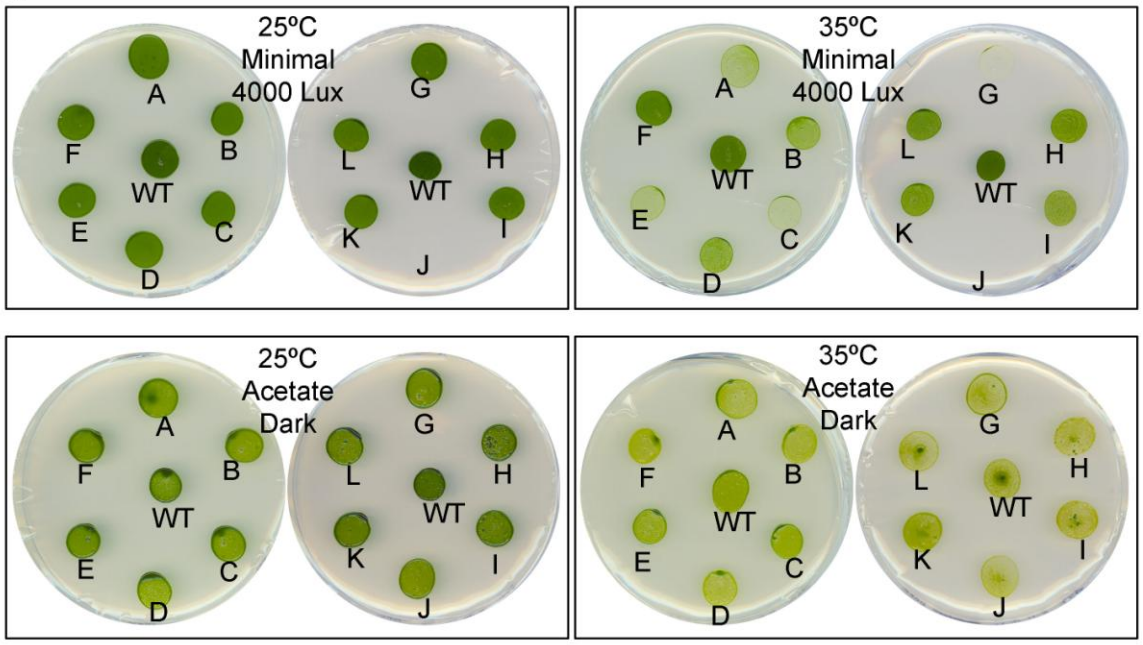
25ºC
Minimal
4000 Lux
A
B
C
D
E
F
WT
G
H
I
J
K
L
35ºC
Minimal
4000 Lux
25ºC
Acetate
Dark
35ºC
Acetate
Dark

B

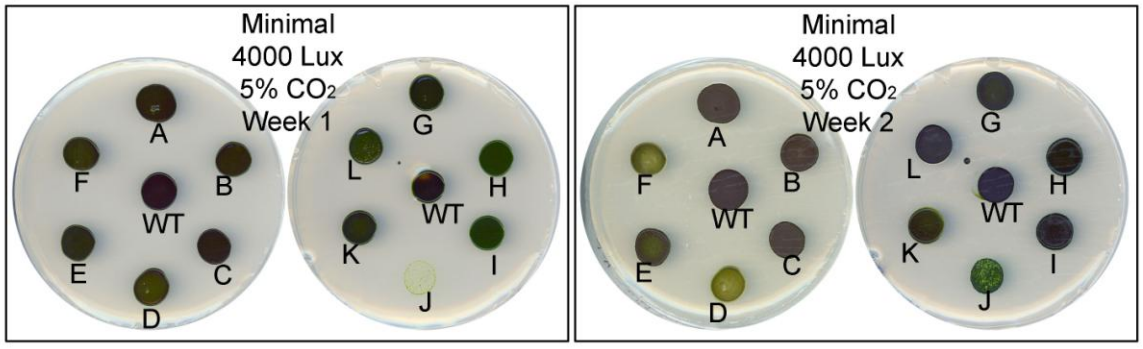
Minimal
4000 Lux
5% $CO_2$
Week 1
Minimal
4000 Lux
5% $CO_2$
Week 2
A
B
C
D
E
F
WT
G
H
I
J
K
L

the 256-258 and 265 phylogenetic-group substitutions does produce a temperature-conditional *Chlamydomonas* mutant (Spreitzer *et al.*, 2005). On the other hand, the temperature-conditional phenotypes of the 30-32Assoc and 86Assoc mutant strains could be attributed to phylogenetic substitutions in a region that affects the interaction between Rubisco and Rubisco activase (Larson *et al.*, 1997; Ott *et al.*, 2000).

For the associated-group mutants that could not be recovered, attempts were also made to transform into the *rbcL*Δ/ABSO and *rbcL*Δ/SSAT strains (Dent *et al.*, 2005; Genkov *et al.*, 2010; Genkov and Spreitzer, unpublished). Interestingly, the 265Assoc mutant produced photosynthetic colonies when transformed in the cell-walled *rbcL*Δ/SSAT strain, which has the Rubisco small subunit substituted with that of *Arabidopsis* (Dent *et al.*, 2005; Genkov *et al.*, 2010; Genkov and Spreitzer, unpublished). However, this 265Assoc/SSAT transformant required 5% v/v $CO_2$ in air for growth, and colonies were visible only after three weeks compared to six days for the wild-type *rbcL* transformants. In fact, spot tests indicated that the 265Assoc/SSAT strain has less photosynthetic growth than wild type even after two weeks on minimal medium with 5% $CO_2$ (spot J, Fig. 10). The other two associated-group mutants, 391-428Assoc and 442-447Assoc, could not be recovered in any of the transformation hosts.

**Rubisco holoenzyme level**

To determine the effects of the mutations on the amount of Rubisco *in vivo*, SDS-PAGE and western blotting were performed. Almost all the associated-group mutant strains expressed equal amounts of Rubisco when compared with wild type except for the

265Assoc/SSAT mutant strain, which had reduced *in vivo* holoenzyme level as evidenced on the western blots (lane J, Fig. 11). The decreased Rubisco holoenzyme level of the 265Assoc/SSAT mutant strain could account for the high-$CO_2$-requiring phenotype (spot J, Fig. 10).

A thermal-inactivation experiment (Chen *et al.*, 1993) was performed to see whether the 265Assoc/SSAT mutant enzyme was unstable (Fig. 12). Whereas the wild-type enzyme was unaffected by a 55ºC incubation, the mutant enzyme lost 80% of its activity at this temperature. Thus, the phylogenetic substitutions I265V/V149Q/I282H/G168P/L326I/M349L/M375L/A398S/C399V/V221C/C256F/K258R, together with the *Arabidopsis* small subunit, caused the 265Assoc/SSAT mutant enzyme to be more unstable than the wild-type enzyme (Fig. 12).

Reductions in holoenzyme levels for 35ºC-grown *Chlamydomonas* cells were observed in the western blots for the 149-282Assoc and 221Assoc mutant strains (lanes E and G, respectively, Fig. 11), which would explain their temperature-conditional phenotypes (spots E and G, respectively, Fig. 10). A previous study has shown that the C256F/K258R/I265V substitutions, which are present in the 149-282Assoc and 221Assoc associated-group mutants, caused a similar reduction in holoenzyme level in *Chlamydomonas* cells grown at 35ºC (Spreitzer *et al.*, 2005). However, the reduction in holoenzyme level was not caused by increased holoenzyme instability, but likely due to increased susceptibility to proteolysis (Du *et al.*, 2003; Spreitzer *et al.*, 2005). Thus, the 149-282Assoc and 221Assoc associated-group substitutions might also alter Rubisco structure sufficiently to increase the susceptibility of the enzymes to proteolysis *in vivo*, especially at elevated 35ºC.

**Figure 11: SDS-PAGE (left) and western-blot analysis (right) of total soluble proteins from *Chlamydomonas* wild type (WT) and associated-group mutants (A to L).** Sixty micrograms of total soluble protein from cells grown in the dark at 25ºC (top) or 35ºC (bottom) were run in each lane. Mutant letter is based on Table 5. LS denotes the Rubisco large subunit, and SS denotes the small subunit.

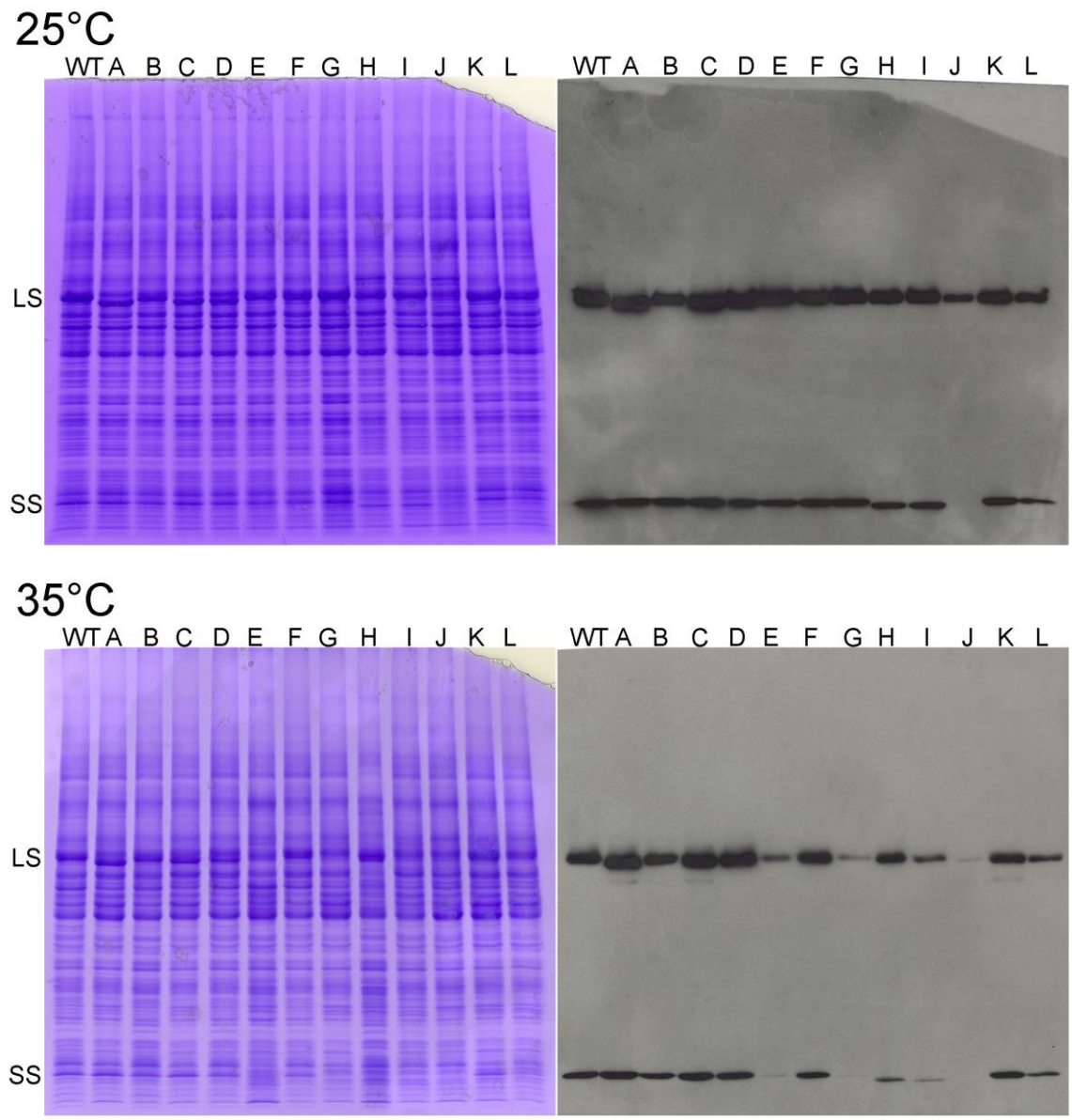
25°C
WT A B C D E F G H I J K L
WT A B C D E F G H I J K L
LS
SS
35°C
WT A B C D E F G H I J K L
WT A B C D E F G H I J K L
LS
SS

**Figure 12: Thermal inactivation of Rubisco purified from *Chlamydomonas* wild type (WT) and the 265Assoc/SSAT mutant.** Five micrograms of Rubisco were pre-incubated at the indicated temperatures for 10 min, and then cooled on ice for 5 min before assaying for carboxylase activity at 25ºC for 1 min. The measured activity after each pre-incubation temperature was normalized to that of 35ºC-pre-incubation. The specific activity after the 35ºC pre-incubation was 1.1 µmol $CO_2$ fixed/min/mg protein for wild-type Rubisco, and 0.1 µmol/min/mg for the 265Assoc/SSAT enzyme.

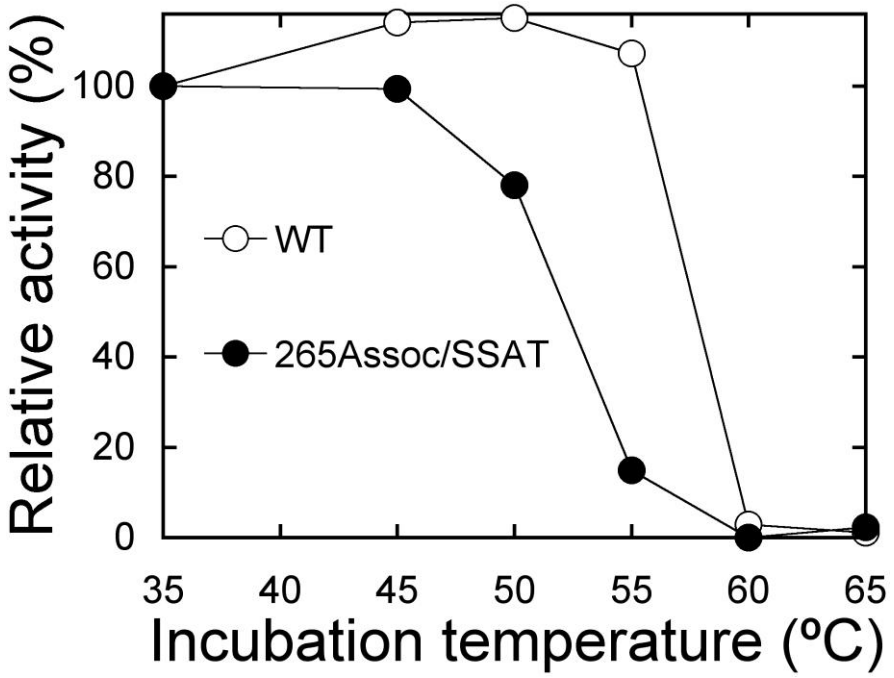
Relative activity (%)
100
80
60
40
20
0
WT
265Assoc/SSAT
35
40
45
50
55
60
65
Incubation temperature (ºC)

**Kinetic properties**

Because Ω defines the rate-limiting step of the carboxylation and oxygenation reactions of Rubisco, and differs between land-plant and *Chlamydomonas* enzymes, Ω was measured for all the associated-group mutant enzymes. Similar to the phylogenetic-group mutant enzymes, none of the associated-group mutant enzymes have increased Ω values (Table 6). The 265Assoc/SSAT mutant enzyme has an increased Ω (Table 6), but this 10% increase can be attributed to substituting the entire small subunit from *Arabidopsis* (Genkov *et al.*, 2010).

Phylogenetic-group mutant 168-399 has a decrease in Ω (Table 3), but when combined with phylogenetic groups 305-474 and 341 to produce the 341Assoc associated-group mutant, the resulting mutant enzyme has Ω restored to the wild-type value (Table 6). Therefore, the 168-399 group substitutions are complemented by the 305-474 and 341 groups. More likely, the 305-474 substitutions are responsible for restoring the Ω value of the 168-399 mutant enzyme because the 305-474 mutant enzyme has an increased $K_o$ (Tables 3 and 4) whereas the 341 mutant enzyme (V341I) has kinetic properties indistinguishable from wild-type Rubisco (Zhu and Spreitzer, 1996).

**Structural analysis of the associated-group mutants**

The Ω-reducing 168-399 phylogenetic-group (G168P/L326I/M349L/M375L/ A398S/C399V) is at the base of loop 6 (Figs. 8 and 13). The other complementary phylogenetic groups 305-474 (R305K/D470E/T471A/I472M/K474T) and 341 (V341I), which restore the Ω value as demonstrated by the 341Assoc associated-group mutant

**Table 6: Ω values of Rubisco purified from *Chlamydomonas* wild type and associated-group mutants.**

| Enzymes (Letter) | Residue substitutions | Ω [a] ($V_cK_o/V_oK_c$) |
|---|---|---|
| Wild type | None | 61 ± 2 |
| 30-32Assoc (A) | V30E/V31T/R32K/D86H/I105L/C369V | 61 ± 2 |
| 42-53Assoc (B) | M42V/C53A/D86H/R305K/D470E/T471A/I472M/ K474T | 60 ± 2 |
| 86Assoc (C) | D86H/V30E/V31T/R32K/M42V/C53A | 55 ± 2 |
| 105-369Assoc (D) | I105L/C369V/V30E/V31T/R32K/V149Q/I282H | 63 ± 2 |
| 149-282Assoc (E) | V149Q/I282H/I105L/C369V/C256F/K258R/I265V | 61 ± 2 |
| 168-399Assoc (F) | G168P/L326I/M349L/M375L/A398S/C399V/I265V/ V341I/V391T/T428V | 57 ± 4 |
| 221Assoc (G) | V221C/C256F/K258R/I265V | 54 ± 2 |
| 235Assoc (H) | V235I/ABSO (spinach small-subunit βA-βB loop) | 56 ± 1 |
| 256-258Assoc (I) | C256F/K258R/V149Q/I282H/V221C/I265V/ ABSO (spinach small-subunit βA-βB loop) | 60 ± 2 |
| 265Assoc/ SSAT (J) | I265V/V221C/V149Q/I282H/G168P/L326I/M349L/ M375L/A398S/C399V/C256F/K258R/ SSAT (*Arabidopsis* small-subunit) | 66 ± 2 |
| 305-474Assoc (K) | R305K/D470E/T471A/I472M/K474T/M42V/C53A/ V341I | 62 ± 3 |
| 341Assoc (L) | V341I/G168P/L326I/M349L/M375L/A398S/C399V/ R305K/D470E/T471A/I472M/K474T | 64 ± 2 |

[a] Values are the means ± S.D. ($n$ - 1) of three separate enzyme preparations.

**Figure 13: Structural comparison of residues in associated group 341Assoc consisting of phylogenetic groups 168-399 (red) at the base of catalytic loop 6, 305-474 (green) at the carboxy-terminal tail, and 341 (blue) in α-helix 6.** Glu-338 in α-helix 6 is in van der Waals contact with Ala-471 in *Chlamydomonas* Rubisco, but caps the N-terminal end of α-helix 6 in spinach Rubisco. The CABP transition-state analog denotes the active site.

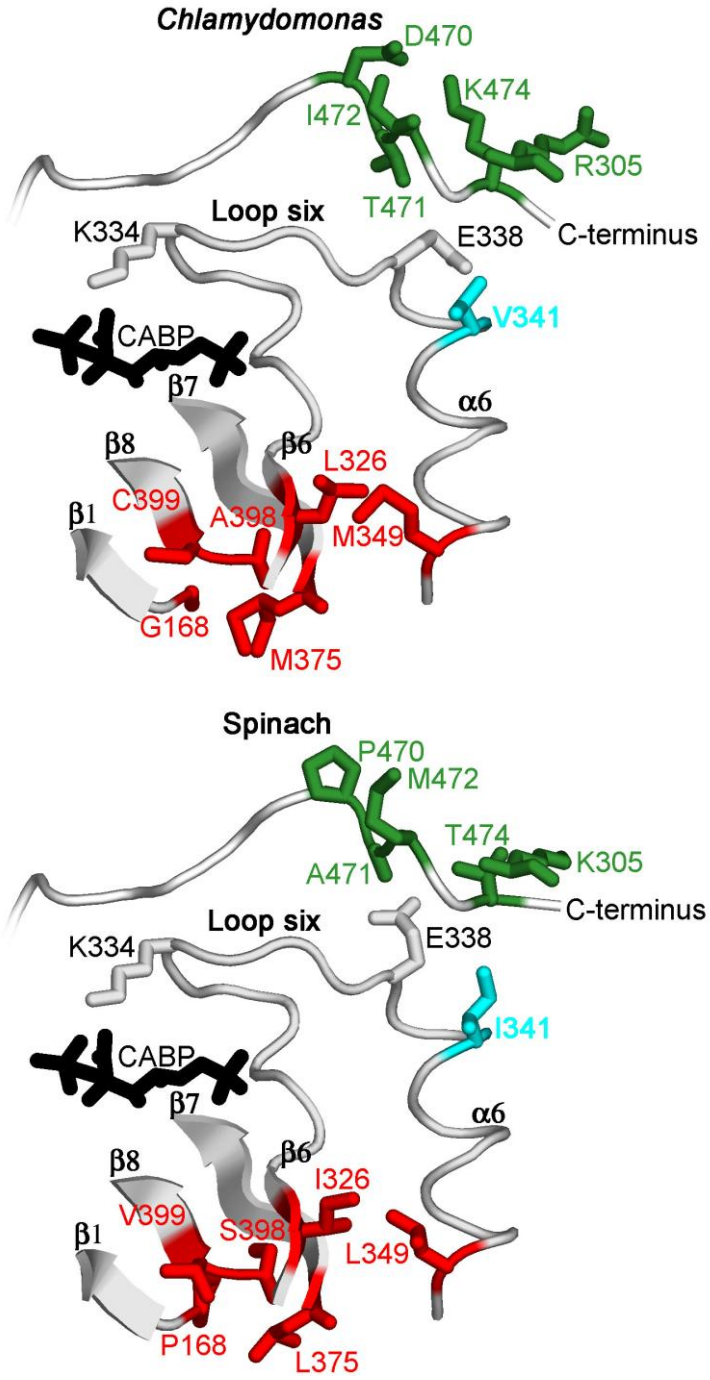
Chlamydomonas
D470
K474
I472
R305
T471
Loop six
K334
E338
C-terminus
V341
CABP
β7
α6
β8
β6
L326
C399
β1
A398
M349
G168
M375
Spinach
P470
M472
T474
A471
K305
C-terminus
Loop six
K334
E338
I341
CABP
β7
α6
β8
β6
I326
V399
β1
S398
L349
P168
L375

enzyme, are in the carboxy terminus (Figs. 9 and 13) and α-helix 6 of the Rubisco large subunit, respectively (Fig. 13). Comparison of the x-ray crystal structures of *Chlamydomonas* and spinach Rubisco indicates that the T471A substitution could change the conformation of the carboxylate side chain of Glu-338 at the amino-terminal end of α-helix 6 (Fig. 13). In spinach Rubisco, Ala-471 is in van der Waals contact with Glu-338, but in *Chlamydomonas*, the bulkier Thr-471 prevents the carboxylate side chain of Glu-338 from occupying the same space. Instead, the negatively-charged side chain is turned towards the amino-terminal end of α-helix 6, and may neutralize the partial positive charge from the α-helix dipole (Fig. 13).

In addition, the phylogenetic V341I substitution enables residue 341 in α-helix 6 to form van der Waal contact with residue 474 in the carboxy terminus through the longer isoleucine side chain as seen in spinach Rubisco (Fig. 13). This may strengthen the interaction between α-helix 6 and the carboxy terminus. Perhaps the increased interaction between α-helix 6 and the carboxy terminus, namely between Glu-338 and Ala-471, and between Ile-341 and Thr-474, complements some subtle structural perturbations caused by the 168-399 phylogenetic substitutions at the base of loop 6 (Fig. 13).

In the 265Assoc associated-group mutant, a combination of the 168-399 phylogenetic-group substitutions (G168P/L326I/M349L/M375L/A398S/C399V) at the base of loop 6 with phylogenetic groups 149-282, 221, 256-258, and 265 (V149Q/I282H, V221C, C256F/K258R and I265V) near the interface between large and small subunits cannot be recovered through photosynthetic selection. However, transforming the 265Assoc mutant gene into a *Chlamydomonas* strain that expresses the *Arabidopsis* small

subunit (Genkov and Spreitzer, unpublished) produces a mutant strain that can grow photosynthetically, albeit at only 5% $CO_2$ in air (Fig. 10). In other words, the land-plant small subunit complements the large-subunit phylogenetic changes in the 265Assoc associated group in *Chlamydomonas*. Because replacement of the small-subunit βA-βB loop with that of spinach complements the large-subunit changes in the penta/ABSO enzyme to produce plant-like kinetic properties (Spreitzer *et al.*, 2005), an attempt was made to transform the 265Assoc mutant gene into the *rbcL*Δ/ABSO *Chlamydomonas* strain to determine whether replacement of the βA-βB loop with that of spinach was sufficient to complement the 265Assoc large-subunit substitutions. Moreover, among the residue changes in 265Assoc are V221C/C256F/K258R/I265V, which are four of the five phylogenetic substitutions in the large subunit of the penta/ABSO mutant (Spreitzer *et al.*, 2005). However, no photosynthetic transformants were recovered in this experiment. Therefore, some other regions of the Rubisco small subunit may complement the 265Assoc substitutions. Because the loop between β-strands C and D of the small subunit, the βC-βD loop, is also variable among species, with photosynthetic bacteria and non-green algae having two additional residues in the loop (Spreitzer, 2003), changes in the βC-βD loop could be responsible for complementing the 265Assoc substitutions (Fig. 14). The *Chlamydomonas* small subunit has Lys-114 in the βC-βD loop, and the corresponding plant residue is Arg-108. Both of these residues form a salt bridge with Asp-397 in the large subunit.

For the 391-428Assoc and 442-447Assoc associated-group substitutions, which cannot be recovered by photosynthetic selection, the substitutions common to both associated groups are V391T/T428V/G442N/D443E/V444I/S447E (Table 6). These are

**Figure 14: Structural comparison of residues in the associated group 265Assoc consisting of phylogenetic groups 149-282 (pale green), 168-399 (red), 221 (bright green), 256-258 (pink), and 265 (purple).** The entire small subunit is colored yellow. Non-phylogenetic residues at the interface between large and small subunits are shown as faded sticks. Residues of the βC-βD loop of the small subunit are labeled (112 to 115 in *Chlamydomonas*; 106 to 109 in spinach). The CABP transition-state analog denotes the active site.

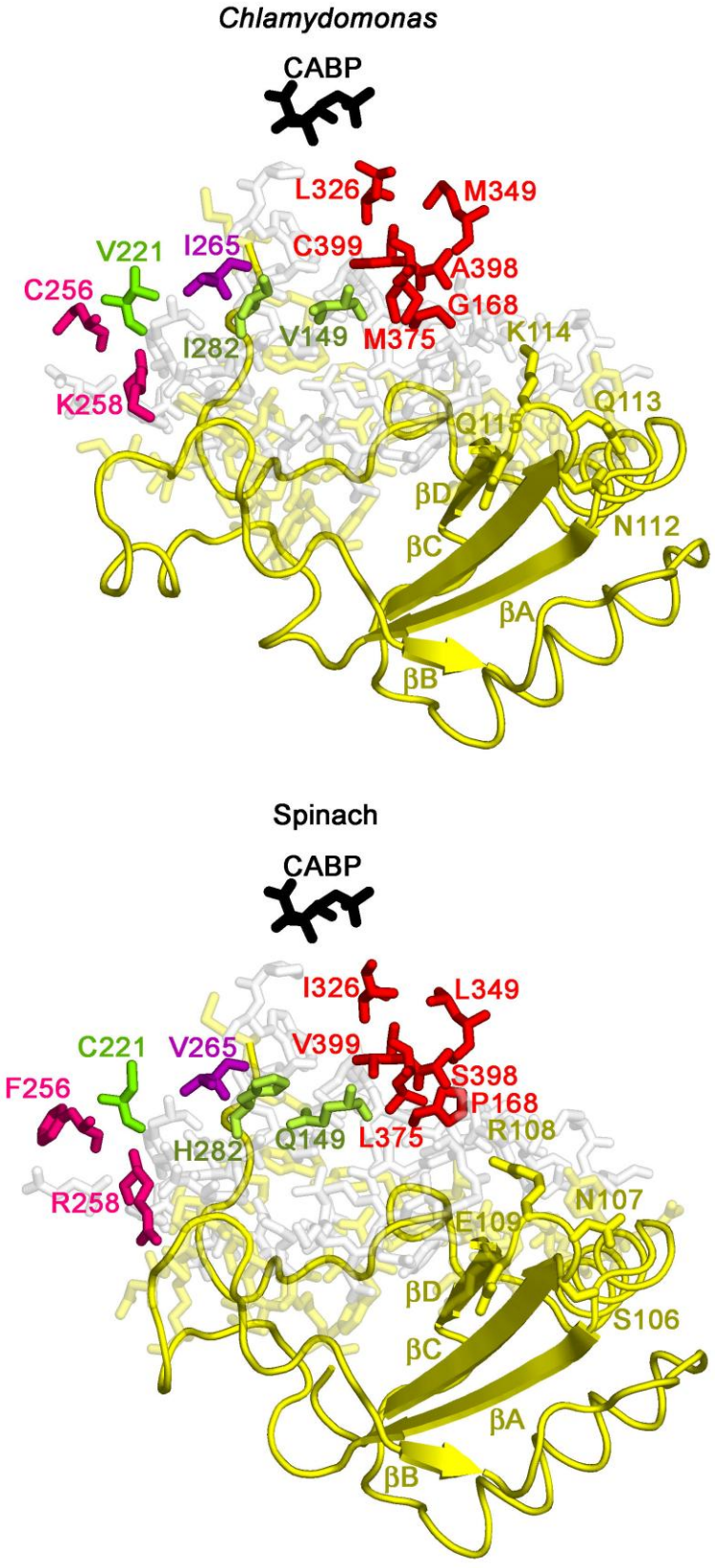
Chlamydomonas
CABP
L326
M349
V221
I265
C399
A398
C256
G168
I282
V149
M375
K114
K258
Q113
Q115
βD
N112
βC
βA
βB
Spinach
CABP
I326
L349
C221
V265
V399
S398
F256
P168
R108
H282
Q149
L375
R258
N107
E109
βD
S106
βC
βA
βB

a combination of the 391-428 and 442-447 phylogenetic-group substitutions (Tables 2 and 5). The 442-447 residues are in α-helix G of the Rubisco large subunit whereas the 391 and 428 residues are in α-helices 7 and 8, respectively (Fig. 15).

Of the 391-428 and 442-447 phylogenetic groups, only phylogenetic residues Gly-442, Asp-443, and Ser-447, which are all in α-helix G, are on the surface of the holoenzyme (Fig. 13). Phylogenetic residues Gly-442 and Asp-443 are substituted with Asn-442 and Glu-443 in most land plants, effectively replacing the residue side chains with longer polar functional groups, thus allowing for better interaction with Arg-446 (Fig. 13). Similarly, phylogenetic residue Ser-447 is more commonly Asp-447 in land plants, which forms a salt bridge with Arg-435 (Fig. 13). Another residue in α-helix G, Trp-451, also has a different conformation between *Chlamydomonas* and Spinach Rubisco (Fig. 13). Because the 442-447 phylogenetic-group substitutions, G442N/D443E/V444I/S447E, caused a decrease in Rubisco holoenzyme level (Fig. 4), and the mutant strain has reduced photosynthetic growth (Fig. 3), changes in electrostatic interactions on the surface of α-helix G involving phylogenetic residues 442, 443 and 447 might affect interactions with chaperones or other protein molecules that assist in the assembly of the hexadecameric Rubisco.

Perhaps the addition of other phylogenetic-residue substitutions in the 391-428Assoc and 442-447Assoc associated-group mutants exacerbate the reduction in Rubisco holoenzyme assembly, which would explain the inability to recover the associated-group mutants in *Chlamydomonas* through photosynthetic selection. The other non-surface phylogenetic residues common to the 391-428Assoc and 442-447Assoc phylogenetic-groups are Val-391, Thr-428, and Val-444. Of these residues, Thr-428 is in

**Figure 15: Structural comparison of phylogenetic residues common to both the 391-428Assoc and 442-447Assoc associated groups consisting of phylogenetic groups 391-428 (brown) in α-helices 7 and 8, and 442-447 (blue) in α-helix G.** Non-phylogenetic residues that might be altered in their interactions because of the phylogenetic changes are shown as white sticks for the large-subunit or yellow sticks for the small subunit. The backbone of large-subunit α-helices 7, 8, and G, and small-subunit N-terminal loop (residues 1-22) are represented as ribbons.

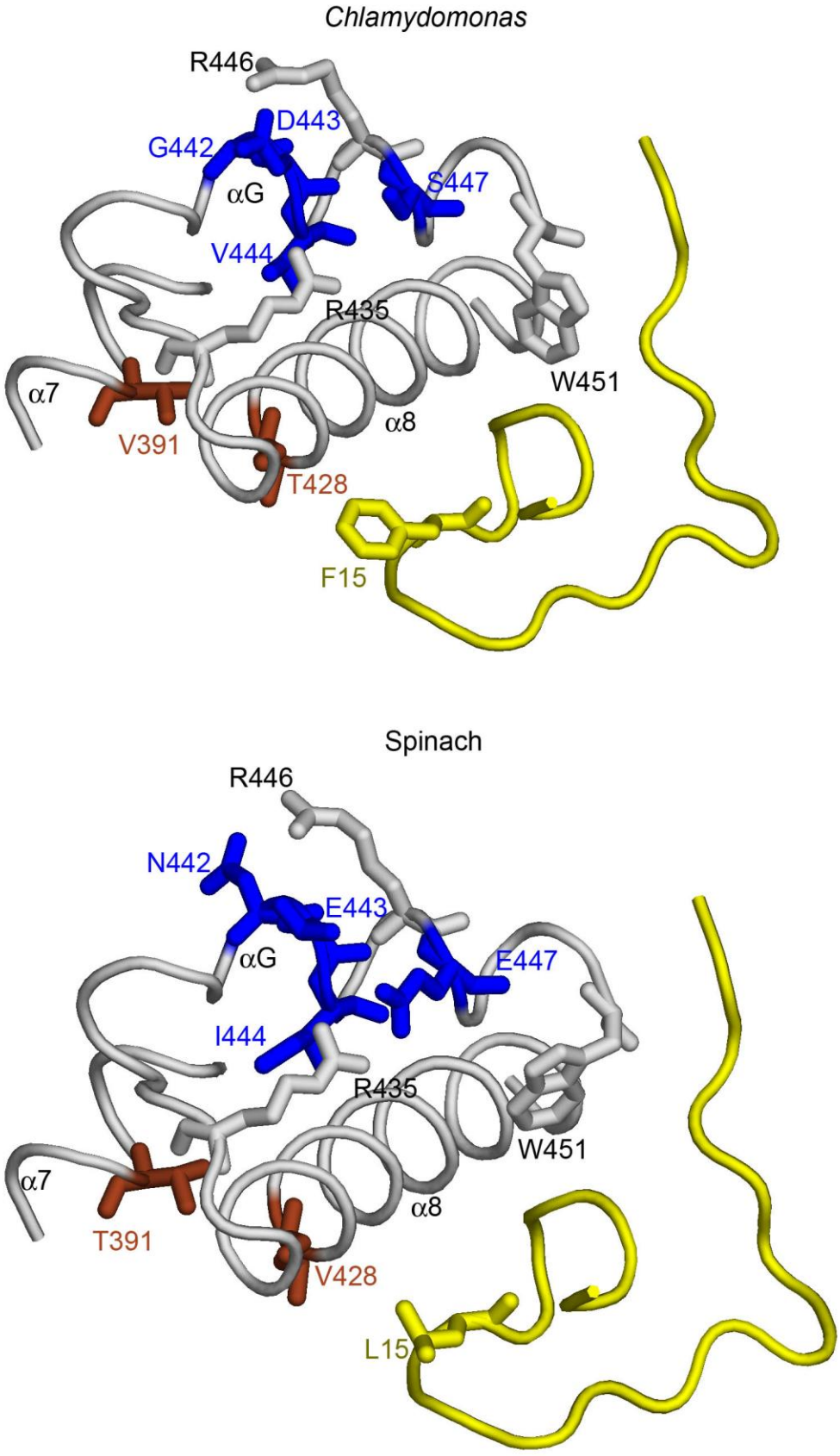
Chlamydomonas
R446
D443
G442
αG
S447
V444
R435
W451
α7
α8
V391
T428
F15
Spinach
R446
N442
E443
αG
E447
I444
R435
W451
α7
α8
T391
V428
L15

van der Waals contact with Phe-15 from the Rubisco small subunit (Fig. 13). In land plants, large-subunit phylogenetic-residue Thr-428 is substituted with Val-428, small-subunit residue Phe-15 is substituted with Leu-15, and the distance between the two residues is greater in plant Rubisco (Fig. 13). A previous study showed that a Rubisco mutant with a small-subunit L18A substitution, which might affect the interaction with residue 15, lacked holoenzyme even though the subunits were expressed (Genkov and Spreitzer, 2009).

A switch in species-specific intermolecular interactions between Rubisco and Rubisco activase was also observed when the surface residues 89 and 94 of the Rubisco large subunit were changed from those of *Chlamydomonas* (non-Solanaceae) to those of tobacco (Solanaceae) (Larson *et al.*, 1997; Ott *et al.*, 2000). Similarly, the surface residues in the 442-447 phylogenetic-group on α-helix G could define a switch region for species-specific interactions between Rubisco and chaperones. *Flaveria* and sunflower Rubisco large subunits can be expressed and assembled in tobacco, and all three species are identical for the surface phylogenetic-residues 442, 443, and 447 in the 442-447 phylogenetic group (Kanevski *et al.*, 1999; Whitney *et al.*, 2011). On the other hand, the Rubisco large subunits from the rhodophyte *Galdieria sulphuraria* and the diatom *Phaeodactylum tricornutum* can be expressed but not assembled in tobacco, and the identities of the residues 442, 443 and 447 from the foreign Rubiscos are different from tobacco (Whitney *et al.*, 2001). Rubisco chaperone RbcX binds specifically to a stretch of seven amino acids in the carboxy terminus of the *Synechococcus* large subunit (Saschenbrecker *et al.*, 2007), which corresponds to residues 464-470 in *Chlamydomonas*. However, a subsequent study indicated that α-helices 8, G, and H

could be involved in chaperone release by undergoing a conformational change of as much as 8 Å (Saschenbrecker *et al.*, 2007; Liu *et al.*, 2010).

It is surprising that none of the associated-group substitutions have significant increases in Ω characteristic of plant Rubisco even though the holoenzyme is being structurally altered to mimic the plant enzyme. The phylogenetic substitutions in the penta/ABSO mutant, and the large/small-subunit region defined by the substitutions, must be truly unique because penta/ABSO is the only phylogenetic mutant enzyme with kinetic properties similar to those of plants (Spreitzer *et al.*, 2005).

## PENTA/ABSO DISSECTION

### Penta/ABSO

The success of the phylogenetic approach was demonstrated by a previous study in which a Rubisco *Chlamydomonas*-to-plant substitution of five large-subunit phylogenetic residues (V221C/V235I/C256F/K258R/I265V), together with the spinach small-subunit βA-βB loop, produced a mutant enzyme with kinetic properties similar to those of plants (Spreitzer *et al.*, 2005). This penta/ABSO enzyme had an increase in Ω by 17% and a decrease in $V_c$ by 50% (Spreitzer *et al.*, 2005). To determine the minimal number of phylogenetic changes that actually plays a role in the catalytic shift of the penta/ABSO enzyme, further dissection of the interactions within the phylogenetic residues and βA-βB loop is warranted. Because five large-subunit phylogenetic residues and the βA-βB loop are changed in the penta/ABSO mutant enzyme, to dissect the structural interactions by creating all possible combinations would require the creation and analysis of $2^6$ (= 64) mutant enzymes. Instead, the five large-subunit phylogenetic residues can be grouped into four phylogenetic groups, and the βA-βB loop can be considered an additional group. To be specific, the residue substitutions in penta/ABSO, V221C/V235I/C256F/ K258R/I265V/ABSO, can be separated into substitutions of phylogenetic groups 221, 235, 256-258, 265, and ABSO (Table 2). Previous studies have shown that just substituting the five separate groups alone do not produce plant-Rubisco kinetic-properties (Du *et al.*, 2003; Karkehabadi *et al.*, 2005; Spreitzer *et al.*, 2005). At a next level, pairwise combinations of the groups could be substituted, but that would still require creating and analyzing ten mutant enzymes. Instead, if only pairs of associated phylogenetic groups are considered, then only five mutant enzymes need to be created

(Table 7). One of these mutant enzymes, C256F/K258R/I265V, was created previously, but it had a 10% decrease in Ω rather than the >30% increase characteristic of plant Rubisco (Du *et al.*, 2003; Spreitzer *et al.*, 2005). The V235I/ABSO mutant enzyme was created as the 235Assoc enzyme (Tables 5 and 6). Thus, only three additional mutant enzymes remained to be created and analyzed.

**Recovery of penta/ABSO-dissection mutants and their phenotypes**

*Chlamydomonas* penta/ABSO-dissection mutants were recovered by chloroplast transformation of the MX3312 (Zhu *et al.*, 2005; Satagopan and Spreitzer, 2004, 2008) and *rbcL*Δ/ABSO *rbcL*-knockout strains followed by photosynthetic selection. The *rbcL*Δ/ABSO strain, which has the small-subunit βA-βB loop from spinach (Spreitzer *et al.*, 2005), was used to create the V235I/ABSO and C256F/K258R/ABSO mutants (Table 7). All the penta/ABSO-dissection mutant strains could grow photoautotrophically, and transformation frequencies were 1-3 X $10^{-6}$ per cells shot. Transformants started to appear on minimal medium within 2 to 4 weeks, which was also observed for wild-type *rbcL* transformants.

Comparison of the growth phenotype between the penta/ABSO-dissection mutants and wild-type *Chlamydomonas* by spot tests (Spreitzer and Mets, 1981) indicated that the C256F/K258R/I265V mutant had reduced photosynthetic growth (spot 4, Fig. 16) as observed previously (Du *et al.*, 2003; Spreitzer *et al.*, 2005). The rest of the mutant strains had somewhat reduced growth on minimal medium at 35ºC in comparison to wild type (Fig. 16). When grown on acetate medium in the dark, the mutant strains were indistinguishable from wild type (Fig. 16). Therefore, the reduction in growth must be

**Table 7: Pairwise combinations of associated phylogenetic groups created to dissect the penta/ABSO mutant.** Phylogenetic groups are defined in Table 2.

| First phylogenetic group | Second Phylogenetic group | Shared non-phylogenetic residues between groups [a] | Necessary residue substitutions |
|---|---|---|---|
| 221 | 256-258 | F218 | V221C/C256F/K258R |
| 221 | 265 | L240 | V221C/I265V |
| 235 | βA-βB loop [b] | Direct contact | V235I/ABSO [c] |
| 256-258 | 265 | A257 | C256F/K258R/I265V [d] |
| 256-258 | βA-βB loop [b] | Direct contact | C256F/K258R/ABSO |

[a] Shared non-phylogenetic residues are within 5 Å from both phylogenetic groups.

[b] Because the small-subunit βA-βB loop also influences catalysis, it is included as a phylogenetic group.

[c] V235I/ABSO was created and analyzed as the 235Assoc mutant enzyme (Tables 5 and Table 6).

[d] The C256F/K258R/I265V mutant strain was created and analyzed previously (Du *et al.*, 2003; Spreitzer *et al.*, 2005).

**Figure 16: Growth phenotypes of *Chlamydomonas* wild type (WT), penta/ABSO-dissection mutants V221C/C256F/K258R (spot 1), V221C/I265V (spot 2), V235I/ABSO (spot 3), C256F/K258R/I265V (spot 4) and C256F/K258R/ABSO (spot 5), and penta/ABSO (V221C/V235I/C256F/K258R/I265V/ABSO) (spot 6).** About 2 X $10^5$ cells were spotted at each position, and grown for one week on minimal medium at 4000 Lux or acetate medium in darkness at either 25 or 35ºC.

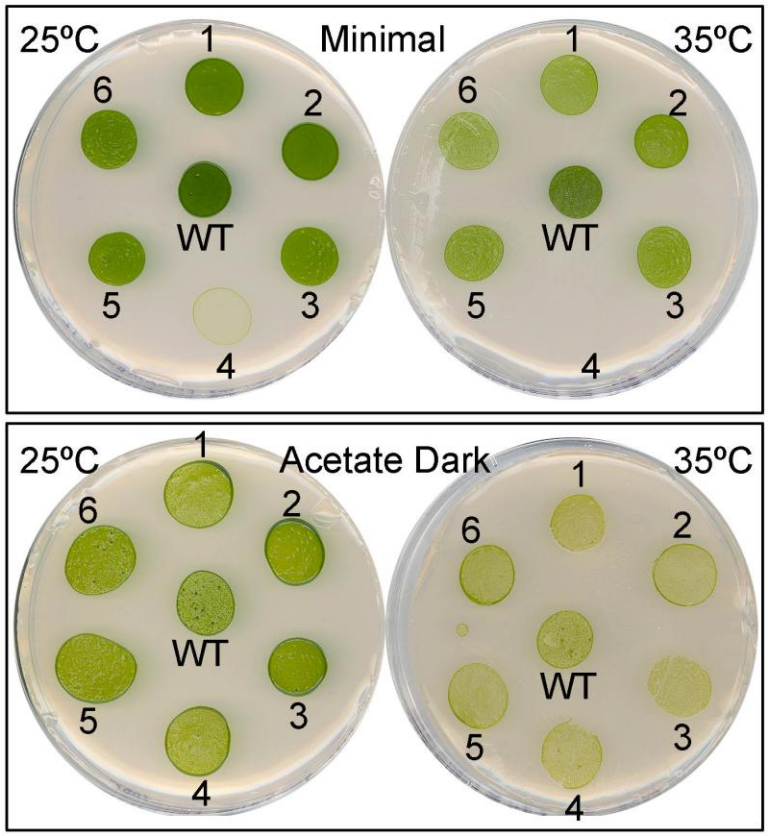
25ºC
Minimal
35ºC
1
2
3
4
5
6
WT
25ºC
Acetate Dark
35ºC
1
2
3
4
5
6
WT

specific to a defect in Rubisco. Previous studies showed that the reduced growth of the C256F/K258R/I265V mutant strain is caused by a decrease in the amount and activity of Rubisco *in vivo* (Du *et al.*, 2003; Spreitzer *et al.*, 2005).

**Kinetic properties**

All the penta/ABSO-dissection mutant enzymes have reduced carboxylase specific activities when measured with saturating $CO_2$ (12.4 mM $NaHCO_3$) (Table 8). The V221C/C256F/K258R, V221C/I265V, V235I/ABSO, and C256F/K258R/ABSO mutant enzymes have carboxylase specific activities of 30%, 64%, 56%, and 44%, respectively, in comparison with the wild-type enzyme. In fact, even the C256F/K258R/I265V enzyme that was analyzed previously had a $V_c$ decreased to 46% of the wild-type value (Du *et al.*, 2003; Spreitzer *et al.*, 2005). Considering that the penta/ABSO enzyme has only 57% of the $V_c$ value of the wild-type enzyme (Spreitzer *et al.*, 2005), the reduction in carboxylase activity seems to be a common feature of changing several phylogenetic residues at a time. However, whereas the penta/ABSO mutant has an Ω value increased by 17% (Spreitzer *et al.*, 2005), none of the dissection mutants has an increase in Ω. Instead, Ω is either unchanged, or reduced by 12% and 7% for the V221C/C256F/K258R and V235I/ABSO mutant enzymes, respectively. There are no significant changes in $O_2$ inhibition among the dissection-mutant enzymes when compared to the wild-type enzyme. However, for the penta/ABSO enzyme, because of a beneficial increase in $K_o$ and decrease in $K_c$, a decrease in $O_2$ inhibition would be expected (Spreitzer *et al.*, 2005). Perhaps all the phylogenetic-residue substitutions in the penta/ABSO mutant are required for the 17% increase in Ω, 54% decrease in $V_c$, 30%

**Table 8: Ω, specific activity, and oxygen inhibition of Rubisco purified from *Chlamydomonas* wild type and penta/ABSO-dissection mutants.**

| Enzyme | RuBP carboxylase activity | | | Ratio (A/B) | Ω [a] $V_cK_o/V_oK_c$ |
|---|---|---|---|---|---|
| | 100% $N_2$ 12.4 mM $NaHCO_3$ | 100% $N_2$ 0.98 mM $NaHCO_3$ (A) | 100% $O_2$ 0.98 mM $NaHCO_3$ (B) | | |
| | *µmol CO2/hr/mg of protein* | | | | |
| Wild type | 103.7 | 28.2 | 11.2 | 2.5 | 60 ± 1 |
| V221C/V235I/C256F/K258R/I265V/ABSO (Penta/ABSO) | | | | | 70 ± 2 [b] |
| V221C/C256F/K258R | 29.8 | 5.7 | 2.7 | 2.1 | 53 ± 1 |
| V221C/I265V | 64.9 | 17.0 | 7.2 | 2.4 | 58 ± 1 |
| V235I/ABSO | 56.4 | 6.8 | 2.8 | 2.4 | 56 ± 1 |
| C256F/K258R/I265V | | | | | 54 ± 2 [b] |
| C256F/K258R/ABSO | 44.0 | 9.9 | 4.4 | 2.3 | 59 ± 1 |

[a] Values are the means ± S.D. ($n$ - 1) of three separate enzyme preparations.

[b] Values are from a previous study (Spreitzer *et al.*, 2005).

decrease in $K_c$, 6% increase in $K_o$, and 37% decrease in $V_o$ (Spreitzer *et al.*, 2005), which represent a shift to the kinetic properties of plant Rubisco. In conclusion, future genetic engineering aimed at improving Rubisco should target all the penta/ABSO phylogenetic residues and the small-subunit βA-βB loop.

It is interesting that Cys-256, which is one of the penta/ABSO residues in van der Waals contact with the small-subunit βA-βB loop, is S-methylated (Taylor *et al.*, 2001). Because plant Rubisco has Phe-256 in place of Cys-256, perhaps S-methylation, which also occurs at phylogenetic residue Cys-369 in *Chlamydomonas* Rubisco (Taylor *et al.*, 2001), is another cause for the differences in kinetic properties between algal and plant Rubisco enzymes. Another posttranslational modification observed in *Chlamydomonas* Rubisco but not in plant Rubisco is hydroxylation of Pro-104 and Pro-151, which are conserved among algal and plant Rubisco enzymes (Taylor *et al.*, 2001).

## POSTTRANSLATIONAL MODIFICATIONS

### Posttranslational modification residues

Four new posttranslational modifications of the Rubisco large subunit were observed in the highest-resolution 1.4-Å x-ray crystal structure of *Chlamydomonas* Rubisco (Taylor *et al.*, 2001). The Cγ atoms of Pro-104 and Pro-151 are hydroxylated, and the Sγ atoms of Cys-256 and Cys-369 are methylated (Taylor *et al.*, 2001; Mizohata *et al.*, 2002). The function of these posttranslational modifications is unknown.

Even though the Pro-104 and Pro-151 residues are conserved among species, hydroxylation of the prolines has not been observed in Rubisco crystal structures from other species (Knight *et al.*, 1990; Taylor *et al.*, 2001; Andersson and Backlund, 2008). Though unlikely, it is also possible that the other Rubisco structures are less well-defined, thus obscuring the hydroxylation modification. Proline hydroxylation has a history of serving as a cellular mechanism for sensing $O_2$ such as for tagging the hypoxia-inducible factor transcription complex for degradation (Jaakkola *et al.*, 2001). In addition, because hydroxyprolines stabilize the triple-helix conformation of collagen (Motooka *et al.*, 2012), the hydroxylation of Pro-104 and Pro-151 in Rubisco could also have a structural effect on the holoenzyme in response to $O_2$ levels. The additional hydroxyl groups might provide extra hydrogen-bonding partners or increase the hydrophilicity of the residues. A chloroplast-localized prolyl 4-hydroxylase has been identified in *Chlamydomonas* that is expressed under anaerobic conditions (Terashima *et al.*, 2010). However, ten other prolyl 4-hydroxylases were also identified in *Chlamydomonas* (Keskiaho *et al.*, 2007), and a crystal-structure is available for one of them (Koski *et al.*, 2007). One of these prolyl 4-hydroxylases plays a role in cell-wall assembly (Keskiaho *et al.*, 2007).

The methylated Cys-256 and Cys-369 residues are phylogenetic residues that are replaced by Phe-256 and Val-369 in plants (Taylor *et al.*, 2001; Du *et al.*, 2003). Perhaps these residues might account for the kinetic differences between algal and plant Rubisco (Jordan and Ogren, 1981b). Methylation of the cysteine residues could prevent formation of disulfide bridges. Methyltransferases have been identified in some plant species, but these chloroplast-localized methyltransferases only methylate Lys-14 of the Rubisco large subunit in plants (Houtz *et al.*, 2008).

Pro-104 and Cys-369 are solvent exposed at the large-subunit interdimeric interface (Knight *et al.*, 1990; Taylor *et al.*, 2001) (Fig. 17). The modification of these residues could occur after formation of the Rubisco holoenzyme. However, because Pro-151 and Cys-256 are inaccessible to solvent, modifications of these residues must occur before assembly. Pro-151 is buried in the large subunit whereas Cys-256, which is in van der Waals contact with small-subunit Val-63, is only slightly exposed to the interior cavity of the holoenzyme at the large/small-subunit interface (Taylor *et al.*, 2001; Spreitzer *et al.*, 2005) (Fig. 17).

To test the importance of the posttranslationally-modified residues, each was separately changed to alanine in *Chlamydomonas* Rubisco. P104A/P151A and C256A/C369A double mutants were also created to assess the essentiality of hydroxylation and methylation. Because Cys-256 and Cys-369 are phylogenetic residues, they were also changed to the common plant residues Phe-256 and Val-369 either singly or as a pair to determine the effect of the plant residues.

**Figure 17: Distribution of posttranslationally modified residues in *Chlamydomonas* Rubisco (PDB 1GK8).** Large subunits are represented in gray and white whereas small subunits are represented in orange and yellow. Surface residues hydroxy-Pro-104 (red) and methyl-Cys-369 (cyan) are shown in the holoenzyme (top). Residues hydroxy-Pro-151 (light green) and methyl-Cys-256 (pink) in the interior are shown by removing four of the front large subunits (bottom).

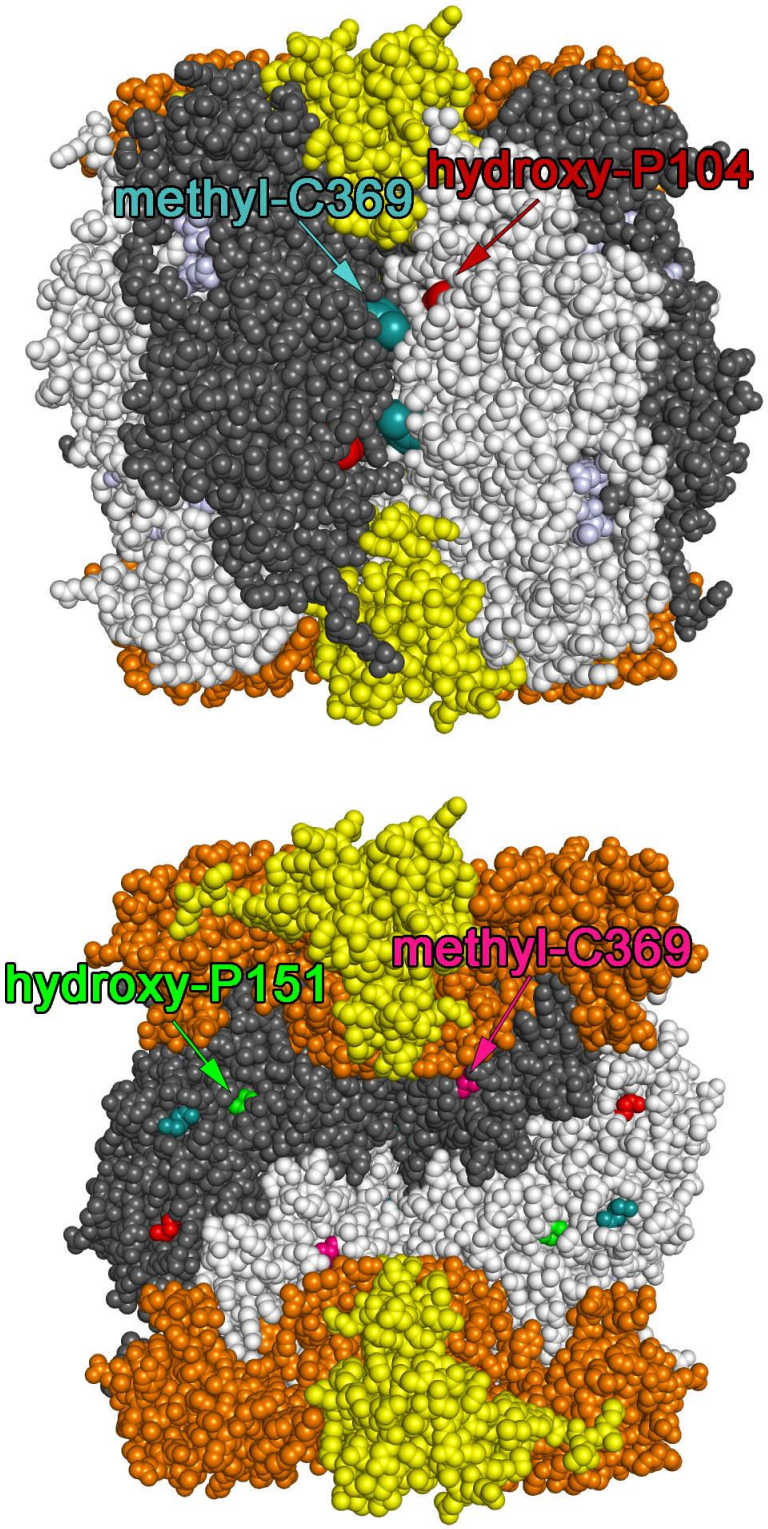
methyl-C369
hydroxy-P104
hydroxy-P151
methyl-C369

**Recovery of modified-residue mutants and their phenotypes**

The *Chlamydomonas* mutants P104A, P151A, P104A/P151A, C256A, C369A, C256A/C369A, C256F, and C256F/C369V were created previously (Spreitzer *et al.*, unpublished), but only the C256F mutant had been analyzed (Du *et al.*, 2003). The C369V Rubisco mutant was created in the current study by chloroplast transformation of the MX3312 *rbcL*-knockout strain followed by photosynthetic selection.

Comparison of the growth phenotypes between the directed mutants and wild type indicated that only the C256A and C256A/C369A mutants had reduced photosynthetic growth, which was even more pronounced at 35ºC (spots 4 and 6 respectively, Fig. 18). The P104A and P104A/P151A mutants also had reduced growth, but only at 35ºC (spots 1 and 3 respectively, Fig. 18).

**Rubisco holoenzyme level**

To determine the effects of the mutant substitutions on the amount of Rubisco *in vivo*, which would depend on holoenzyme expression, stability, or assembly, SDS-PAGE and western analysis were performed. Only the C256A and C256A/C369A mutant strains had reduced holoenzyme levels when grown at both 25 and 35ºC (lanes 4 and 6 respectively, Fig. 19). The P104A/P151A mutant had some decrease in holoenzyme at 35ºC (lane 3, Fig. 19). The decreased Rubisco holoenzyme levels of the C256A and C256A/C369A mutant strains could account for their decreased photosynthetic growth at 25 and 35ºC (spots 4 and 6, Fig. 18). The slight decrease in holoenzyme level of the 35ºC-grown P104A/P151A mutant (lane 3, Fig. 19) may account for its decreased growth at 35ºC (spot 3, Fig. 18).

**Figure 18: Growth phenotypes of *Chlamydomonas* wild type (WT) and posttranslational-residue mutants P104A (spot 1), P151A (spot 2), P104A/P151A (spot 3), C256A (spot 4), C369A (spot 5), C256A/C369A (spot 6), C256F (spot 7), C369V (spot 8) and C256F/C369V (spot 9).** About 2 X $10^5$ cells were spotted on each position, and grown for one week at the conditions indicated.

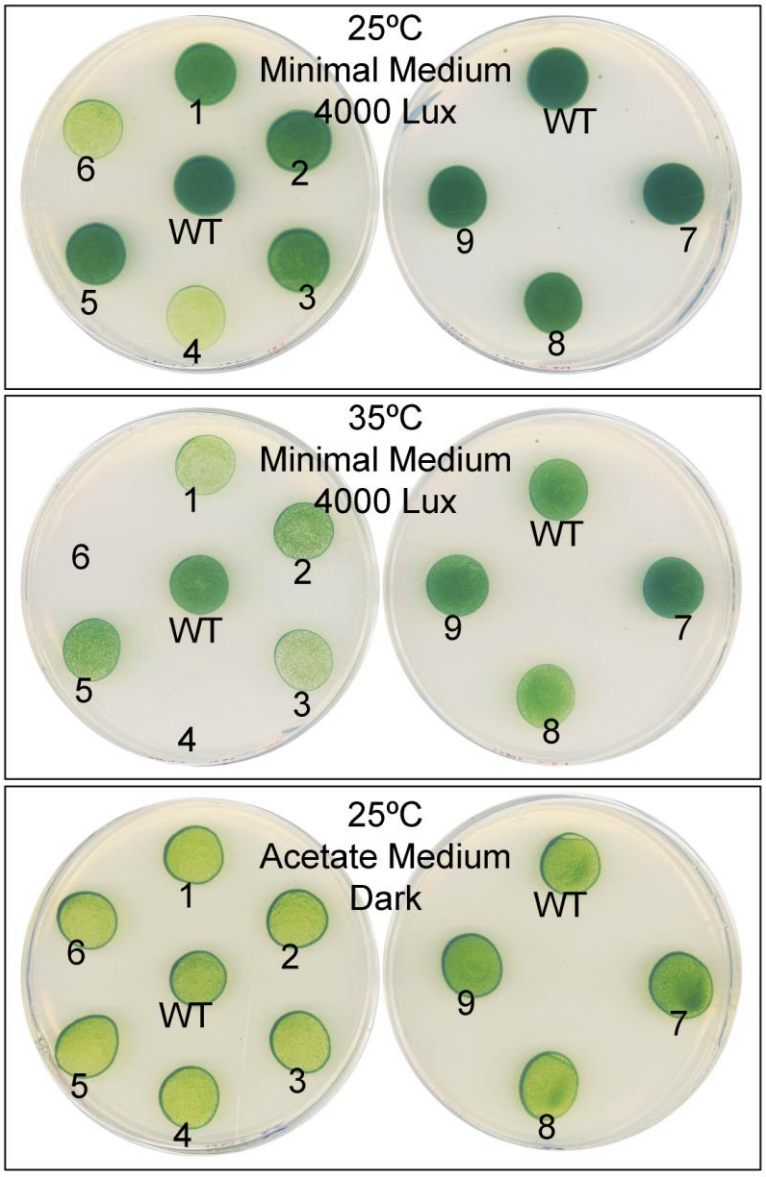
25ºC
Minimal Medium
4000 Lux
1
2
3
4
5
6
WT
WT
7
8
9
35ºC
Minimal Medium
4000 Lux
1
2
3
4
5
6
WT
WT
7
8
9
25ºC
Acetate Medium
Dark
1
2
3
4
5
6
WT
WT
7
8
9

**Figure 19: SDS-PAGE (left) and western-blot analysis (right) of total soluble protein from *Chlamydomonas* wild type (WT) and posttranslational-residue mutants P104A (lane 1), P151A (lane 2), P104A/P151A (lane 3), C256A (lane 4), C369A (lane 5), C256A/C369A (lane 6), C256F (lane 7), C369V (lane 8) and C256F/C369V (lane 9).** Sixty micrograms of total soluble protein from dark-grown cells were run in each lane. LS denotes the Rubisco large subunit, and SS denotes the small subunit.

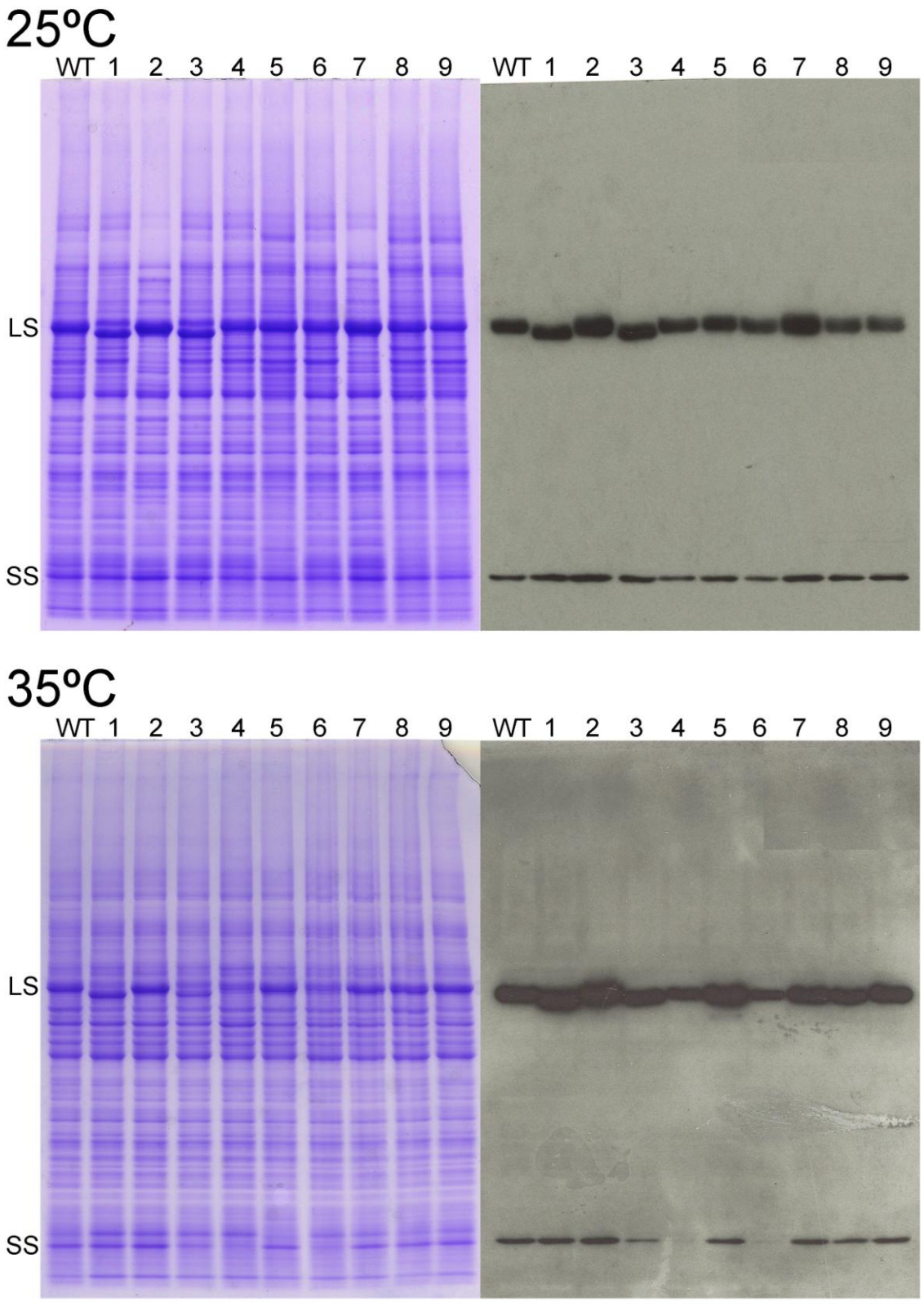
25ºC
WT 1 2 3 4 5 6 7 8 9
WT 1 2 3 4 5 6 7 8 9
LS
SS
35ºC
WT 1 2 3 4 5 6 7 8 9
WT 1 2 3 4 5 6 7 8 9
LS
SS

Thermal inactivation experiments (Chen *et al.*, 1993) were performed to determine whether the mutant enzymes are unstable (Fig. 20). All the mutant enzymes had similar temperature inactivation profiles (Fig. 20), indicating that they are not inherently unstable. Perhaps the P104A/P151, C256A, and C256A/C369A mutants have reduced holoenzyme levels because the mutations increase the susceptibility of the holoenzyme to proteolysis *in vivo*.

**Kinetic properties**

Among the hydroxy-Pro-to-Ala mutant enzymes, only P104A and P104A/P151A have reduced $V_c$ of over 50%, and increased $K_c$ of 18% and 36%, respectively, which are compensated by increased $K_o$ of about 80% (Table 9). Because the P104A/P151A enzyme has kinetic properties similar to those of the P104A enzyme, the changes in kinetic properties may be caused by the P104A mutation alone. The kinetic properties of the P151A enzyme are similar to those of the wild-type enzyme. The P151A and P104A/P151A enzymes have significant reductions in $\Omega$ of 5% and 8%, respectively (Table 9).

More pronounced changes in kinetic properties were observed for the methyl-Cys-to-Ala mutant enzymes. C256A and C256A/C369A enzymes have reduced $V_c$ of over 79%, and increased $K_c$ of 29% and 39%, respectively. These negative effects are compensated by increased $K_o$ values of 36% and 70%, respectively (Table 9). Because the kinetic properties of the C256A and C256A/C369A enzymes are similar, changes in the kinetic properties of the C256A/C369A enzyme may be caused by the C256A substitution alone. Methyl-Cys-256 is one of the phylogenetically-substituted residue in

**Figure 20: Thermal inactivation of Rubisco purified from *Chlamydomonas* wild type (WT) and posttranslational-residue mutants P104A, P151A, P104A/P151A, C256A, C369A, C256A/C369A, C256F, C369V, and C256F/C369V.** Five micrograms of Rubisco were pre-incubated at the indicated temperatures for 10 min, cooled on ice for 5 min, and assayed for carboxylase activity at 25ºC for 1 min. The measured activity after each pre-incubation temperature was normalized to that of the 35ºC pre-incubation. The specific activity after the 35ºC pre-incubation was 1.1 µmol $CO_2$/min/mg protein for wild-type Rubisco, 0.8 µmol $CO_2$/min/mg for mutant P104A, 1.3 µmol $CO_2$/min/mg for mutant P151A, 0.9 µmol $CO_2$/min/mg for mutant P104A/P151A, 0.5 µmol $CO_2$/min/mg for mutant C256A, 1.4 µmol $CO_2$/min/mg for mutant C369A, 0.3 µmol $CO_2$/min/mg for mutant C256A/C369A, 0.9 µmol $CO_2$/min/mg for mutant C256F, 1.0 µmol $CO_2$/min/mg for mutant C369V, and 1.1 µmol $CO_2$/min/mg for mutant C256F/C369V.

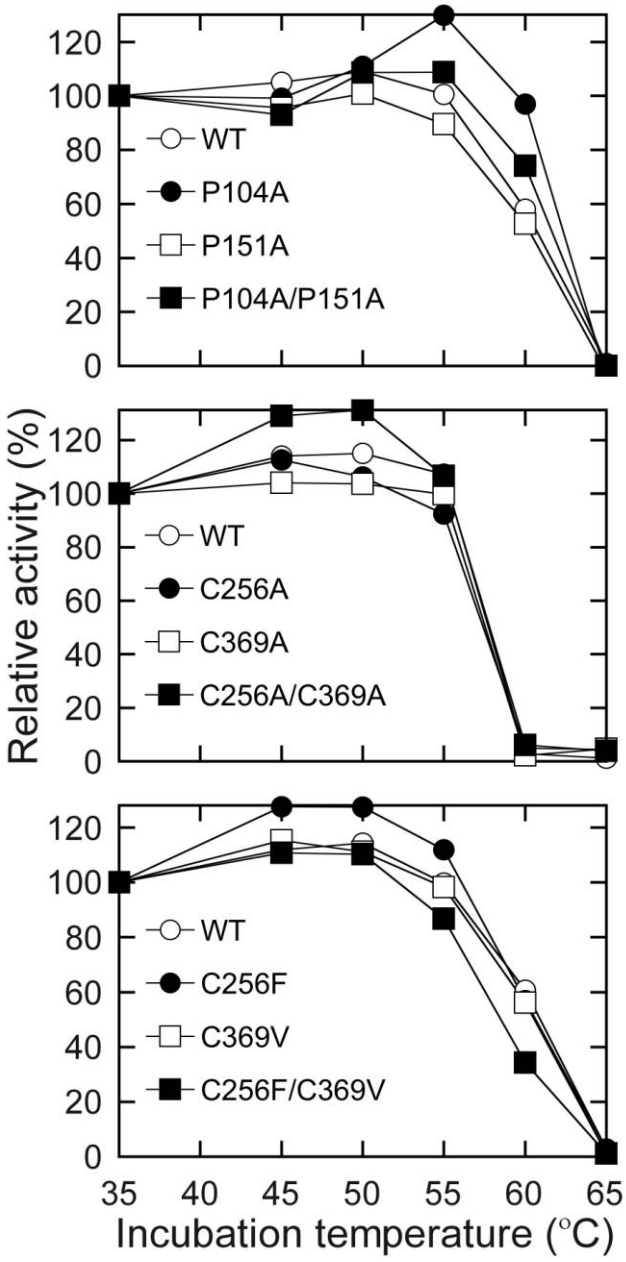
Relative activity (%)
120
100
80
60
40
20
0
WT
P104A
P151A
P104A/P151A
WT
C256A
C369A
C256A/C369A
WT
C256F
C369V
C256F/C369V
35
40
45
50
55
60
65
Incubation temperature (°C)

**Table 9: Kinetic properties of Rubisco purified from *Chlamydomonas* wild type and posttranslational mutants.**

| Enzyme | $\Omega$ [a] | $V_c$ [a] | $K_c$ [a] | $K_o$ [a] | $V_c/K_c$ [b] | $K_o/K_c$ [b] | $V_c/V_o$ [b] |
|---|---|---|---|---|---|---|---|
| | $V_cK_o/V_oK_c$ | *µmol/hr/mg* | *µM* $CO_2$ | *µM* $O_2$ | | | |
| WT | 60 ± 1 | 134 ± 12 | 28 ± 2 | 569 ± 51 | 4.9 | 21 | 2.9 |
| P104A | 58 ± 2 | 50 ± 2 | 33 ± 5 | 1062 ± 62 | 1.5 | 32 | 1.8 |
| P151A | 57 ± 1 | 98 ± 14 | 24 ± 4 | 574 ± 42 | 4.1 | 24 | 2.3 |
| P104A/P151A | 55 ± 3 | 55 ± 8 | 38 ± 6 | 1031 ± 306 | 1.5 | 27 | 2.0 |
| C256A | 50 ± 3 | 28 ± 7 | 36 ± 6 | 771 ± 174 | 0.8 | 22 | 2.3 |
| C369A | 51 ± 2 | 113 ± 15 | 28 ± 2 | 581 ± 61 | 4.1 | 21 | 2.5 |
| C256A/C369A | 54 ± 3 | 24 ± 6 | 39 ± 8 | 965 ± 71 | 0.6 | 25 | 2.2 |
| C256F [c] | 59 | 91 | 34 | 602 | 2.7 | 18 | 3.3 |
| C369V | 65 ± 3 | 124 ± 22 | 21 ± 4 | 582 ± 30 | 5.9 | 28 | 2.3 |
| C256F/C369V | 58 ± 4 | 86 ± 16 | 31 ± 2 | 645 ± 69 | 2.8 | 21 | 2.8 |

[a] Values are the means ± S.D. ($n$ - 1) of three separate enzyme preparations.

[b] Calculated values.

[c] Values are from Du *et al.* (2003).

the penta/ABSO mutant (Spreitzer *et al.*, 2005). In terms of Ω, the C256A, C369A and C256A/C369A enzymes have decreases by 17%, 15%, and 10%, respectively (Table 9). In contrast, the phylogenetic substitutions of the methyl-Cys residues (C256F, C369V and C256F/C369V) do not cause any significant changes to the kinetic properties of the enzymes except for a small increase in Ω for the C369V mutant.

**Structural analysis of posttranslationally-modified mutant enzymes**

Of the two hydroxylated proline residues in *Chlamydomonas* Rubisco, only Pro-104 seems to play a role in catalysis based on the measured kinetic properties of the Pro-to-Ala mutants (Table 9). Moreover, unlike Pro-151, Pro-104 is solvent exposed, which would allow the modification to take place after the assembly of the holoenzyme, and might provide a means for modulating enzyme activity in response to environmental conditions such as $CO_2$ and $O_2$ concentrations. The hydroxyl group of hydroxy-Pro-104 is in van der Waals contact with the backbone carbonyl oxygens of large-subunit residues Arg-79 and Lys-81 (Fig. 21), which are both in a stretch of loop region known as the 60s loop in the N-terminal domain of the large subunit (Knight *et al.*, 1990; Duff *et al.*, 2000; Spreitzer and Salvucci, 2002). Active-site residues Glu-60, Thr-65, and Trp-66 are also located in the 60s loop (Knight *et al.*, 1990; Duff *et al.*, 2000; Spreitzer and Salvucci, 2002). Perhaps hydroxy-Pro-104 influences catalysis through the interaction with the 60s loop. In addition to being located in the 60s loop, Arg-79 forms a hydrogen bond with the carbonyl oxygen of Gln-113 in the small-subunit βC-βD loop (Fig. 21). Therefore, the modification state of Pro-104 might also influence small-subunit structure.

Of the two methylated cysteine residues in *Chlamydomonas* Rubisco, only

**Figure 21: Structural interactions from hydroxy-Pro-104 (*red*) to the catalytic 60s loop and the small subunit.** The large-subunit 60s loop is represented in white ribbon. Residues that interact with hydroxy-Pro-104 (Arg-79, Lys-81 and Ile/Leu-105) or active-site residues (Glu-60, Thr-65 and Trp-66) are represented as sticks. The small subunit is represented in yellow. Small-subunit residue Gln-113/Asn-107 that interacts with Arg-79 is represented as sticks. The CABP transition-state analog (black) denotes the active site.

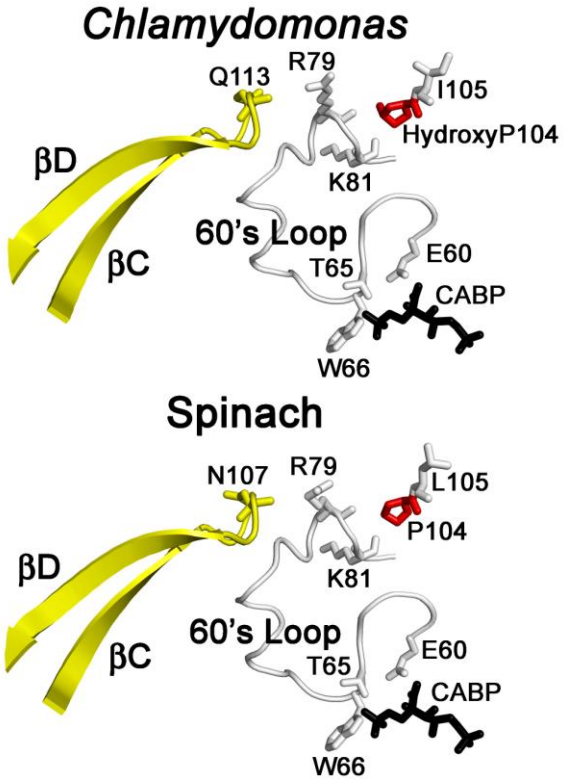
Chlamydomonas
Q113
R79
I105
HydroxyP104
βD
K81
60's Loop
βC
T65
E60
CABP
W66
Spinach
N107
R79
L105
P104
βD
K81
60's Loop
βC
T65
E60
CABP
W66

Cys-256 influences catalysis (Table 9). The methylation of Cys-256 enables contact with small-subunit residue Val-63, which is absent in the shorter βA-βB loop of plants (Fig. 22). Changes in the interaction between the small-subunit βA-βB loop and the large subunit could partially account for the shift in kinetic properties of the penta/ABSO mutant enzyme (Spreitzer *et al.*, 2005). Therefore, Cys-256 could be one of the large-subunit residues mediating the interaction between the large and small subunits in a methylation-dependent manner. Moreover, when Cys-256 is replaced with the phylogenetically-related Phe-256, which has a longer and bulkier side chain, the changes in kinetic properties are less drastic than that of replacing with Ala-256, which has a shorter side chain. Perhaps the loss of interaction between residue 256 and small-subunit residue 63 is the reason for this change in catalysis.

In conclusion, among the four posttranslational modifications observed in the large subunit of *Chlamydomonas* Rubisco, only hydroxylation of Pro-104 and methylation of Cys-256 provide potential mechanisms for controlling Rubisco catalysis. Hydroxy-Pro-104 and methyl-Cys-256 can form networks of interactions to the small-subunit βC-βD and βA-βB loops, respectively, whereas the unmodified Pro-104 and Cys-256 are unable to participate in the interactions. Based on a previous study (Spreitzer *et al.*, 2005) and also the analysis of the 265Assoc/SSAT associated-group mutant enzyme (Fig. 14), interactions between the large subunit and small-subunit βA-βB and βC-βD loops could affect the function of Rubisco.

**Figure 22: Comparison of structural interactions of methyl-Cys-256/Phe-256 (red) and the small subunit.** The large subunit is represented in white. Residues within 4 Å of methyl-Cys/Phe-256 are represented as sticks. The small subunit is represented in yellow. The CABP transition-state analog (black) that denotes the active site is 20Å away from this region.

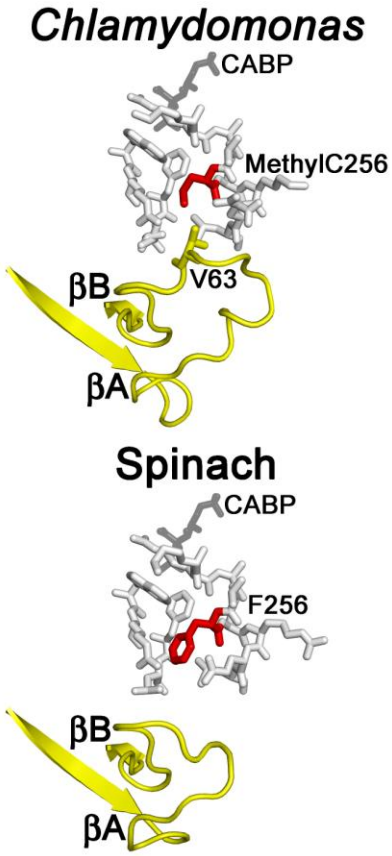
Chlamydomonas
CABP
MethylC256
βB
V63
βA
Spinach
CABP
F256
βB
βA

# CONCLUSION

Ever since the discovery of the role that Rubisco plays in photosynthesis and photorespiration (Bowes *et al.*, 1971), engineering the enzyme for increased photosynthesis or decreased photorespiration has been touted as a means to increase crop productivity (Spreitzer and Salvucci, 2002). Considering that the kinetic properties of Rubisco are variable among species (Jordan and Ogren, 1981b), modifying the enzyme to produce the desired kinetic properties seems possible. However, the active-site residues, which at first glance would seem like obvious targets for engineering, are conserved among species, and any changes in the active-site residues are detrimental to Rubisco function (Gutteridge *et al.*, 1993; Hartman and Harpel, 1994; Zhu and Spreitzer, 1994). Therefore, the variable non-active-site residues, known as phylogenetic residues, and the corresponding structural regions of the holoenzyme must define targets for engineering. Because engineering of eukaryotic Rubisco is most amenable in *Chlamydomonas*, this alga is a suitable host for testing out engineered Rubisco enzymes, and also provides a system for genetic selection. In the present study, phylogenetic residues, grouped according to their distribution in the x-ray crystal structure of *Chlamydomonas* Rubisco (Taylor *et al.*, 2001) were changed to those most common in land plants. Phylogenetic substitutions that altered the kinetic properties of Rubisco defined non-active-site regions of the holoenzyme that influence catalysis. Complementary phylogenetic substitutions between separate regions of the holoenzyme were also observed.

Phylogenetic substitutions (G168P/L326I/M349L/M375L/A398S/C399V) at the base of loop 6 reduced Ω by 5%, which was consistent with a previous study in the same region of the holoenzyme (Zhu and Spreitzer, 1996). Further substitutions

(R305K/D470E/T471A/I472M/K474T) at the carboxy terminus of the large subunit complement the base-of-loop-6 substitutions, and restore the Ω value of the enzyme back to normal. This indicates that the phylogenetic residues at the base of loop 6 and at the carboxy terminus form complementary interactions, possibly affecting catalytic loop 6, which is located between the two structural regions. However, because land plant Rubisco has a greater Ω value, other regions of the holoenzyme must also affect catalysis.

When the base-of-loop-6 substitutions were combined with several substitutions at the large/small-subunit interface region at the bottom of the α/β barrel, a mutant enzyme was created that requires the presence of the land-plant *Arabidopsis* small subunit to enable viable photosynthetic growth in *Chlamydomonas*. Perhaps the large-subunit residues that were changed in the mutant enzyme define a network of interactions between the small subunit and the active site. Though the βA-βB and βC-βD loops of the small subunit could be involved in the large/small-subunit interaction, defining the exact small-subunit residues that are responsible for complementing the large-subunit changes would be an avenue for future research.

A couple of associated-group mutants with phylogenetic substitutions in α-helices 7, 8, and G cannot be recovered as photosynthetic transformants in any of the available *Chlamydomonas rbcL*-knockout hosts. Therefore, phylogenetic differences in the three α helices, especially surface α-helix G, might be important for species-specific assembly of the holoenzyme. In fact, creating all the other phylogenetic substitutions did not complement the changes in the three α helices, and failed to produce a functional Rubisco enzyme in *Chlamydomonas*. If the species-specific assembly region of Rubisco could be defined in the future, it might be possible to express the high-Ω non-green algal Rubisco

in crop plants, which might increase net $CO_2$ fixation, and it might also be possible to express eukaryotic Rubisco in *E. coli*, which would expedite structure-function studies of the enzyme.

Because none of the phylogenetic substitutions in the current study produced a corresponding shift in the kinetic properties of Rubisco, the focus was turned to the previously created penta/ABSO phylogenetic mutant that has plant-like kinetic properties. Further dissection of the substitutions within the penta/ABSO mutant indicated that all of the residue substitutions are required for the shift in catalysis, which means that the five large-subunit phylogenetic residues at the bottom of the α/β barrel, and the small-subunit βA-βB loop in the same region, are important targets for attempts at engineering an improved Rubisco enzyme.

Some of the posttranslationally-modified residues also play a role in Rubisco catalysis. Alanine substitutions of hydroxy-Pro-104 and methyl-Cys-256 affect the kinetic properties of Rubisco negatively by reducing $V_c$ and Ω values. Therefore, targeting the modified residues or the modification states of the residues might be another avenue for Rubisco engineering. A variety of nuclear non-*RbcS* mutations that affect Rubisco properties were previously recovered in *Chlamydomonas* (Spreitzer *et al.*, 1992; Gotor *et al.*, 1994), and may have lesions in the posttranslational modification pathway of Rubisco. If the genetic loci of the catalysis-influencing nuclear mutations could be identified in the future, other players that are involved in the modification of Rubisco might be defined, and serve as additional targets for engineering.

In conclusion, the present study narrowed down the primary region for Rubisco engineering to only the interface area between the large-subunit bottom-of-the-α/β-barrel

region and the small-subunit βA-βB loop. Other structural interactions, such as those between the large-subunit regions at the base of loop 6 and the carboxy terminus, and between the base of loop 6, the bottom of the α/β barrel and the small-subunit βC-βD loop, also influence Rubisco function. These regions may also be worthy targets for molecular-evolution experiments.

## LITERATURE CITED

Andersson, I. (2008) Catalysis and regulation in Rubisco. *J. Exp. Bot.* **59**: 1555-1568.

Andersson, I., and Backlund, A. (2008) Structure and function of Rubisco. *Plant Physiol. Biochem.* **46**: 275-291.

Andrews, T. J., and Lorimer, G. H. (1985) Catalytic properties of a hybrid between cyanobacterial large subunits and higher plant small subunits of ribulose bisphosphate carboxylase/oxygenase. *J. Biol. Chem.* **260**: 4632-4636.

Birnboim, H. C., and Doly, J. (1979) A rapid alkaline extraction procedure for screening recombinant plasmid DNA. *Nucleic Acids Res.* **7**: 1513-1523.

Bowes, G., Ogren, W. L., and Hageman, R. H. (1971) Phosphoglycolate production catalyzed by ribulose diphosphate carboxylase. *Biochem. Biophys. Res. Commun.* **45**: 716–722.

Boynton, J. E., and Gillham, N. W. (1993) Chloroplast transformation in *Chlamydomonas*. *Methods Enzymol*. **217**: 510-536.

Boynton, J. E., Gillham, N. W., Harris, E. H., Hosler, J. P., Johnson, A. M., Jones, A. R., Randolph-Anderson, B. L., Robertson, D., Klein, T. M., and Shark, K. B. (1988) Chloroplast transformation in *Chlamydomonas* with high velocity microprojectiles. *Science* **240**: 1534-1538.

Bradford, M. M. (1976) A rapid and sensitive method for the quantitation of microgram quantities of protein utilizing the principle of protein-dye binding. *Anal. Biochem.* **72**: 248-254.

Chen, Z., Chastain, C. J., Al-Abed, S. R., Chollet, R., and Spreitzer, R. J. (1988) Reduced $CO_2/O_2$ specificity of ribulose-bisphosphate carboxylase/oxygenase in a temperature-sensitive chloroplast mutant of *Chlamydomonas*. *Proc. Natl. Acad. Sci. U. S. A.* **85**: 4696-4699.

Chen, Z., Hong, S., and Spreitzer, R. J. (1993) Thermal instability of ribulose-1,5-bisphosphate carboxylase/oxygenase from a temperature-conditional chloroplast mutant of *Chlamydomonas reinhardtii*. *Plant Physiol.* **101**: 1189-1194.

Chen, Z., and Spreitzer, R. J. (1989) Chloroplast intragenic suppression enhances the low $CO_2/O_2$ specificity of mutant ribulose bisphosphate carboxylase/oxygenase. *J. Biol. Chem.* **264**: 3051-3053.

Chen, Z., and Spreitzer, R. J. (1991) Proteolysis and transition-state-analogue binding of mutant forms of ribulose-1,5-bisphosphate carboxylase/oxygenase from *Chlamydomonas reinhardtii*. *Planta* **183**: 597-603.

Chen, Z., and Spreitzer, R. J. (1992) How various factors influence the $CO_2/O_2$ specificity of ribulose-1,5-bisphosphate carboxylase/oxygenase. *Photosynth. Res.* **31**: 157-164.

Chen, Z., Yu, W., Lee, J. H., Diao, R., and Spreitzer, R. J. (1991) Complementing amino acid substitutions within Loop-6 of the α/β-barrel active site influence the carbon dioxide/oxygen specificity of chloroplast ribulose-1,5-bisphosphate carboxylase/oxygenase. *Biochemistry* **30**: 8846-8850.

Cheng, Z. Q., and McFadden, B. A. (1998) A study of conserved in-loop and out-of-loop glycine residues in the large subunit of ribulose bisphosphate carboxylase/oxygenase by directed mutagenesis. *Protein Eng.* **11**: 457-465.

Christeller, J. T., and Tolbert, N. E. (1978) Phosphoglycolate phosphatase: Purification and properties. *J. Biol. Chem.* **253**: 1780-1785.

Chua, N.-H. (1980) Electrophoretic analysis of chloroplast proteins. *Methods enzymol.* **69**: 434-446.

Cleland, W. W., Andrews, T. J., Gutteridge, S., Hartman, F. C., and Lorimer, G. H. (1998) Mechanism of Rubisco: The carbamate as general base. *Chem. Rev.* **98**: 549-561.

Cloney, L. P., Bekkaoui, D. R., and Hemmingsen, S. M. (1993) Co-expression of plastid chaperonin genes and a synthetic plant Rubisco operon in *Escherichia coli*. *Plant Mol. Biol.* **23**: 1285-1290.

Dent, R. M., Haglund, C. M., Chin, B. L., Kobayashi, M. C., and Niyogi, K. K. (2005) Functional genomics of eukaryotic photosynthesis using insertional mutagenesis of *Chlamydomonas reinhardtii*. *Plant Physiol.* **137**: 545-556.

Dron, M., Rahire, M., Rochaix, J. D., and Mets, L. (1983) First DNA sequence of a chloroplast mutation: A missense alteration in the ribulose bisphosphate carboxylase large subunit gene. *Plasmid* **9**: 321-324.

Du, Y. C., Hong, S., and Spreitzer, R. J. (2000) *RbcS* suppressor mutations improve the thermal stability and $CO_2/O_2$ specificity of *rbcL*-mutant ribulose-1,5-bisphosphate carboxylase/oxygenase. *Proc. Natl. Acad. Sci. U. S. A.* **97**: 14206-14211.

Du, Y. C., Peddi, S. R., and Spreitzer, R. J. (2003) Assessment of structural and functional divergence far from the large subunit active site of ribulose-1,5-bisphosphate carboxylase/oxygenase. *J. Biol. Chem.* **278**: 49401-49405.

Du, Y. C., and Spreitzer, R. J. (2000) Suppressor mutations in the chloroplast-encoded large subunit improve the thermal stability of wild type ribulose-1,5-bisphosphate carboxylase/oxygenase. *J. Biol. Chem.* **275**: 19844-19847.

Duff, A. P., Andrews, T. J., and Curmi, P. M. (2000) The transition between the open and closed states of Rubisco is triggered by the inter-phosphate distance of the bound bisphosphate. *J. Mol. Biol.* **298**: 903-916.

Ellis, R. J. (1979) The most abundant protein in the world. *Trends Biochem. Sci.* **4**: 241-244.

Finer, J., Vain, P., Jones, M., and McMullen, M. (1992) Development of the particle inflow gun for DNA delivery to plant cells. *Plant Cell Rep.* **11**: 323-328.

Finkemeier, I., Laxa, M., Miguet, L., Howden, A. J., and Sweetlove, L. J. (2011) Proteins of diverse function and subcellular location are lysine acetylated in *Arabidopsis*. *Plant Physiol.* **155**: 1779-1790.

Genkov, T., Du, Y. C., and Spreitzer, R. J. (2006) Small-subunit cysteine-65 substitutions can suppress or induce alterations in the large-subunit catalytic efficiency and holoenzyme thermal stability of ribulose-1,5-bisphosphate carboxylase/oxygenase. *Arch. Biochem. Biophys.* **451**: 167-174.

Genkov, T., Meyer, M., Griffiths, H., and Spreitzer, R. J. (2010) Functional hybrid Rubisco enzymes with plant small subunits and algal large subunits: Engineered *rbcS* cDNA for expression in *Chlamydomonas*. *J. Biol. Chem.* **285**: 19833-19841.

Genkov, T., and Spreitzer, R. J. (2009) Highly-conserved small-subunit residues influence Rubisco large-subunit catalysis. *J. Biol. Chem.* **284**: 30105-30112.

Getzoff, T. P., Zhu, G., Bohnert, H. J., and Jensen, R. G. (1998) Chimeric *Arabidopsis thaliana* ribulose-1,5-bisphosphate carboxylase/oxygenase containing a pea small subunit protein is compromised in carbamylation. *Plant Physiol.* **116**: 695-702.

Gibson, J. L., and Tabita, F. R. (1977) Isolation and preliminary characterization of two forms of ribulose-1,5-bisphosphate carboxylase from *Rhodopseudomonas capsulata*. *J. Bacteriol.* **132**: 818-823.

Gotor, C., Hong, S., and Spreitzer, R. J. (1994) Temperature-conditional nuclear mutation of *Chlamydomonas reinhardtii* decreases the $CO_2/O_2$ specificity of chloroplast ribulose bisphosphate carboxylase/oxygenase. *Planta* **193**: 313-319.

Goloubinoff, P., Christeller, J. T., Gatenby, A. A., and Lorimer, G. H. (1989) Reconstitution of active dimeric ribulose bisphosphate carboxylase from an unfolded state depends on two chaperonin proteins and Mg-ATP. *Nature* **342**: 884-889.

Gutteridge, S., Lorimer, G. H., and Pierce J. (1988). Details of the reactions catalyzed by mutant forms of Rubisco. *Plant Physiol. Biochem.* **26**: 675-682.

Gutteridge, S., Rhoades, D. F., and Herrmann, C. (1993) Site-specific mutations in a loop region of the C-terminal domain of the large subunit of ribulose bisphosphate carboxylase/oxygenase that influence substrate partitioning. *J. Biol. Chem.* **268**: 7818-7824.

Harpel, M. R., Larimer, F. W., and Hartman, F. C. (1991) Functional analysis of the putative catalytic bases His-321 and Ser-368 of *Rhodospirillum rubrum* ribulose bisphosphate carboxylase/oxygenase by site-directed mutagenesis. *J. Biol. Chem.* **266**: 24734-24740.

Harpel, M. R., Larimer, F. W., and Hartman, F. C. (1998) Multiple catalytic roles of His-287 of *Rhodospirillum rubrum* ribulose 1,5-bisphosphate carboxylase/oxygenase. *Protein Sci.* **7**: 730-738.

Harpel, M. R., Larimer, F. W., and Hartman, F. C. (2002) Multifaceted roles of Lys-166 of ribulose bisphosphate carboxylase/oxygenase as discerned by product analysis and chemical rescue of site-directed mutants. *Biochemistry* **41**: 1390-1397.

Hollingshead, S., and Vapnek, D. (1985) Nucleotide sequence analysis of a gene encoding a streptomycin/spectinomycin adenylyltransferase. *Plasmid* **13**: 17-30.

Hong, S., and Spreitzer, R. J. (1994) Nuclear mutation inhibits expression of the chloroplast gene that encodes the large subunit of ribulose-1,5-bisphosphate carboxylase/oxygenase. *Plant Physiol.* **106**: 673-678.

Hong, S., and Spreitzer, R. J. (1997) Complementing substitutions at the bottom of the barrel influence catalysis and stability of ribulose bisphosphate carboxylase/oxygenase. *J. Biol. Chem.* **272**: 11114-11117.

Houtz, R. L., Magnani, R., Nayak, N. R., and Dirk, L. M. (2008) Co- and post-translational modifications in Rubisco: Unanswered questions. *J. Exp. Bot.* **59**: 1635-1645.

Houtz, R. L., Stults, J. T., Mulligan, R. M., and Tolbert, N. E. (1989) Post-translational modifications in the large subunit of ribulose bisphosphate carboxylase/oxygenase. *Proc. Natl. Acad. Sci. U. S. A.* **86**: 1855-1859.

Ishikawa, C., Hatanaka, T., Misoo, S., Miyake, C., and Fukayama, H. (2011) Functional incorporation of sorghum small subunit increases the catalytic turnover rate of Rubisco in transgenic rice. *Plant Physiol.* **156**: 1603-1611.

Jaakkola, P., Mole, D. R., Tian, Y. M., Wilson, M. I., Gielbert, J., Gaskell, S. J., von Kriegsheim, A., Hebestreit, H. F., Mukherji, M., Schofield, C. J., Maxwell, P. H., Pugh, C. W., and Ratcliffe, P. J. (2001) Targeting of HIF-α to the von Hippel-Lindau ubiquitylation complex by $O_2$-regulated prolyl hydroxylation. *Science* **292**: 468-472.

Jordan, D. B., and Ogren, W. L. (1981a) A sensitive assay procedure for simultaneous determination of ribulose-1,5-bisphosphate carboxylase and oxygenase activities. *Plant Physiol.* **67**: 237-245.

Jordan, D. B., and Ogren, W. L. (1981b) Species variation in the specificity of ribulose biphosphate carboxylase/oxygenase. *Nature* **291**: 513-515.

Johnson, X., Wostrikoff, K., Finazzi, G., Kuras, R., Schwarz, C., Bujaldon, S., Nickelsen, J., Stern, D. B., Wollman, F. A., and Vallon, O. (2010) MRL1, a conserved pentatricopeptide repeat protein, is required for stabilization of *rbcL* mRNA in *Chlamydomonas* and *Arabidopsis*. *Plant Cell* **22**: 234-248.

Kanevski, I., Maliga, P., Rhoades, D. F., and Gutteridge, S. (1999) Plastome engineering of ribulose-1,5-bisphosphate carboxylase/oxygenase in tobacco to form a sunflower large subunit and tobacco small subunit hybrid. *Plant Physiol.* **119**: 133-142.

Kannappan, B., and Gready, J. E. (2008) Redefinition of Rubisco carboxylase reaction reveals origin of water for hydration and new roles for active-site residues. *J. Am. Chem. Soc.* **130**: 15063-15080.

Kapralov, M. V., and Filatov, D. A. (2006): Molecular adaptation during adaptive radiation in the Hawaiian endemic genus *Schiedea*. *PLoS ONE* **1**: e8.

Kapralov, M. V., and Filatov, D. A. (2007) Widespread positive selection in the photosynthetic Rubisco enzyme. *BMC Evol. Biol.* **7**: 73.

Kapralov, M. V., Kubien, D. S., Andersson, I., and Filatov, D. A. (2011) Changes in Rubisco kinetics during the evolution of C4 photosynthesis in *Flaveria* (Asteraceae) are associated with positive selection on genes encoding the enzyme. *Mol. Biol. Evol.* **28**: 1491-1503.

Karkehabadi, S., Peddi, S. R., Anwaruzzaman, M., Taylor, T. C., Cederlund, A., Genkov, T., Andersson, I., and Spreitzer, R. J. (2005) Chimeric small subunits influence catalysis without causing global conformational changes in the crystal structure of ribulose-1,5-bisphosphate carboxylase/oxygenase. *Biochemistry* **44**: 9851-9861.

Karkehabadi, S., Satagopan, S., Taylor, T. C., Spreitzer, R. J., and Andersson, I. (2007) Structural analysis of altered large-subunit loop-6/carboxy-terminus interactions that influence catalytic efficiency and $CO_2/O_2$ specificity of ribulose-1,5-bisphosphate carboxylase/oxygenase. *Biochemistry* **46**: 11080-11089.

Keskiaho, K., Hieta, R., Sormunen, R., and Myllyharju, J. (2007) *Chlamydomonas reinhardtii* has multiple prolyl 4-hydroxylases, one of which is essential for proper cell wall assembly. *Plant Cell* **19**: 256-269.

Khrebtukova, I., and Spreitzer, R. J. (1996) Elimination of the *Chlamydomonas* gene family that encodes the small subunit of ribulose-1,5-bisphosphate carboxylase/oxygenase. *Proc. Natl. Acad. Sci. U. S. A.* **93**: 13689-13693.

Knight, S., Andersson, I., and Branden, C. I. (1990) Crystallographic analysis of ribulose-1,5-bisphosphate carboxylase from spinach at 2.4 Å resolution: Subunit interactions and active site. *J. Mol. Biol.* **215**: 113-160.

Kolesinski, P., Piechota, J., and Szczepaniak, A. (2011) Initial characteristics of RbcX proteins from *Arabidopsis thaliana*. *Plant Mol. Biol.* **77**: 447-459.

Koski, M. K., Hieta, R., Bollner, C., Kivirikko, K. I., Myllyharju, J., and Wierenga, R. K. (2007) The active site of an algal prolyl 4-hydroxylase has a large structural plasticity. *J. Biol. Chem.* **282**: 37112-37123.

Kubien, D. S., Whitney, S. M., Moore, P. V., and Jesson, L. K. (2008) The biochemistry of Rubisco in *Flaveria*. *J. Exp. Bot.* **59**: 1767-1777.

Kuehn, G. D., and Hsu, T. C. (1978) Preparative-scale enzymic synthesis of D-[$^{14}$C]ribulose 1,5-bisphosphate. *Biochem. J.* **175**: 909-912.

Laing, W. A., Ogren, W. L., and Hageman, R. H. (1974) Regulation of soybean net photosynthetic $CO_2$ fixation by the interaction of $CO_2$, $O_2$, and ribulose 1,5-diphosphate carboxylase. *Plant Physiol.* **54**: 678-685.

Larson, E. M., O'Brien, C. M., Zhu, G., Spreitzer, R. J., and Portis, A. R., Jr. (1997) Specificity for activase is changed by a Pro-89 to Arg substitution in the large subunit of ribulose-1,5-bisphosphate carboxylase/oxygenase. *J. Biol. Chem.* **272**: 17033-17037.

Liu, C., Young, A. L., Starling-Windhof, A., Bracher, A., Saschenbrecker, S., Rao, B. V., Rao, K. V., Berninghausen, O., Mielke, T., Hartl, F. U., Beckmann, R., and Hayer-Hartl, M. (2010) Coupled chaperone action in folding and assembly of hexadecameric Rubisco. *Nature* **463**: 197-202.

Lorimer, G. H. (1981) Ribulosebisphosphate carboxylase: Amino acid sequence of a peptide bearing the activator carbon dioxide. *Biochemistry* **20**: 1236-1240.

Maeda, N., Kanai, T., Atomi, H., and Imanaka, T. (2002) The unique pentagonal structure of an archaeal Rubisco is essential for its high thermostability. *J. Biol. Chem.* **277**: 31656-31662.

Maul, J. E., Lilly, J. W., Cui, L., dePamphilis, C. W., Miller, W., Harris, E. H., and Stern, D. B. (2002) The *Chlamydomonas reinhardtii* plastid chromosome: Islands of genes in a sea of repeats. *Plant Cell* **14**: 2659-2679.

Merchant, S. S., Prochnik, S. E., Vallon, O., Harris, E. H., Karpowicz, S. J., Witman, G. B., *et al.* (2007) The *Chlamydomonas* genome reveals the evolution of key animal and plant functions. *Science* **318**: 245-250.

Miller, E. M., and Nickoloff, J. A. (1995) *Escherichia coli* electrotransformation. *Methods Mol. Biol.* **47**: 105-113.

Miziorko, H. M., and Lorimer, G. H. (1983) Ribulose-1,5-bisphosphate carboxylase-oxygenase. *Annu. Rev. Biochem.* **52**: 507-535.

Mizohata, E., Matsumura, H., Okano, Y., Kumei, M., Takuma, H., Onodera, J., Kato, K., Shibata, N., Inoue, T., Yokota, A., and Kai, Y. (2002) Crystal structure of activated ribulose-1,5-bisphosphate carboxylase/oxygenase from green alga *Chlamydomonas reinhardtii* complexed with 2-carboxyarabinitol-1,5-bisphosphate. *J. Mol. Biol.* **316**: 679-691.

Motooka, D., Kawahara, K., Nakamura, S., Doi, M., Nishi, Y., Nishiuchi, Y., Kang, Y. K., Nakazawa, T., Uchiyama, S., Yoshida, T., Ohkubo, T. and Kobayashi, Y. (2012) The triple helical structure and stability of collagen model peptide with 4(*s*)-hydroxyprolyl-pro-gly units. *Biopolymers* **98**: 111-121.

Mueller-Cajar, O., Morell, M., and Whitney, S. M. (2007) Directed evolution of Rubisco in *Escherichia coli* reveals a specificity-determining hydrogen bond in the form II enzyme. *Biochemistry* **46**: 14067-14074.

Mueller-Cajar, O., and Whitney, S. M. (2008) Evolving improved *Synechococcus* Rubisco functional expression in *Escherichia coli*. *Biochem. J.* **414**: 205-214.

Newman, S. M., Boynton, J. E., Gillham, N. W., Randolph-Anderson, B. L., Johnson, A. M., and Harris, E. H. (1990) Transformation of chloroplast ribosomal RNA genes in *Chlamydomonas*: Molecular and genetic characterization of integration events. *Genetics* **126**: 875-888.

Newman, S. M., Gillham, N. W., Harris, E. H., Johnson, A. M., and Boynton, J. E. (1991) Targeted disruption of chloroplast genes in *Chlamydomonas reinhardtii*. *Mol. Gen. Genet.* **230**: 65-74.

Nozaki, H., Onishi, K., and Morita, E. (2002) Differences in pyrenoid morphology are correlated with differences in the *rbcL* genes of members of the *Chloromonas* lineage (*Volvocales, Chlorophyceae*). *J. Mol. Evol.* **55**: 414-430.

Ott, C. M., Smith, B. D., Portis, A. R.,Jr, and Spreitzer, R. J. (2000) Activase region on chloroplast ribulose-1,5-bisphosphate carboxylase/oxygenase: Nonconservative substitution in the large subunit alters species specificity of protein interaction. *J. Biol. Chem.* **275**: 26241-26244.

Parikh, M. R., Greene, D. N., Woods, K. K., and Matsumura, I. (2006) Directed evolution of Rubisco hypermorphs through genetic selection in engineered *E.coli*. *Protein Eng. Des. Sel.* **19**: 113-119.

Papworth, C., Bauer, J. C., and Braman, J. (1996) Site-directed mutagenesis in one day with >80% efficiency. *Strategies* **9**: 3-4.

Portis, A. R., Jr. (2003) Rubisco activase: Rubisco's catalytic chaperone. *Photosynth Res.* **75**: 11-27.

Ranty, B., Lundqvist, T., Schneider, G., Madden, M., Howard, R., and Lorimer, G. (1990) Truncation of ribulose-1,5-bisphosphate carboxylase/oxygenase (Rubisco) from *Rhodospirillum rubrum* affects the holoenzyme assembly and activity. *EMBO J.* **9**: 1365-1373.

Read, B. A., and Tabita, F. R. (1992) A hybrid ribulose bisphosphate carboxylase/oxygenase enzyme exhibiting a substantial increase in substrate specificity factor. *Biochemistry* **31**: 5553-5560.

Read, B. A., and Tabita, F. R. (1994) High substrate specificity factor ribulose bisphosphate carboxylase/oxygenase from eukaryotic marine algae and properties of recombinant cyanobacterial Rubisco containing algal residue modifications. *Arch. Biochem. Biophys.* **312**: 210-218.

Saito, Y., Ashida, H., Sakiyama, T., de Marsac, N. T., Danchin, A., Sekowska, A., and Yokota, A. (2009) Structural and functional similarities between a ribulose-1,5-bisphosphate carboxylase/oxygenase (Rubisco)-like protein from *Bacillus subtilis* and photosynthetic Rubisco. *J. Biol. Chem.* **284**: 13256-13264.

Salvucci, M. E., Portis, A. R., Jr., and Ogren, W. L. (1985) A soluble chloroplast protein catalyzes ribulosebisphosphate carboxylase/oxygenase activation *in vivo*. *Photosynth. Res.* **7**: 193–201.

Saschenbrecker, S., Bracher, A., Rao, K. V., Rao, B. V., Hartl, F. U., and Hayer-Hartl, M. (2007) Structure and function of RbcX, an assembly chaperone for hexadecameric Rubisco. *Cell* **129**: 1189-1200.

Satagopan, S., and Spreitzer, R. J. (2004) Substitutions at the Asp-473 latch residue of *Chlamydomonas* ribulose bisphosphate carboxylase/oxygenase cause decreases in carboxylation efficiency and $CO_2/O_2$ specificity. *J. Biol. Chem.* **279**: 14240-14244.

Satagopan, S., and Spreitzer, R. J. (2008) Plant-like substitutions in the large-subunit carboxy terminus of *Chlamydomonas* Rubisco increase $CO_2/O_2$ specificity. *BMC Plant. Biol.* **8**: 85.

Savir, Y., Noor, E., Milo, R., and Tlusty, T. (2010) Cross-species analysis traces adaptation of Rubisco toward optimality in a low-dimensional landscape. *Proc. Natl. Acad. Sci. USA* **107**: 3475-3480.

Schmidt, G. W., and Mishkind, M. L. (1986) The transport of proteins into chloroplasts. *Annu. Rev. Biochem.* **55**: 879-912.

Schneider, G., Lindqvist, Y., Branden, C. I., and Lorimer, G. (1986) Three-dimensional structure of ribulose-1,5-bisphosphate carboxylase/oxygenase from *Rhodospirillum rubrum* at 2.9 Å resolution. *EMBO J.* **5**: 3409-3415.

Schneider, G., Knight, S., Andersson, I., Branden, C. I., Lindqvist, Y., and Lundqvist, T. (1990) Comparison of the crystal structures of L2 and L8S8 Rubisco suggests a functional role for the small subunit. *EMBO J.* **9**: 2045-2050.

Schreuder, H. A., Knight, S., Curmi, P. M., Andersson, I., Cascio, D., Branden, C. I., and Eisenberg, D. (1993) Formation of the active site of ribulose-1,5-bisphosphate carboxylase/oxygenase by a disorder-order transition from the unactivated to the activated form. *Proc. Natl. Acad. Sci. U. S. A.* **90**: 9968-9972.

Smith, S. A., and Tabita, F. R. (2003) Positive and negative selection of mutant forms of prokaryotic (cyanobacterial) ribulose-1,5-bisphosphate carboxylase/oxygenase. *J. Mol. Biol.* **331**: 557-569.

Somerville, C. R., and Ogren, W. L. (1982) Genetic modification of photorespiration. *Trends Biochem. Sci.* **7**: 171-174.

Spreitzer, R. J. (1993) Genetic dissection of Rubisco structure and function. *Annu. Rev. Plant Physiol. Plant Mol. Biol.* **44**: 411-434.

Spreitzer, R. J. (1998) Genetic Engineering of Rubisco. *In*: Rochaix, J. D., Goldschmidt-Clermont, M., and Merchant, S. (eds.) *The Molecular Biology of Chloroplasts and*

*Mitochondria in Chlamydomonas*. Kluwer Academic Publishers, Dordrecht, pp. 515-527.

Spreitzer, R. J. (1999) Questions about the complexity of chloroplast ribulose-1,5-bisphosphate carboxylase/oxygenase. *Photosynthesis Res.* **60**: 29-42.

Spreitzer, R. J. (2003) Role of the small subunit in ribulose-1,5-bisphosphate carboxylase/oxygenase. *Arch. Biochem. Biophys.* **414**: 141-149.

Spreitzer, R. J., Al-Abed, S. R., and Huether, M. J. (1988a) Temperature-sensitive, photosynthesis-deficient mutants of *Chlamydomonas reinhardtii*. *Plant Physiol.* **86**: 773-777.

Spreitzer, R. J., Brown, T., Chen, Z., Zhang, D., and Al-Abed, S. R. (1988b) Missense mutation in the *Chlamydomonas* chloroplast gene that encodes the Rubisco large subunit. *Plant Physiol.* **86**: 987-989.

Spreitzer, R. J., and Chastain, C. J. (1987) Heteroplasmic suppression of an amber mutation in the *Chlamydomonas* chloroplast gene that encodes the large subunit of ribulose bisphosphate carboxylase/oxygenase. *Curr. Genet.* **11**: 611-616.

Spreitzer, R. J., Goldschmidt-Clermont, M., Rahire, M., and Rochaix, J. (1985) Nonsense mutations in the *Chlamydomonas* chloroplast gene that codes for the large subunit of ribulose bisphosphate Carboxylase/Oxygenase. *Proc. Natl. Acad. Sci. U. S. A.* **82**: 5460-5464.

Spreitzer, R. J., Jordan, D. B., and Ogren, W. L. (1982) Biochemical and genetic analysis of an RuBP carboxylase/oxygenase-deficient mutant and revertants of *Chlamydomonas reinhardii*. *FEBS Lett.* **148**: 117-121.

Spreitzer, R. J., and Mets, L. J. (1980) Non-mendelian mutation affecting ribulose-1,5-bisphosphate carboxylase structure and activity. *Nature* **285**: 114-115.

Spreitzer, R. J., and Mets, L. J. (1981) Photosynthesis-deficient mutants of *Chlamydomonas reinhardii* with associated light-sensitive phenotypes. *Plant Physiol.* **67**: 565-569.

Spreitzer, R. J., Peddi, S. R., and Satagopan, S. (2005) Phylogenetic engineering at an interface between large and small subunits imparts land-plant kinetic properties to algal Rubisco. *Proc. Natl. Acad. Sci. U. S. A.* **102**: 17225-17230.

Spreitzer, R. J., and Salvucci, M. E. (2002) Rubisco: Structure, regulatory interactions, and possibilities for a better enzyme. *Annu. Rev. Plant. Biol.* **53**: 449-475.

Spreitzer, R. J., Thow, G., and Zhu, G. (1995) Pseudoreversion substitution at large-subunit residue 54 influences the $CO_2/O_2$ specificity of chloroplast ribulose-bisphosphate carboxylase/oxygenase. *Plant Physiol.* **109**: 681-685.

Spreitzer, R. J., Thow, G., Zhu, G., Chen, Z., Gotor, C., Zhang, D., and Hong, S. (1992) Chloroplast and nuclear mutations that affect Rubisco structure and function in *Chlamydomonas reinhardtii. In* Murata, N. (ed.) *Research in Photosynthesis, Vol III.* Kluwer Academic Publishers, Dordrecht, pp. 593-600.

Svab, Z., and Maliga, P. (1993) High-frequency plastid transformation in tobacco by selection for a chimeric *aadA* gene. *Proc. Natl. Acad. Sci. U. S. A.* **90**: 913-917.

Tabita, F. R. (1999) Microbial ribulose-1,5-bisphosphate carboxylase/oxygenase: A different perspective. *Photosynth. Res.* **60**: 1-28.

Tabita, F. R., Hanson, T. E., Li, H., Satagopan, S., Singh, J., and Chan, S. (2007) Function, structure, and evolution of the Rubisco-like proteins and their Rubisco homologs. *Microbiol. Mol. Biol. Rev.* **71**: 576-599.

Tabita, F. R., Hanson, T. E., Satagopan, S., Witte, B. H., and Kreel, N. E. (2008a) Phylogenetic and evolutionary relationships of Rubisco and the Rubisco-like proteins and the functional lessons provided by diverse molecular forms. *Philos. Trans. R. Soc. Lond. B. Biol. Sci.* **363**: 2629-2640.

Tabita, F. R., Satagopan, S., Hanson, T. E., Kreel, N. E., and Scott, S. S. (2008b) Distinct form I, II, III, and IV Rubisco proteins from the three kingdoms of life provide clues about Rubisco evolution and structure/function relationships. *J. Exp. Bot.* **59**: 1515-1524.

Taylor, T. C., and Andersson, I. (1997) Structure of a product complex of spinach ribulose-1,5-bisphosphate carboxylase/oxygenase. *Biochemistry* **36**: 4041-4046.

Taylor, T. C., Backlund, A., Bjorhall, K., Spreitzer, R. J., and Andersson, I. (2001) First crystal structure of Rubisco from a green alga, *Chlamydomonas reinhardtii*. *J. Biol. Chem.* **276**: 48159-48164.

Terashima, M., Specht, M., Naumann, B., and Hippler, M. (2010) Characterizing the anaerobic response of *Chlamydomonas reinhardtii* by quantitative proteomics. *Mol. Cell. Proteomics* **9**: 1514-1532.

Thow, G., Zhu, G., and Spreitzer, R. J. (1994) Complementing substitutions within loop regions 2 and 3 of the α/β-barrel active site influence the $CO_2/O_2$ specificity of chloroplast ribulose-1,5-bisphosphate carboxylase/oxygenase. *Biochemistry* **33**: 5109-5114.

Towbin, H., Staehelin, T., and Gordon, J. (1979) Electrophoretic transfer of proteins from polyacrylamide gels to nitrocellulose sheets: Procedure and some applications. *Proc. Natl. Acad. Sci. U. S. A.* **76**: 4350-4354.

Uemura, K., Anwaruzzaman, Miyachi, S., and Yokota, A. (1997) Ribulose-1,5-bisphosphate carboxylase/oxygenase from thermophilic red algae with a strong specificity for $CO_2$ fixation. *Biochem. Biophys. Res. Commun.* **233**: 568-571.

Wang, Z. Y., Snyder, G. W., Esau, B. D., Portis, A. R., Jr., and Ogren, W. L. (1992) Species-dependent variation in the interaction of substrate-bound ribulose-1,5-bisphosphate carboxylase/oxygenase (Rubisco) and Rubisco activase. *Plant Physiol.* **100**: 1858-1862.

Whitney, S. M., and Andrews, T. J. (2001) Plastome-encoded bacterial ribulose-1,5-bisphosphate carboxylase/oxygenase (Rubisco) supports photosynthesis and growth in tobacco. *Proc. Natl. Acad. Sci. U. S. A.* **98**: 14738-14743.

Whitney, S. M., Baldet, P., Hudson, G. S., and Andrews, T. J. (2001) Form I Rubiscos from non-green algae are expressed abundantly but not assembled in tobacco chloroplasts. *Plant J.* **26**: 535-547.

Whitney, S. M., Sharwood, R. E., Orr, D., White, S. J., Alonso, H., and Galmes, J. (2011) Isoleucine 309 acts as a C4 catalytic switch that increases ribulose-1,5-bisphosphate carboxylase/oxygenase (Rubisco) carboxylation rate in *Flaveria*. *Proc. Natl. Acad. Sci. U. S. A.* **108**: 14688-14693.

Wildman, S. G. (2002) Along the trail from fraction I protein to Rubisco (ribulose bisphosphate carboxylase-oxygenase). *Photosynth. Res.* **73**: 243-250.

Wildman, S. G., and Bonner, J. (1947) The proteins of green leaves: Isolation, enzymatic properties and auxin content of spinach cytoplasmic proteins. *Arch. Biochem.* **14**: 381-413.

Wolfenden, R., and Snider, M. J. (2001) The depth of chemical time and the power of enzymes as catalysts. *Acc. Chem. Res.* **34**: 938-945.

Yanisch-Perron, C., Vieira, J., and Messing, J. (1985) Improved M13 phage cloning vectors and host strains: Nucleotide sequences of the M13mp18 and pUC19 vectors. *Gene* **33**: 103-119.

Yu, G. X., Park, B. H., Chandramohan, P., Geist, A., and Samatova, N. F. (2005) An evolution-based analysis scheme to identify $CO_2/O_2$ specificity-determining factors for ribulose 1,5-bisphosphate carboxylase/oxygenase. *Protein Eng. Des. Sel.* **18**, 589-596

Zhu, G., Jensen, R. G., Bohnert, H. J., Wildner, G. F., and Schlitter, J. (1998) Dependence of catalysis and $CO_2/O_2$ specificity of Rubisco on the carboxy-terminus of the large subunit at different temperatures. *Photosynth. Res* **57**: 71–79.

Zhu, G., Kurek, I., True, T., Zhang, X., Majumdar, M., Liu, L., and Lassner, M. (2005) Enhancing photosynthesis by improving Rubisco carboxylase activity and specificity, and Rubisco activase thermostability through DNA shuffling. *In* Photosynthesis: fundamental aspects to global perspectives. Proceedings of 13th International Congress on Photosynthesis, pp. 841–843. Lawrence, KS, USA

Zhu, G., and Spreitzer, R. J. (1994) Directed mutagenesis of chloroplast ribulose bisphosphate carboxylase/oxygenase. substitutions at large subunit Asparagine-123 and Serine-379 decrease $CO_2/O_2$ specificity. *J. Biol. Chem.* **269**: 3952-3956.

Zhu, G., and Spreitzer, R. J. (1996) Directed mutagenesis of chloroplast ribulose-1,5-bisphosphate carboxylase/oxygenase: Loop-6 substitutions complement for structural stability but decrease catalytic efficiency. *J. Biol. Chem.* **271**: 18494-18498.